MITIGATION OF AMMONIA AND HYDROGEN SULFIDE EMISSIONS FROM LIVESTOCK OPERATIONS USING TiO$_2$ AND ZnO NANOPARTICLES

A Thesis submitted to the College

of Graduate and Postdoctoral Studies

in partial fulfillment of the requirements

for the degree of Master of Science

in the Department of Chemical and Biological Engineering

University of Saskatchewan

Saskatoon

By

Suraj Kumar

PERMISSION TO USE

In presenting this thesis in partial fulfillment of the requirements for a Postgraduate degree from the University of Saskatchewan, I agree that the Libraries of this University may make it freely available for inspection. I further agree that permission for copying of this thesis in any manner, in whole or in part, for scholarly purposes may be granted by the professor or professors who supervised my thesis work or, in their absence, by the Head of the Department, the Dean of the college in which my thesis work was done. It is understood that any copying or publication or use of this thesis or parts there of for financial gain shall not be allowed without my written permission. It is also understood that due recognition shall be given to me and to the University of Saskatchewan in any scholarly use which may be made of any material in my thesis. Requests for permission to copy or to make other use of material in this in whole or part should be addressed to:

Head of the Department of Chemical and Biological Engineering.

3B48 Engineering Building,

University of Saskatchewan, 57 Campus Dr,

Saskatoon, Saskatchewan S7N 5A9 Canada.

OR,

Dean

College of Graduate and Postdoctoral Studies

University of Saskatchewan

116 Thorvaldson Building, 110 Science Place

Saskatoon, Saskatchewan S7N 5C9

Canada.

ABSTRACT

Hazardous gases such as ammonia (NH_3) and hydrogen sulfide (H_2S) are produced as part of a variety of industrial processes and in livestock production facilities. The emission of these gases poses severe risks to human and animal health, property values as well as to the environment. Several techniques including biological and physicochemical methods have been applied to remove these gases from contaminated air streams. However, most of the work focused on individual ammonia or hydrogen sulfide removal, and use of nanoparticles for simultaneous removal of these two gases has not been done yet. Thus, this work is focused on simultaneous removal of ammonia and hydrogen sulfide from livestock operations using ZnO and TiO_2 nanoparticles.

Adsorption capacities and isotherms at various temperatures (22 °C, 70 °C, 140 °C and 280 °C) in the concentration range 50-50, 100-100, 200-200, 300-300, 400-400, 500-550 ppmv of NH_3-H_2S in laboratory scale packed-bed adsorption column was studied and developed. The equilibrium adsorption capacities of both ammonia and hydrogen sulfide increased with an increase of gas concentration. Equilibrium adsorption capacity of hydrogen sulfide increase with the increase of temperature, while there is decrease adsorption capacity of ammonia due to an increase in temperature (22 °C to 280 °C). Control experiments showed that orientation of ZnO and TiO_2 nanoparticles layers in the column, as well as utilization of a homogeneous mixture of ZnO and TiO_2, had no impact on adsorption capacities (12 mg/g for NH_3 and 25.14 mg/g for H_2S). Among the evaluated isotherms, Langmuir-Freundlich best described the equilibrium adsorption data. To understand the mechanism of simultaneous removal of NH_3 and H_2S from gaseous streams, characterization of the unused and exposed adsorbents was conducted by CNHS and TGA. Finally, semi-pilot scale trials using gases emitted from swine manure showed the effectiveness of nanoparticles in the removal of H_2S and NH_3 from representative gases.

ACKNOWLEDGEMENTS

DEDICATION

I dedicate this thesis to my parents Mr. and Mrs. Saw who have always been there for me.

TABLE OF CONTENTS

LIST OF TABLES

LIST OF FIGURES

ABBREVIATIONS

AC: Activated Carbon

ACF: Activated Carbon Fiber

ASABE: American Society of Agricultural and Biological Engineers

ATSDR: Agency for Toxic Substances and Disease Registry

BET: Brunauer–Emmett–Teller

CNFs: Carbon nanofibers

DF: Degree of Freedom

EPA: Environmental Protection Agency.

OSHA: Occupational Safety and Health Administration

PPMV: Parts per million by volume

PM: Particulate matter

TLV: Threshold limit value

VOCs: Volatile organic compounds

WHO: World Health Organization

CHAPTER 1
INTRODUCTION

Air in livestock production facilities contains contaminants such as gases, odor, dust, and microorganisms (Casey et al. 2006). These contaminants are emitted from feed, animal, and manure. Among these sources, manure contributed the most significant fraction of the gas emission, which can be generated from fresh or deposited animal manure (Hartung and Phillips, 1994). Air contaminant emissions from livestock operations are primarily originated by gases produced from fresh or deposited animal manure, of which the gases of great concern are ammonia and hydrogen sulfide (Watts, 2000). Ammonia is formed by the bacterial and enzymatic breakdown of nitrogen-containing compounds in the feces, while hydrogen sulfide originates from the excreta through the anaerobic bacterial activity on sulfur-containing amino acids (Hartung and Phillips, 1994).

The emission of these gases continues to be a major concern for the swine industry because they pose serious risks to human and animal health, property values as well as to the environment (Casey et al. 2006). It has been documented that excessive levels of certain gases present in swine confinement units can cause illnesses and in extreme cases, even death. Ammonia (NH_3) and hydrogen sulfide (H_2S) are highly toxic gases which could potentially be fatal to human and animals at certain concentration levels.

Hog farmers have been reported to experience toxic or inflammatory effects on the respiratory system. In addition, residents near swine production facilities have suffered a tangible economic setback from a decline in their real property values of up to 9% (Palmquist et al. 1997). Several studies have shown that livestock gases contribute to environmental acidification and eutrophication, and pollution of ground and surface waters (Xue et al. 1998). To address concerns associated with both gases emissions, a number of studies have been conducted aiming to control NH_3 and H_2S, as well as other odor and gaseous emissions from the swine manure.

These include diet manipulation, manure additive, oil sprinkling, and biofiltration. Diet manipulation involves the modification of animal feed to reduce the production of gas and odor

(ASABE, 2007). This technique alone does not reduce the problems of hazardous gas emission since gas and odor are still produced (ASABE, 2007).

The application of manure additives is a more universal and commercially available method used to alleviate odor and gaseous emissions from livestock operations including NH_3 and H_2S. Additives are usually useful over a limited period, and thus frequent application is required (McCrory and Hobbs, 2001).

Oil sprinkling method has demonstrated that sprinkling a small amount of oil in swine facilities can reduce dust and gas concentrations substantially (Ouellette et al. 2006). This technique requires careful attention so that the areas near fans, heaters, and surrounding feeders are not affected, as oil could interfere with equipment operation. Cost and safety are a major concern too.

Biofilters which utilize the activity of microorganisms immobilized on media such as peat, compost or wood chips, are shown to be effective in the treatment of NH_3 and H_2S (Nicolai and Janni, 2001; Oliver, 2015). However, due to high operating costs associated with aeration, significant pressure drops, plugging of the biofilter as a result of biomass overgrowth, use of biofilters was restricted (Riskowski, 2003). Thus, an adequate gas mitigating measure is needed to address these concerns.

Therefore, this study is designed to explore a novel technology to help resolve the problem of hazardous gases emitting in swine barns. An example of this approach is to explore the application of nanotechnology, which currently has a broad range of uses ranging from pharmaceuticals, bioengineering, pigments, and electronics to optical and magnetic devices or structures and coatings with unique properties. In recent years, advances in nanotechnology have produced new materials with a scale of 1 to 100 nanometers in at least one dimension such as nanotubes, nanowires, and nanoparticles (EPA, 2007). With inherent properties different from their bulk counterpart, these nanomaterials were proven to be effective in environmental remediation applications such as air purification (Kim et al. 2008), and groundwater and wastewater treatments (Hu et al. 2005).

While some of these applications are already fully developed, the potential of nanotechnology in addressing issues regarding hazardous gas emissions such as ammonia and hydrogen sulfide from swine facilities has not yet been explored fully. In fact, most of the work to date has focused on the removal of individual ammonia or hydrogen sulfide in other applications and at temperature ranges higher than those encountered in swine barns. Thus, this work has been initiated to fill this gap by evaluating the application of commercially-available nanoparticles in reducing the levels of odor and gaseous emissions from swine barns by studying simultaneous removal of NH_3 and H_2S by a binary nanoparticle mixture of ZnO and TiO_2.

CHAPTER 2

LITERATURE REVIEW, KNOWLEDGE GAP, AND RESEARCH OBJECTIVES

Many industrial processes including livestock production emit hazardous gases such as hydrogen sulfide (H_2S) and ammonia (NH_3), and odors. The principal livestock operations associated with the emission of H_2S and NH_3 are swine, cattle, and poultry (Atia, 2013). Canada has a large swine industry that is ranked sixth in swine production globally with about 15 million pigs as recorded in 2016 (Statistics Canada, 2016). Because emission of hazardous gases (i.e., H_2S and NH_3) from such industry poses a risk to workers, animals, and environment, therefore, development of innovative technology that can be applied with ease and with reasonable cost is essential to mitigate the emission of these hazardous gases.

2.1 Ammonia

Ammonia is a colorless gas, lighter than air, highly water-soluble, and has a sharp, pungent odor with detection threshold between 5 and 18 ppmv (Casey et al. 2006). Ammonia also reacts rapidly with atmospherically-formed sulfuric and nitric acids to contribute to ambient levels of fine particles. Agriculture (livestock waste and fertilizer application) is the most significant source of NH_3 globally (Moran et al. 2016). Clarisse et al. (2009) reported that atmospheric NH_3 is emitted primarily from livestock waste (39%) and volatilization of NH_3-based fertilizers (17%). Heald et al. (2012) were one of the opinions that deposition of atmospheric NH_3 near an intensive agricultural area would dominate the overall load of reactive nitrogen from the atmosphere. NH_3 emissions from agriculture sources have become a growing concern from environmental scientists and government regulators (Aneja et al. 2003).

Gaseous NH_3 has a mean life of about 14 – 36 hours depending on the weather conditions. It also contributes to the formation of ground-level ozone, $PM_{2.5}$ and PM_{10} and ammonium nitrate particles (Bejan et al. 2013; Webb et al. 2014). To be more specific, in the vapor phase, ammonia would react with other compounds to form particulates. NH_3 and (NHx) are essential components

responsible for acidification in addition to sulfur compounds (SOx), nitrogen oxides, and volatile organic components. When exposed to 20 –50 ppmv NH$_3$, the gas can irritate the eyes. It is lighter than air and can cause various respiratory diseases to animals if exposed to a significant gas level for an extended period (McAllister and McQuitty, 1965).

Livestock production is a major contributor of ammonia emissions (ApSimon et al. 1987; Allen et al. 1988; Battye et al. 1994; Sommer and Hutchings, 1995; Kurvits and Marata, 1998; Koerkamp et al. 1998; Hobbs et al. 1999; Aneja et al. 2001). Ammonia is produced inside livestock facilities, in open feedlots, in manure storage facilities, during manure handling and treatment and when manure is added to soils. The total annual global emissions of NH$_3$ is about 54 Mtones NH$_3$-N. Globally, livestock production is responsible for about 50% of ammonia emissions (Olivier et al. 1998).

Koerkamp et al. (1998) reported that ammonia was usually produced from manure and animal waste through different pathways including aerobic decomposition of uric acid (reaction 2.1) and urea hydrolysis (reaction 2.2):

$$C_5H_4O_3N_4 + 1.5O_2 + 4H_2O \longrightarrow 5CO_2 + 4NH_3 \tag{2.1}$$

$$CO\,(NH_2)_2 \; + H_2O \longrightarrow CO_2 + 2NH_3 \tag{2.2}$$
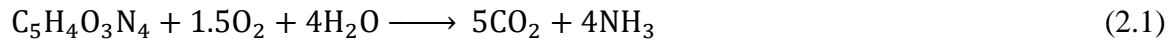
2.2 Hydrogen Sulfide

Hydrogen sulfide is formed by bacterial sulfate reduction and the decomposition of sulfur-containing organic compounds in manure under anaerobic conditions (Arogo et al. 2000) by the following reactions.

$$SO_4{}^{2-} + \text{organic matter} \xrightarrow{\textit{Anaerobic bacteria}} S_{2-} + nH_2O + CO_2 \tag{2.3}$$

$$S_2^- + 2H^+ \longrightarrow H_2S \tag{2.4}$$
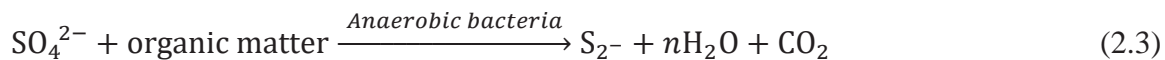
Hydrogen sulfide is colorless, heavier than air, highly soluble in water and has the characteristic odor of rotten eggs at low concentrations. At concentrations around 30 ppb, the H_2S odor can be detected by over 80% of the population (Schiffman et al. 2000).

Hydrogen sulfide in livestock buildings is mainly present in shallow barn gutters, underground or outdoor holding storage tanks, and earthen manure storage facilities. Ni et al. (2000, 2002) and Heber et al. (2004) reported that H_2S concentration in swine buildings under normal operating conditions is usually low (under 5 ppmv). Levels of H_2S can be high for swine manure, compared to other animal wastes because of the high protein content. Hydrogen sulfide concentrations as high as 1000 mg L^{-1} have been recorded in swine operations (Chenard et al. 2003).

2.3 Effects of NH_3 and H_2S on human, animals, and environment

The emission of NH_3 and H_2S imposes serious adverse effects on human, animals, and the environment. The current United States Occupational Safety and Health Administration (OSHA) Threshold Level Volume (TLV) for ammonia is 25 ppmv with a short-term exposure limit of 35 ppmv. Exposure to 300 to 500 ppmv for 30 to 60 minutes might be hazardous to health (ATSDR, 2006).

Ammonia (NH_3) reacts with other pollutants in the atmosphere to produce secondary particulate species, NH_3 plays a vital role in determining the overall acidity of precipitation, cloud water and airborne particulate matter (PM or aerosols) (Behera and Sharma, 2011).

Ammonia is the most prevalent alkaline gas in the atmosphere, and it readily combines with acidic species such as sulfur dioxide (SO_2), nitric acid (HNO_3) and sulfuric acid (H_2SO_4) to form aerosols such as ammonium nitrate (NH_4NO_3), ammonium bisulfate (NH_4HSO_4), and ammonium sulfate (($NH_4)_2SO4$). These aerosols may cause haze and impair visibility characteristics in the atmosphere (Apsimon and Kruse, 1991; Barthelmie and Pryor, 1998).

Similarly, H_2S gas is also very toxic to human, animals, and environment. Exposure to H_2S can cause unconsciousness and even death in workers and animals. Hydrogen sulfide is detectable as

with its odor at concentrations as low as 0.005 ppmv. According to the American Conference of Governmental Industrial Hygienists, the threshold limit value (TLV), or maximum allowable concentration for humans is 1 ppmv. The World Health Organization (WHO) recommends that exposure to hydrogen sulfide at five parts per billion must not exceed 30 minutes. Hydrogen sulfide can stay in the atmosphere for about 18 hours. While in the atmosphere, it can be transformed into sulfur dioxide (SO_2) and eventually sulfuric acid (H_2SO_4) which is the primary component of acidic deposition (ATSDR, 2006). It contributes to the deterioration of production facilities and equipment due to its corrosive nature (Asaad et al. 2008). Considering the hazardous effects of NH_3 and H_2S gases, removal of these gases is very much needed.

2.4 Hazardous gas emission control strategies

There are many strategies that have been proven effective in reducing hazardous gas concentration in swine production. Some of these techniques are discussed in the following sections.

2.4.1 Diet manipulation

Ammonia and other nitrogenous gases result from the digestion of protein, part of which is lost in manure and urine. Diet manipulation involves the modification of animal feed to reduce the production of hazardous gas and odor (ASABE, 2007). Animal feed can be altered to make it more digestible, or the feed composition can be changed. Godbout et al. (2001) reported the impact of dietary manipulations using low protein diet and canola oil application on gas and odor emission. With diet containing 16% protein and 15% soybean hull, ammonia emissions were decreased by more than 38%, but reduction in hydrogen sulfide and carbon dioxide emissions were not observed. Ammonia emissions could be reduced in dairy cows by 20% to 30% by manipulating dietary crude protein types and levels. Feeding a reduced crude protein, an amino acid–supplemented diet is also an active tool for reducing ammonia emissions from growing-finishing swine housing. Phase feeding is a commonly used practice for meeting livestock nutrient needs without exceeding them. Some studies suggested that dietary manipulation has the potential to reduce the cost of feed (Clark et al. 2005). Additional research is needed to find if diet manipulation has any adverse effects on livestock health, products quality or productivity.

2.4.2 Manure additives

Livestock manures contain several compounds, many of which are a potential source of malodorous gases. Some of those compounds are directly volatilized and can contribute to odor, while other compounds are converted to potentially odorous gases through a microbial breakdown. Odor control additives can change the nature of the odor itself, work on the complex microbial community that integrates the odorous compounds or convert the physio-chemical environment to suppress the release of odorous gases.

Manure additives are used to adsorb NH_3 and H_2S directly, reduce the manure pH, inhibit the microbial activity causing generation of odors and other gases, or to promote immobilization of microbes to reduce emissions of hazardous gases from manure (Arogo et al. 2000).

Moore et al. (1995) reported that alum addition to poultry manure resulted in 99% decrease in ammonia emissions. Alum additions have also been shown to decrease ammonia emission from beef cattle manure (Shi et al. 2001). Meisinger et al. (2001) reported that the addition of 2.5 wt.% alum to raw dairy slurry reduced ammonia volatilization by 60%.

Moreno et al. (2010) investigated the use of Na-nitrite and Na-molybdate to control H_2S emission from swine manure in large scale. Nitrite impact was not persistent, and simultaneous addition of nitrite and molybdate had a synergistic effect on reducing H_2S emission only with aged manure. The costs associated with molybdate mediated control of H_2S emission amounted to less than 1% of the total costs of a complete growth cycle. The use of manure additives may not be economically feasible. The costs of the chemical additives vary widely, and they can cost prohibitive for smaller operations. One disadvantage of using acidifying agents to suppress the ammonia emissions from manure is that it will favor the condition for the release of more hydrogen sulfide to the environment.

2.4.3 Oil sprinkling

The term sprinkle means that the oil is applied under low pressures and gives a shower effect and spray means that the oil is applied at high pressure and gives a fog-like effect (Takai and Pederson, 1999). Numerous studies have shown that sprinkling a small amount of oil in swine facilities can extensively reduce dust and gas concentrations.

The oil spraying or sprinkling of small quantities of vegetable oils on building interior surfaces has been shown as a reliable technique for particulate matter (PM) control in swine housing for many years (Maghirang et al. 1995) with 50 to 90% reductions in PM (Godbout et al. 2001; Zhang et al. 1996). Canola oil is primarily used in Canada and Northern Europe whereas soybean oil is used in the United States for the experimental research. In both cases, it appears that 5.0 mL/m^2 is the optimum dosage and both oils have similar cost (Takai and Pederson, 1999).

Oil sprinkling is an emerging technology that is a promising control measure for emission of air pollutants inside livestock buildings (Zhang et al. 1996). Paszek et al. (2001) reported that daily sprinkling of soybean oil inside swine finishing buildings by a soaker system significantly reduced the indoor concentration and emissions of NH$_3$ (30 % reduction of NH$_3$ and H$_2$S). Oil applications higher than 10 mL/m^2 could create a hazardous working environment due to slippery surfaces (Zhang et al. 1996). The application of oil sprinkling will require effective maintenance of machines and the animal production facilities (Schmidt and Heber, 2004) and thus increase in costs.

2.4.4 Biofiltration

Biofiltration can be defined as the removal and oxidation of harmful gases, mainly VOCs, from contaminated air. Gas treatment using biological processes can also be described as diffusion of the gaseous phase into an aqueous phase, where microorganisms convert biodegradable pollutant components into harmless products. In biofilters, gas is blown through a bed of compost or soil, in which the natural microorganisms presented into the support consume the organic pollutants or

inert support where a particular microorganism or pool of microorganisms are cultivated (Soccol et al. 2003).

Biofiltration is an effective method for reducing the emissions of NH_3, odor, and H_2S from livestock buildings (Nicolai and Janni, 2001). Biofilters usually consist of ventilation fans that flow the air from the building through ducts into a plenum below the biofilter media. The air passes through the biofilter media where the microorganisms treated the air before it is emitted into the atmosphere. The effectiveness of a biofilter is dependent on proper selection and management of the filter medium to provide appropriate conditions for the microbial population including temperature, the concentration of gases, oxygen level, acidity, nutrients and moisture contents. The operating cost of biofilters can be very high (Riskowski, 2003).

Armeen et al. (2008) suggested a treatment system (a combination of biosrubber and biofiltration) reduce the NH_3 and H_2S compounds of polluted air from animal facilities and the effect of NH_3 and H_2S on biofilter performance. It was proposed that the most effective biofilter performance be reached by a mixture of polystyrene (75% by volume) and peat moss (25% by volume).

Oliver (2015) studied spatial and temporal fungal dynamics in full-scale woodchip biofilters. Using wooden baits and microbial measures, fungi were characterized and shown to tolerate media desiccation. Additionally, successional patterns at the taxa and guild level were studied, and the development of a dominant fungal community was identified. Using a lab-scale biofilter system, fungi were shown to improve the capture of methane, particularly after periods of low-concentration inlet emissions.

The dynamics and potential abilities of fungi in biofilters treating livestock production emission can be used to guide the connection between fungi and biofilter function and has potential to improving biofilter performance and better protect air quality (Oliver, 2015).

The previous research showed that biofilters could treat contaminated air at the high rate. However, many subjects could be improved in this system about designation criteria (size of biofilters), bed materials and the relationship between microorganisms and the system.

2.5 Adsorption

Adsorption is a process where the substance (sorbate) is captured on the surface of the adsorbent or sorbent. It is a process that occurs when a gas or liquid solute accumulates on the surface of a solid, forming a molecular or atomic film. It is the adhesion of atoms, ions, biomolecules or molecules of gas, liquid, or dissolved solids to a surface and this process forms a film of the adsorbate (the molecules or atoms being accumulated) on the surface of the adsorbent. It is a surface phenomenon and a consequence of surface energy. Other atoms do not wholly surround the atoms on the surface of the adsorbent and thus, can attract adsorbates (Dabrowski, 2001).

The two types of adsorption processes are physisorption and chemisorption. Physical adsorption mechanism is a direct consequence due to the presence of weak Van der Waals forces. It is a phenomenon in which molecules in a gas bulk phase concentrate onto a surface to form a condensed phase. Physical sorption process is reversible and can adsorb multiple layers of molecules whereas chemical sorption process is irreversible and usually adsorb a single layer of molecules (Noble and Terry, 2004).

The adsorbate (gas or liquid) molecules which attract onto the adsorbent (solid) surfaces are primarily held at the micropores in their majority and some extent to mesopores of the solid adsorbent. These phenomena are physical, and hence, this process can be reversed using heat or pressure (Ruthven, 1984). Since physical adsorption is due to attraction forces, heat is released due to the change in energy level of the adsorbate molecules between gaseous and adsorbed phases; therefore, physical adsorption is an exothermic process (Horvath and Suzuki, 1999).

Chemisorption, on the other hand, involves a chemical reaction between surface and adsorbate, resulting in an altered electronic density distribution. In this process, the attraction force is given by chemical reactions between adsorbate and adsorbent resulting in chemical bond formation not completely reversible as physical adsorption (Rouquerol et al. 2013).

Adsorption mechanisms can be steric, kinetic or equilibrium. The steric mechanism is a function of the shape of a molecule such as molecular sieving where small molecules can be adsorbed while

the large molecules are excluded. The kinetic mechanism involves the relative accessibility of the adsorbate to the solid surface while the equilibrium mechanism is influenced by the thermodynamic equilibrium state of the fluid and solid phases (Dabrowski, 2001). These mechanisms help to treat environmental pollution using adsorbent columns. Influent is passed through the adsorbents, and the concentration of the effluent is at a minimum until it reaches the breakthrough. The effluent concentration exceeded the maximum allowable solute concentration when the bed will be saturated, and the effluent concentration will be the same as the influent concentration until the column reaches its exhaustion point. Adsorption of sorbate takes place in the mass transfer zone, and through time it moves down the adsorbent column.

2.6 Adsorption isotherms and adsorption capacity

Adsorption isotherms describe the relationship between gas and solid phase concentrations of adsorbate at constant temperature (Hines and Maddox, 1985). Adsorption isotherms show the equilibrium amount of gas/material adsorbed per unit mass of adsorbent as a function of concentration or partial pressure of the gas in the bulk phase (Hines and Robert, 1985). It represents the relationship between the concentration of the adsorbate in the bulk phase and the amount of material adsorbed onto the solid at a constant temperature. Although temperature and pH are constant, the concentration of the adsorbate changes until equilibrium is reached (Brezonik and Arnold, 2011).

Various empirical adsorption isotherms have been developed including Langmuir, Freundlich, BET, and Langmuir-Freundlich. The isotherms can be obtained by calculating the adsorbed amount of adsorbate using the overall mass balance. The adsorption system must first reach equilibrium; that is, the state in which the temperature of the bed has been restored to its initial state, and there is no mass transfer. The adsorption equilibrium data were fitted into Langmuir, Freundlich, and Langmuir-Freundlich expressions, represented by Equations 2.5, 2.6, and 2.7, respectively.

$$q = \frac{q_s K P}{1 + K P} \tag{2.5}$$

$$q = B P^{1/n} \tag{2.6}$$

$$q = \frac{q_s k^{1/n} P^{1/n}}{1 + k^{1/n} P^{1/n}} \tag{2.7}$$

where q refers to equilibrium adsorption capacity (mg adsorbed gas/g adsorbent), q_s is the maximum equilibrium adsorption capacity (mg adsorbed gas/g adsorbent), P is the partial pressure of gas (kPa), K is Langmuir or Langmuir-Freundlich equilibrium constant, B is Freundlich constant and n is Freundlich or Langmuir- Freundlich constant.

The temperature dependency of K in Langmuir and Langmuir-Freundlich isotherms can be expressed by Van't Hoff equation:

$$K = K_O \exp\left(\frac{-\Delta H}{RT}\right) \tag{2.8}$$

where ΔH is the enthalpy of adsorption (kJ/ mol), T is temperature (K), and R is the universal gas constant (kJ/ mol/ K). The variation of B and m with temperature can be expressed by Equations. 2.9 and 2.10, respectively (Ismadji et al. 2015).

$$B = B_O \exp\left(\frac{-\eta RT}{A_O}\right) \tag{2.9}$$

$$m = \frac{A_O}{RT} \tag{2.10}$$

where A_o and η are characteristic adsorption energy of surface and Clapeyron constant parameter, in addition to the above three isotherms, Langmuir-Freundlich isotherm was extended to incorporate the dependency of q_s on temperature using Equation 2.11 (Helminen et al. 2000).

$$q = q_{so}\exp(-\alpha(T - T_o)) \tag{2.11}$$

where α is the thermal expansion coefficient (K^{-1}) and $q_{s0,}$ is maximum equilibrium adsorption capacity (mg adsorbed gas/g adsorbent) at the reference temperature T_o (273 K).

The time required by adsorbent takes to get saturated described by breakthrough curves. It also shows the variation in adsorbate uptake with time. Figure 2.1 shows a schematic diagram of a typical breakthrough curve.

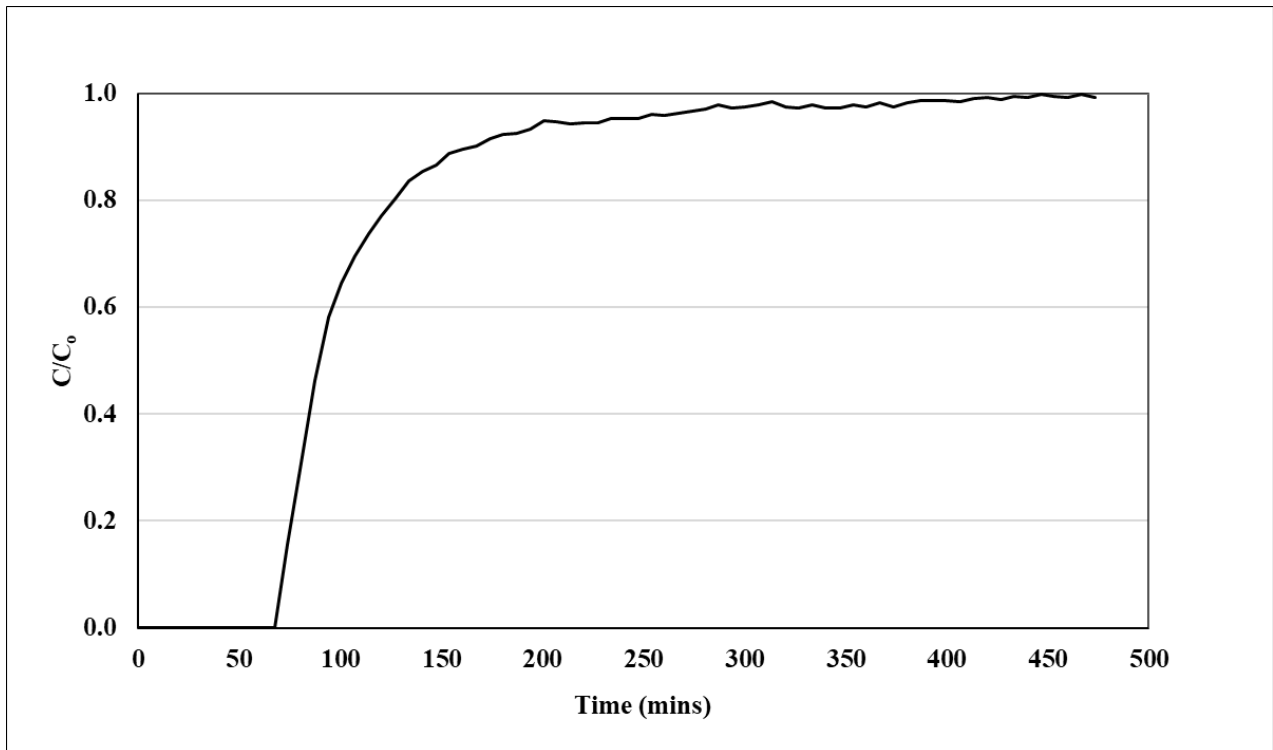**Figure 2.1.** Schematic diagram of a breakthrough curve, where C is the effluent gas concentration and Co is the influent gas concentration.

Amount of the adsorbate adsorbed per unit mass of the adsorbent at a given gas-phase concentration under equilibrium conditions is known as adsorption capacity. Equilibrium capacity also known as saturation capacity is the capacity of the adsorbent under equilibrium conditions.

The equilibrium established at a given temperature and pressure for a given concentration of gas depends on the properties of both the adsorbate and adsorbent. The adsorbent properties include the pore size distribution, size, shape, and chemical composition

2.7 Nanotechnology

Nanotechnology is called the science that develops materials by manipulating matter at the atomic and molecular level. Nanotechnology can also be defined as the study of matter within the size range of 10^{-6} to 10^{-9} meters. Nano-materials have high surface area per unit mass. Nanotechnology covers the design, construction, and utilization of functional structures with at least one dimension in 1 – 100 nanometers. At this scale, materials exhibit properties different from a macro scale. This technology is not only about the size of materials but about the manipulation of the structure and ability of materials to function more efficiently (Masciangioli and Zhang, 2003). Metallic nanoparticles have different physical and chemical properties from bulk metals (e.g., lower melting points, higher specific surface areas, specific optical properties, mechanical strengths, and specific magnetizations), properties that might prove attractive in various industrial applications.
In general, their classification depends very much on the specific application.

Nanomaterials can be grouped into four main types based on the materials that are used in making them. These are carbon-based materials which are made from carbon; dendrimers which are made from polymers; metal-based materials which are made from metals; and composites which are a combination of nanoparticles with other nanoparticles or larger materials. They have a wide range of potential applications in chemical, biomedical and electronics industry. One of the promising applications is adsorption. Appropriate large-scale structures need to be designed and built with nanoscale units to perform various separation applications including various gases.

2.7.1 Application of nanoparticles for adsorption of ammonia

There are three different families of adsorbents which have been used for the removal of gaseous ammonia. The first type is porous adsorbents such as carbon structures and zeolites. The second family includes porous materials impregnated with metallic nanoparticles, and the third category

is pure metal oxide nanoparticles. Having in mind the small size of ammonia molecule and its high basicity, adsorbents require a unique structure and acidic surface area. Activated carbon is one of the most commonly used adsorbents in removing ammonia due to its large surface area, high porosity and low cost (Rodrigues et al. 2007). However, the presence of functional groups in both acidic and basic nature on its surface constitutes a disadvantage for ammonia retention. Therefore, an increase in the density of acidic functional group and adjustment of the pore size is necessary to overcome this problem.

Introduction of acidic groups to the surface can be achieved via dry oxidation, wet oxidation, and impregnation with metal ions. The enhancement effect of oxidizing agents on the formation of acidic functional groups of activated carbon and ammonia adsorption is reported widely in the literature (Kaneoko et al. 1992; Mangun et al. 1999; Park et al. 2005; Huang et al. 2008).

Kaneko et al. (1992) studied the effect of temperature on the oxidation degree of pitch activated carbon fiber (ACF) in dry air and showed that the microporosity of ACF was not affected significantly even at a very high temperature and that the pore volume and surface area increased with increasing temperature of oxidation. It was found that at low pressure, the adsorption capacity of 6.7 mg NH_3 g^{-1} increased with the increase of temperature to 10 times higher than that of untreated ACF resulting in adsorption capacity of 125 mg NH_3 g^{-1}.

Mangun et al. (1999) investigated the enhancement effect of the surface acidity of activated carbon fiber (ACF) on ammonia adsorption by applying various oxidation methods including acid wash and dry air oxidation. The oxidation degree increased with the intensity of treatment such as increasing concentration of acid, contact time and heat temperature was emphasized by analyzing the textural properties such as surface area and pore volume. Due to the addition of functionalized groups, modification of the carbon surface by aqueous solution resulted in a reduction of micropore volume and surface area.

Also, there was a principal difference in the changes of the structural properties between ACF samples oxidized in dry air in comparison with an acid wash; the results showed that the adsorption capacity was increased significantly by 8 and 30 times, respectively. Indeed, the results suggested

that the interaction was derived from chemical forces and not structural properties (Mangun et al. 1999).

Park et al. (2005) showed the effect of ozone and nitric acid treatment on the formation of oxygen-containing functional groups in activated carbon fibers (ACF) and carbon nanofibers (CNFs) in conjunction to ammonia removal efficiency. Ozone and acid treatment increased the amount of functionalized group, while wet oxidation ozone treatment decreased surface area and pore volume along with the formation of the functional group. The effect of additional functionality on ammonia adsorption at low pressure was observed for all samples at low pressure even though nanofibers have much smaller surface area.

The adsorption capacity obtained for ACF indicated that there was no difference between the enhancement effect of ozone and acid treatment as obtained from adsorption capacity for ACF. It was also concluded that at lower pressure ammonia adsorption was governed predominantly by chemical forces as the ratio between the ammonia adsorbed to the total functional groups on all carbon samples was almost one (Park et al. 2005).

The removal of ammonia in adsorption processes using metal impregnated has been discussed extensively due to the contribution of metal ions in forming acidic functionalized groups on the surface of carbon-based materials. Metal oxide and metal chlorides-based composites are found to significantly increase adsorption capacity through selective acid-base interaction with polar molecules such as ammonia when compared to non-impregnated materials (Leuch et al. 2005; Petit et al. 2007; Romero et al. 2011; Barpaga and Levan, 2016).

Leuch et al. (2005) investigated the effect of metal oxide impregnates such as copper, zinc, and ferrous oxides on activated carbon fiber cloth in conjunction with their concentration and calcination temperature. They showed that modification of the support increased ammonia removal efficiency. The adsorption capacity increased to four times in case of ferrous oxides-supported activated carbon.

17

Petit et al. (2007) showed the influence of metal chloride (Zn, Cu, Ni) impregnates on ammonia uptake on BPL carbon samples. They investigated the interaction of ammonia with the surface concerning the amount of ammonia strongly and weakly adsorbed on the surface. The results indicated that most ammonia was retained on the surface by weak forces (Van der Waals bonding), all modified samples showed improved capacity. Also, copper chloride samples showed the highest removal efficiency of 67.7 mg /g by forming strong chemical interactions and complexes with ammonia.

Romero et al. (2012) reported that carbon samples incorporated with a mixture of metal chlorides and metal oxides ($CuO/ZnO/NiO/CuCl_2$) were useful for the removal of ammonia in a mixture with SO_2.

Petit et al. (2007) also studied the efficiency of activated carbon impregnated with tungsten and molybdenum oxides (W_2O_3 and MoO_3) in removing ammonia. They concluded that the presence of higher number of functionalized groups on the carbon surface is the molecular mass of the impregnate. Number of molecules measure the amount, the lower the mass of the metal atom, the higher the number of functionalized groups.

Rezaei et al. (2017) studied MgO, ZnO, CuO, and TiO_2 nanoparticles along with activated charcoal (AC) for ammonia adsorption under various atmospheric pressure in a packed bed column. They concluded that TiO_2 had the highest equilibrium adsorption capacity followed by AC, ZnO, MgO, and CuO.

Rezaei et al. (2017) also studied TiO_2-AC composites with different TiO_2 loadings by sol-gel method and evaluated adsorption of gaseous ammonia using a continuous flow packed-bed column. The equilibrium adsorption capacity of AC at room temperature (22 °C) increased from 2.48 to 3.22, 5.48, 7.07, and 7.73 mg NH_3 g^{-1} by 10, 20, 30, and 40% TiO_2 loadings, respectively. They reported that ammonia adsorption capacity of TiO_2 nanoparticles in TiO_2-AC (30%) composite was higher than that of commercial TiO_2 nano-particles (40 nm), due to the smaller size of TiO_2 nanoparticles deposited on AC. The addition of TiO_2 to AC changed the multilayer adsorption of ammonia to monolayer adsorption.

2.7.2 Application of nanoparticles for adsorption of hydrogen sulfide

Adsorption on metal oxides has shown H_2S removal at temperatures as high as 1500 °C for oxides of many metals such as Fe, Cu, Zn, Co, W, Mo, Ca, Ba, and Sr are reported to be efficient adsorbents at high temperatures (Westmoreland et al. 1976).

Lew et al. (1992) studied the adsorption of H_2S on pure zinc oxide and zinc titanates. The authors concluded that zinc titanate reduces more slowly to volatile zinc; therefore, it can be used at higher temperatures and that to increase the effectiveness of the adsorbents and their H_2S breakthrough capacities, the number of active sites must be increased. This can be achieved by substituting the metal oxide on the surface of different supports such as TiO_2, SiO_2 Al_2O_3, and zeolites.

Li et al. (1997) showed an H_2S reduction down to 5-10 ppmv from a gas stream containing several thousand ppmv at temperatures between 650-850 °C using CuO-CeO_2 adsorbent. They reported that ZnO based adsorbents were compared with copper oxides and found that CuO can be used at higher temperatures than ZnO based adsorbents. They also reported a reduction of H_2S concentration from several thousand ppmv to sub-ppmv levels using CuO and Cu_2O sorbents.

Bandosz et al. (1999) studied the use of activated carbon as an H_2S removing agent. They showed that the surface functional groups (containing oxygen and phosphorous) and the porosity of carbon significantly contribute to the H_2S removal. They also discovered that functional groups present on the carbon surface act as a catalyst for H_2S oxidation.

Jun et al. (2001) prepared Zn-Ti based adsorbents using a mixture of zinc oxide, titanium oxide, nickel oxide and cobalt oxide together with bentonite as an inorganic binder. These adsorbents showed good sulfur removing capacity even after 15 cycles of regeneration. These adsorbents found to be efficient while conventional Zn-Ti sorbents deactivate much earlier. Nickel and cobalt helped to stabilize the structure of the adsorbent and worked as the active sites for desulfurization reaction.

Wang et al. (2008) showed the effectiveness of SBA-15 supported zinc oxide (ZnO) nanoparticles in the removal of H_2S. At 523 K, using the ultrasonic method and incipient wetness impregnation, SBA-15 supported zinc oxide (ZnO) nanoparticles were prepared.

Nassar and Pereira-Almao (2010) studied the adsorption of $H_2S(g)$ into different in situ prepared colloidal metal oxides in oil and matrix under recovery conditions, namely, ZnO, CuO, NiO, and Al_2O_3 at the temperature range of 25 to 200 °C. They studied in an oil sand-packed bed column at 200 mg H_2S L^{-1} and gas flow rate of 110 mL min^{-1} and concluded that there is an increase in the adsorption efficiency of ZnO with an increase in temperature.

Habibi et al. (2010) fabricated nano-ZnO sample with a rod-like morphology and comparatively studied together with a nano-spherical ZnO sample under feed gas concentration ranged between 5000-10000 mg H_2S L^{-1} and flow rate of 1100 mL min^{-1}. Results indicated breakthrough adsorption capacity also decreases with decreased in temperature (250 to 150 °C).

Awume et al. (2017) studied that adsorption of H_2S by ZnO nanoparticles in the feed gas concentration (80-1700 mg L^{-1}), nanoparticle size (18, 80-200 nm), gas flow rate (200 and 450 mL min^{-1}) and temperature (1-41°C). It was found that the adsorption rate and capacities increased with increases of H_2S concentration and the effect was more noticeable for the lower concentration. The increase of gas flow rate shortened the residence time and led to lower adsorption capacities. They concluded that the equilibrium adsorption capacity was not affected by the change of temperature in the range 1 to 22 °C but increased marginally when the temperature increased to 41 °C.

2.8 Knowledge gap and objectives of the research

Hazardous gas treatment techniques including diet manipulation, oil sprinkling and biofiltration have been applied to mitigate hazardous gas emission in swine production facilities. In recent years, nanotechnology has been applied for capturing of hazardous gases like H_2S and NH_3 and has shown promising results. However, most of the earlier research has focused on the removal of individual NH_3 or H_2S and simultaneous removal of NH_3 and H_2S have not been investigated as

part of the earlier research. This is important that as in practical situations such as livestock operations hazardous emissions include both NH_3 and H_2S. Therefore, in this work, simultaneous removal of H_2S and NH_3 was investigated using a binary nanoparticle adsorbent comprised of ZnO and TiO_2 nanoparticles.

The primary goal of this project was to develop a treatment approach whereby nanomaterials were used to remove NH_3 and H_2S simultaneously from the contaminated air streams, especially those emitted from swine production facilities. The specific objectives of this research were:

1. To determine the effects of NH_3 and H_2S concentrations and temperature on adsorption process using pre-mixed gases in a laboratory scale system.
2. To develop the adsorption isotherms and identify a suitable expression to describe the results.
3. To do a preliminary characterization of unused and exposed nanoparticles.
4. To use a semi-pilot scale system to evaluate the effectiveness of the developed approach in the treatment of gases emitted from stored swine manure.

CHAPTER 3
MATERIALS AND METHODS

3.1 Chemicals and gases

ZnO (99%), and TiO_2 (99.5%) nanoparticles were obtained from US Research Nanomaterials Inc. The average particle size of TiO_2 was 40 nm, and ZnO had a size range of 35-45 nm. Two premixed gases one containing 1000 ppmv ammonia balanced with helium and the other containing 1000 ppmv hydrogen sulfide balanced with helium were obtained from Praxair and used to prepare gas mixtures with the desired ammonia and hydrogen sulfide concentrations. These gases were used to evaluate the adsorption of NH_3 and H_2S on nanoparticles and the effects of operating conditions on adsorption in the laboratory-scale system.

3.2 Design of experiments

Design of experiments for laboratory scale experiments was done using Taguchi methods (Minitab version 18). It is a suitable method because it allows the experimenter to observe the variance of certain parameters during an experiment. This means it can be used to analyze how several factors in the experiments affect the output parameter. Its main advantage is to allow an understanding to be gained in the relationship between factor and parameter, or input and output. An orthogonal array allows an equal assessment of each factor through a specific Design of Experiment (DOE). Using this method allows the experimenter to cut down the number of required experiments required. Variables were chosen as concentration and temperature while levels were range of temperature and concentrations of gases. Table 3.1 shows the design of experiments table in which the total number of experiments in the laboratory scale experiments were 24 (6 x 4 = 24). In addition to these experiments, also some control experiments and repeats were done.

Table 3.1. Orthogonal array for DOE with Taguchi Method.

Level	Variable 1	Variable 2	
	Concentration(ppmv) (NH$_3$/ H$_2$S)	Temperature (°C)	Flow rate (mL min $^{-1}$)
1	50-50	22	100
2	100-100	70	
3	200-200	140	
4	300-300	280	
5	400-400		
6	500-550		

3.3 Laboratory scale experiments
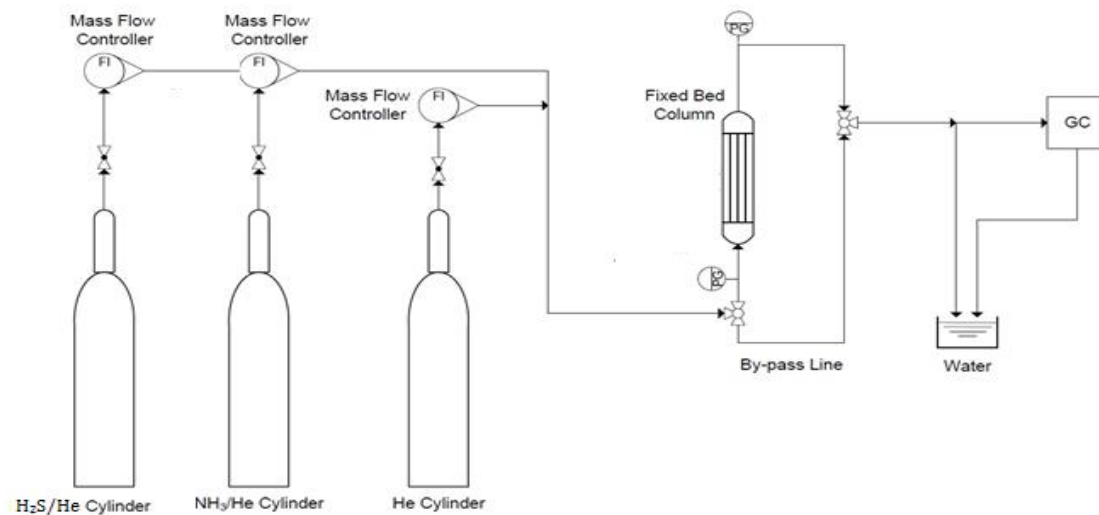
3.3.1 Experimental set-up

The apparatus used for the laboratory experiments included the following: a glass adsorption column, mass flow meters (Aalborg, US), Tygon tubing, sampling ports, differential pressure transducer (Honeywell, US), thermocouple (Omega K type, Stamford, USA) and a glass bottle containing scrubber solution (1 M NaOH solution). The adsorption column was a Pyrex glass tube with 29.5 cm length and 10 mm inside diameter. Two pressure gauges were located at the inlet and outlet of the column to measure the pressure drop across the column.

The schematic diagram and photograph of the experimental setup are shown in Figure 3.1 (Awume et al. 2017). Packed bed column was used to conduct laboratory scale experiments in continuous mode. The column was located inside a walking fume hood. The premixed gases (1000 ppmv NH$_3$-balanced He and 1000 ppmv H$_2$S – balanced He) were diluted with helium to achieve desired ammonia and hydrogen sulfide concentrations in the range 50-550 ppmv through an adsorption column packed with the designated adsorbent (0.2 g) to generate breakthrough curves. The adsorbent consisting of a layer of ZnO and silicon carbide and another layer TiO$_2$ and silicon

carbide. The outlet of the adsorption column was directed to an online gas chromatograph (GC) to measure the concentration of NH$_3$ and H$_2$S. To prevent choking of the flow during the GC injections, a bleed line was devised at the outlet of the column. The empty space of the column was filled with glass beads to prevent expansion of the bed and to assist with mixing and heating of the incoming gas.

The outlets from the GC and the bleed line were passed through sodium hydroxide solution (1 M) to capture any residual NH$_3$ and H$_2$S from the gas stream. Tygon tubing was used to connect the various components of the system. Flow rates of ammonia, hydrogen sulfide, and helium were set using three mass flow controllers (Model GFC17, Aalborg Instruments, and Controls).

The temperature of the column was controlled at the desired level with an accuracy of ± 0.1 $^\circ$C using a heating tape (HTS/Amptek Co.) connected to an Omega CN 7500 controller. All connecting tube lines were stainless steel to prevent adsorption of ammonia and hydrogen sulfide in the tubes. Helium gas was used to test the system for leakages before each experiment. For safety purposes, the system was installed inside a walking fume hood, and a personal H$_2$S and NH$_3$ monitor was used by the researchers while carrying out the experiments.

(A)
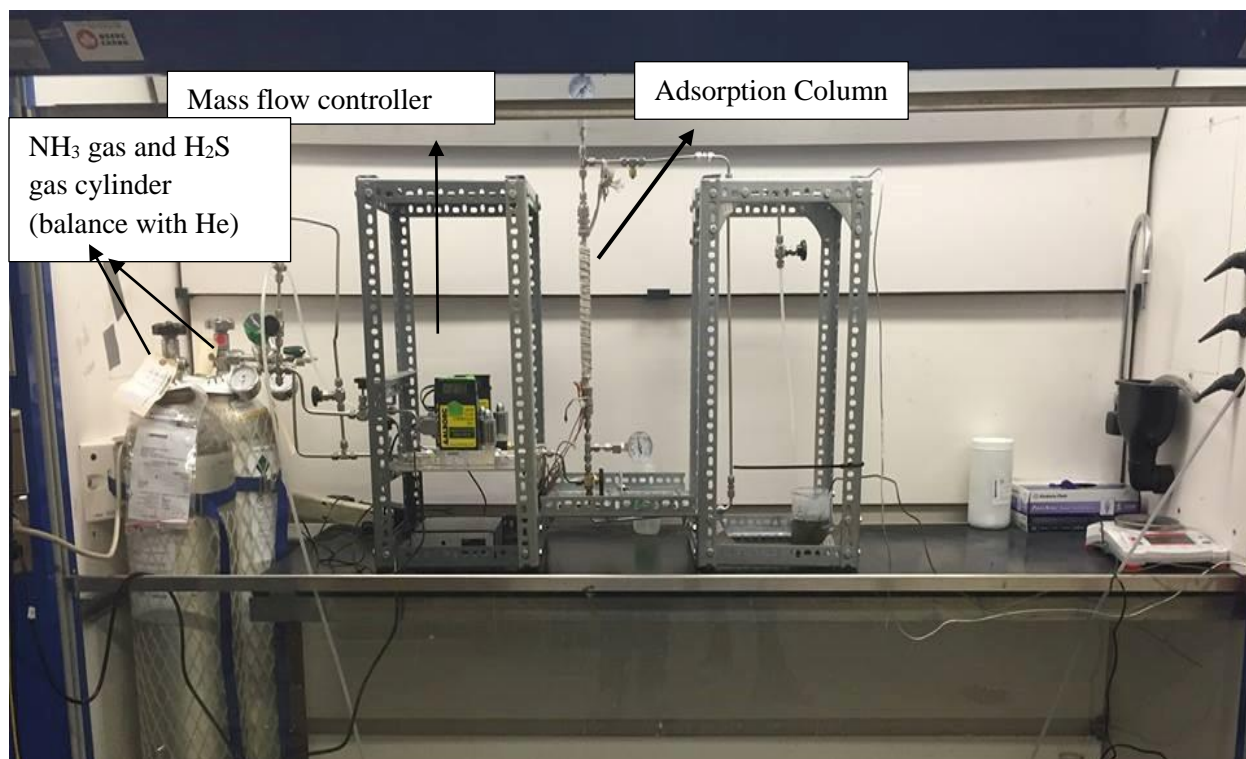
(B)

Figure 3.1. Schematic diagram (A) and photograph (B) of the experimental setup.

3.3.2 Experimental procedures

A series of laboratory scale experiments were conducted to investigate the simultaneous adsorption of NH_3 and H_2S gas on nanoparticles. Effect of feed gas concentrations and temperatures as described in detail in the latter parts were investigated. The premixed gas (1000 ppmv NH_3 and 1000 ppmv H_2S both balanced with helium) were diluted with helium to achieve desired concentrations of H_2S and NH_3.

In a typical experimental run, 0.2 g of ZnO nanoparticles (H_2S adsorbent) mixed with 0.8 g of silicon carbide mesh size 120 (125 microns); and 0.2 g TiO_2 nanoparticles (NH_3 adsorbent) mixed with 0.8 g of silicon carbide were loaded into the column in bilayer form (ZnO nanoparticles as first layer and TiO_2 nanoparticles as second layer). Silicon carbide was used to increase the depth of the bed and to prevent channeling of the flow through the packed bed (Rezaei et al. 2017). It was also chosen because it does not absorb NH_3 and H_2S based on control experiments.

Between two layers of adsorbent, a thin layer of glass wool was placed. The remaining space of the column was filled with glass beads. Before starting the adsorption experiments, all the lines and the column were flushed with helium to remove air from the system.

The adsorption of ammonia and hydrogen sulfide from the gas mixture with designated concentrations at a specified flow rate was then started and continued until the equilibrium state was reached (i.e., outlet concentration reached approximately 95% of the inlet concentration).

Experiments to evaluate the effects of NH_3 and H_2S concentrations were conducted by varying NH_3 and H_2S concentrations within the range of 50 to 500 ppmv of each gas in the mixture (i.e., NH_3-H_2S concentrations: 50-50, 100-100, 200-200, 300-300, 400-400, 500-550 ppmv, respectively). Experiments with all indicated concentrations were carried out at temperature 22, 70, 140 and 280°C to investigate the effect of temperature on simultaneous NH_3 and H_2S adsorption. Various temperature and concentration range are chosen as lower temperature range used to address the situation in the livestock and higher temperature range used in an industry setting. Also, the earlier works (Awume et al. 2017 and Rezaei et., 2017) were in the higher

temperature range. To compare results obtained from individual ZnO and TiO$_2$, above concentration and temperature range were used.

The gas flow rate was kept constant at 100±0.2 mL min^{-1} (Rezaei et al. 2017). Adsorption capacities were calculated from the integration of breakthrough curves and expressed as mg of NH$_3$ or H$_2$S per g of adsorbent. The breakthrough point is defined as the time where ammonia and hydrogen sulfide concentration in the outlet was approximately 5% of the inlet concentration.

In an additional experimental run, the layers of nanoparticles were reversed (i.e., TiO$_2$ as the first layer and ZnO as the second layer) to see the effect of orientation on adsorption capacity. The gas concentrations were 500 ppmv NH$_3$ and 550 ppmv H$_2$S, the gas flow rate and temperature were set at 100±0.2 mL min^{-1} and 22 °C respectively. The amount of nanoparticles and silicon carbide were similar to previous runs. To assess the effect of adsorbents homogeneity (instead of separate layers), both nanoparticles (ZnO and TiO$_2$) along with silicon carbide were mixed and loaded as one layer in adsorption column for the experimental run of 500 ppmv of NH$_3$ and 550 ppmv of H$_2$S.

The breakthrough curves were generated by plotting C/C$_o$ versus time, where C represents the effluent gas concentration (mg L^{-1}) and C$_o$ represents the influent gas concentration in the feed stream. The breakthrough point was defined as the point where the ratio of the NH$_3$ or H$_2$S level in the effluent and that of the influent was approximately 0.05 (Guo et al. 2007).

The breakthrough adsorption capacity was calculated using the experimental data from the start of the experiment to the breakthrough time. The bed was said to have reached a saturation point when effluent gas concentration stabilized, and thus system reached an equilibrium state. The equilibrium adsorptive capacity was calculated using the experimental data from the initiation of the experiment to the equilibrium point.

3.3.3. Adsorption kinetics and isotherms

The experimental data were used to identify suitable adsorption isotherms (Equations 2.5, 2.6 and 2.7) describing the adsorption of NH_3 and H_2S on ZnO/TiO_2 nanoparticles in the mixture of gases (NH_3 and H_2S). The isotherms were generated by plotting the amount of NH_3, or H_2S adsorbed versus gas phase NH_3 or H_2S concentrations at different temperatures.

Experimental data were fitted non-isothermally into each model, and the values of parameters were determined using lsqnonlin optimization function in MATLAB R2006a to minimize the sum of squares of differences between the experimental and calculated equilibrium adsorption capacities. The coefficient of determination (R^2) and Fisher coefficient (F_c), defined by Equations 3.1 and 3.2, respectively, were used to identify the most suitable model (Brown, 2001; Froment et al. 2011):

$$R^2 = 1 - \frac{\sum_i \sum_j (q_{exp,ij} - q_{cal,ij})^2}{\sum_i \sum_j (q_{exp,ij} - q_{mean})^2} \tag{3.1}$$

$$F_c = \frac{\sum_i \sum_j \frac{\left(q_{cal,ij}\right)^2}{NP}}{\sum_i \sum_j \frac{\left(q_{exp,ij} - q_{mean}\right)^2}{DF}} \tag{3.2}$$

where q_{exp} and q_{cal} are the experimental and calculated equilibrium adsorption capacities, respectively and q_{mean} is the average value of experimental equilibrium adsorption capacities. Finally, i refers to i^{th} temperature level (5, 70, 140, and 280 °C) and j refers to j^{th} ammonia partial pressure (0.005, 0.010, 0.020, 0.030, 0.051 kPa) at temperature level i. NP is the number of fitting parameters, and DF is the degrees of freedom (i.e., the difference between the number of experimental data points and the number of fitting parameters).

Calculation of equilibrium adsorption capacity which was done by integration is described in detail in Appendices C and using equation C.1.

**3.4 Semi pilot scale trials with representative gases**

3.4.1 Experimental setup

Experiments were conducted using gases emitted from swine manure stored in containers to simulate the actual conditions in the swine barn and to assess the performance of adsorbent in the removal of NH_3 and H_2S from manure gas. The manure slurry samples were collected from the under-floor manure pit of a grow-finish room at the swine barn at the Prairie Swine Centre Inc. (SK, Canada). Grow-finish rooms house the pigs at the grow-finish production stage (about 14-16 weeks after nursery until they reach a market weight of 115-120 kg). Before collection of the manure samples, the manure in the pit was mixed thoroughly using a mechanical agitator to minimize manure variation in the collected samples. After mixing, twelve clean 65-L containers were each filled with 30 L of manure slurry. The containers were covered and stored for 6-7 weeks at 20 °C to allow sufficient time for anaerobic digestion and production of manure gases (Zhang et al. 1990; Awume et al. 2017).

Experimental setup consists of centrifugal fan (Model Keho, Edwards's group, Lethbridge, AB), filter pad (Model HPE30651 Electrostatic hammock filter pad, True Blue company, Indiana, USA), PVC adsorption column thermal anemometer (VelociCalc 9545-A, TSI Inc., Shoreview, MN, USA), ammonia and hydrogen sulfide sensors, rubber tubing and galvanized ducts. For adsorption column, clear cylinder PVC tubing 7.5 cm internal diameter and length of 25 cm was used. Centrifugal pump generated the flow of gases from manure containers through an adsorption column. Metallic mesh filter material with glass wool and filter material was placed at the top of the column, while a layer of filter material was placed in the bottom of the column.

About 34.25 gram of TiO_2 (40 nm size) was placed at the top of the layer, and about 34.25 gram of ZnO (35-45 nm size) was placed the bottom of the column (Awume et al. 2017). Then the column was filled with spherical beads. The bed depth was 2.54 cm. The column was connected to the manure containers using 10 cm flexible rubber tubing and to the centrifugal fan using 10 cm galvanized ducts.

Two gas monitoring sensors (ammonia and hydrogen sulfide) were installed before and after the adsorption column to analyze influent and effluent gas samples concentrations. The gas flow rate was controlled and set to 27 L s^{-1} in the pre-run to make sure the nanoparticles were fluidized, using damper at the exhaust of the centrifugal fan and with vents installed on the galvanized duct upstream of the fan (Awume et al. 2017). A thermal anemometer was used to measure the gas flow rate. The manure containers had a cover with an outlet connected to the adsorption column by the flexible rubber tubing. A stirrer was also fixed at the top of the container to agitate the manure during the tests. Figure 3.2 shows the schematic diagram and picture of the setup (Awume et al. 2017).
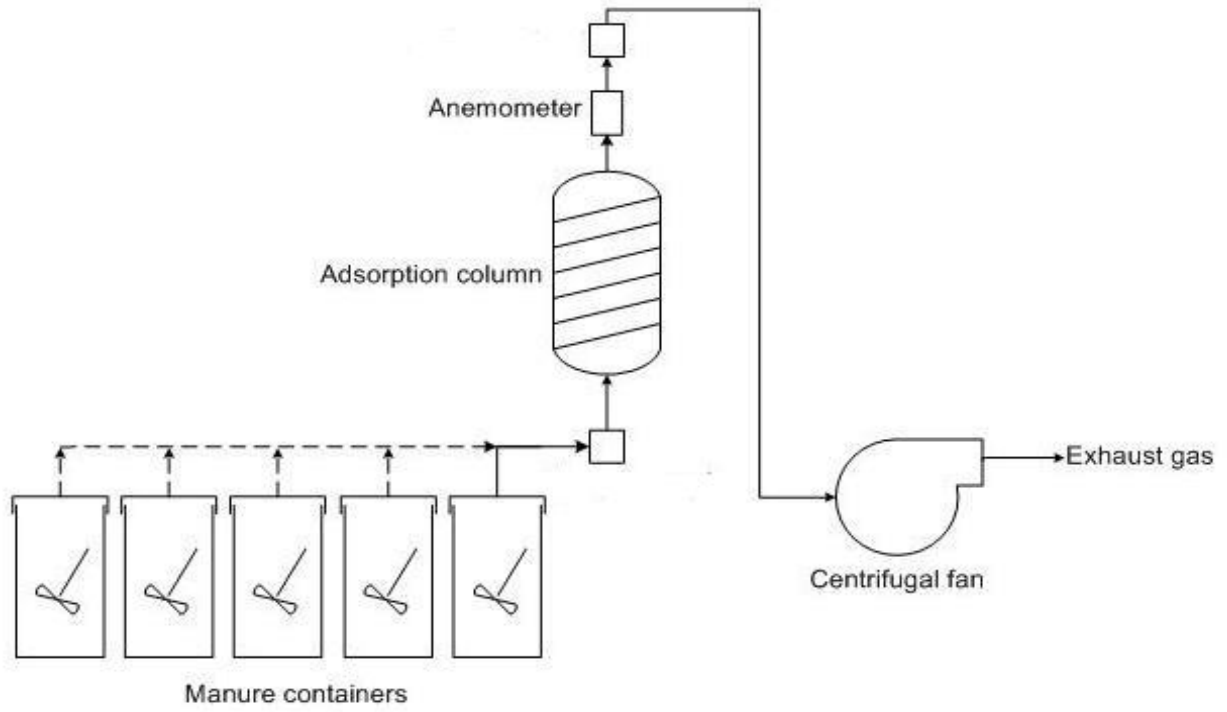
(A)
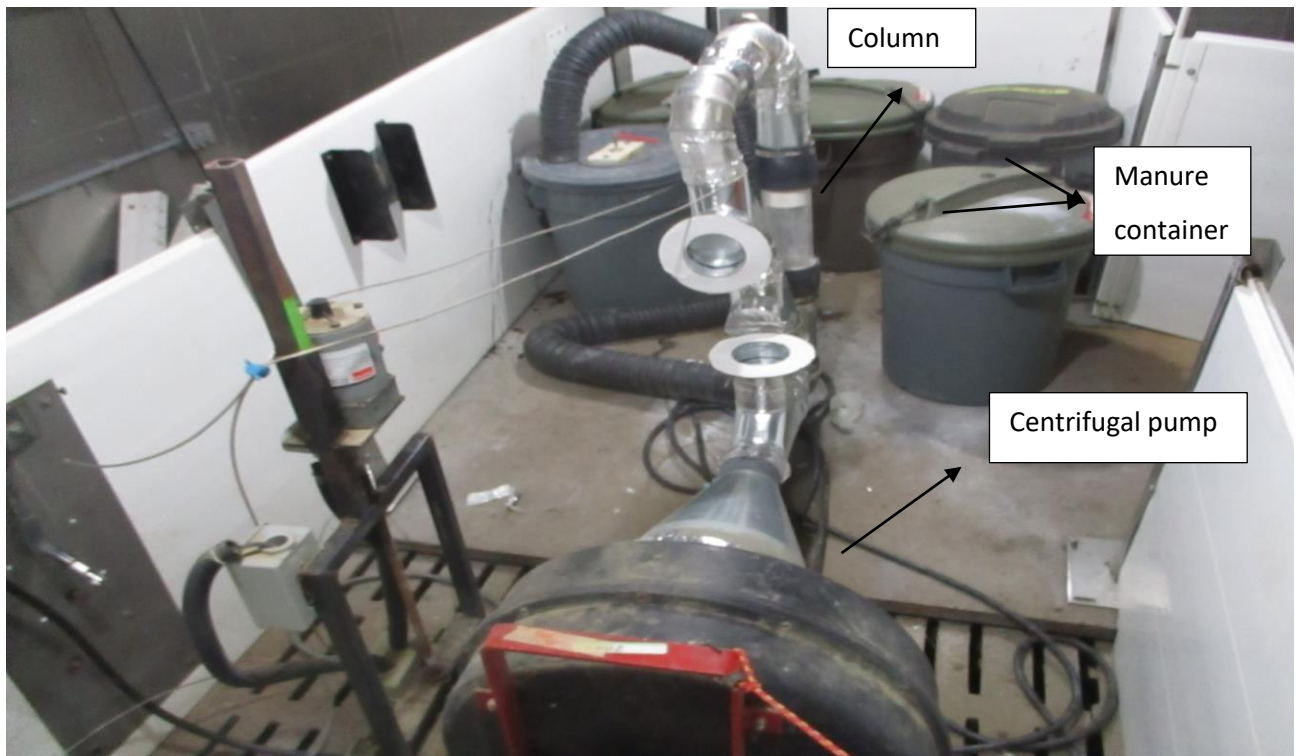
(B)

Figure 3.2. Schematic diagram (A) and photograph (B) of semi-pilot adsorption experimental set up.

3.4.2 Experimental procedure

The manure in swine barns contains many gases including ammonia and hydrogen sulfide. To stimulate emission of these gases, manure was agitated during manure pit drainage, and high gas concentrations were generated for relatively short periods. This was achieved using 12 containers partially filled with the swine manure. The ten containers were used to generate manure gas for approximately 100 minutes (20 minutes for each manure container). The other two manure containers were used to run control tests without nanoparticles to check for potential adsorption by any part of the set-up. The required gas stream was generated using five manure containers (in the first run of experiments) in sequence whereby each container provided the representative gas for 20 min (five cycles). In each cycle, a manure container was agitated intermittently (2 min agitation at 5 min intervals) during which centrifugal fan withdrew the headspace gas and passed it through the adsorption column. Following this, the next container was connected to the feed line, and the cycle was repeated.

A total of five runs was done for reproducibility of results. The centrifugal fan was started immediately after agitation of the first container and provided a gas flow rate of 27 L s^{-1}. Based on blank tests, this flow rate was sufficient to fluidize the nanoparticles without carryover.

Prior to the start of the run, clean air was used to test the system for leakages before and after loading the column. The samples were analyzed by ammonia and hydrogen sulfide gas sensors at both the influent and effluent where the sensors were installed.

A second experimental run was conducted after one week to assess the reproducibility of the results obtained in the first test. In this test, five new manure containers were used to generate manure gas (approximately 30 minutes from each container).

The same amount of nanoparticles were used. About 34.25 gram of TiO_2 (40 nm size) and 34.25 gram of ZnO (35-45 nm size) unused nanoparticles were used.

The five manure containers were used in sequence whereby each container provided the representative gas for 30 min (five cycles). In each cycle, a manure container was agitated intermittently (1 min agitation at 5 min intervals) during which centrifugal fan withdrew the headspace gas and passed it through the adsorption column. After the 30-minute period, the flexible tubing connection was moved to the next manure container, and the same procedure was repeated. The experimental procedure was carried out in the same way as the first experimental run. The manure was agitated for 1 minute before gas samples were taken to generate a measurable amount of NH_3 and H_2S.

3.5 Analytical techniques

In the laboratory scale experiments, ammonia and hydrogen sulfide concentrations were measured by an online gas chromatograph (Varian Gas Chromatograph 3800) with a thermal conductivity detector (TCD) connected to a CP-Pora PLOT Amines column (Agilent Technologies, CP7591). The GC oven temperature was set at 100 $^{\circ}$C, and TCD filament at 250 °C and the column flow rate was maintained at 8 mL min^{-1} with a split ratio of 1. GC was recalibrated if the error in the measured concentration of the calibration gas was more than 10%.

Ammonia and hydrogen sulfide concentrations in semi pilot-scale experiments were determined by an ammonia and hydrogen sulfide analyzer (Drager Pac 7000, Germany). The detection limit for hydrogen sulfide and ammonia sensors was 300 ppmv, with gas readings recorded at every 10 seconds. Both analyzers were calibrated using zero and span gases prior to their use in the experiment.

The characterization of unused and exposed nanoparticles was done by CHNS and TGA (Thermogravimetric analysis) to understand the nature of adsorbed species. These characterization techniques were chosen because Thermalgravimetric analysis (TGA) is a method of thermal analysis in which the mass of a sample is measured over time as the temperature changes while CHNS analysis reveals the surface attachment of adsorbed species.

The saturated adsorbents (ZnO and TiO_2) were obtained in an experimental run with 500 ppmv NH_3-550 ppmv H_2S at a gas flow rate of 100 mL min^{-1}. The quantity of adsorbent was 0.2 g and experiments were conducted at room temperature. Samples for TGA and CHNS were saturated with ammonia and hydrogen sulfide at room temperature. Saturated samples were carefully transferred to ait tight glass tube without silicon carbide. The weight percent of nitrogen on the saturated samples was determined using a CHNS analyzer (Vario EL III, Elementar Americans Inc, USA). Thermogravimetric analysis (TGA) was performed on the exposed adsorbents using a Q500 thermogravimetric analyzer (TA Instruments) to a temperature range of 22 to 800 °C with a ramping rate of 7 - 10 °C min^{-1} was used.

# CHAPTER 4
RESULTS AND DISCUSSION

4.1. Laboratory scale experiments

To study the effects of feed concentration and temperature on NH_3 and H_2S adsorption on ZnO and TiO_2 nanoparticles in the mixture of gases (NH_3 and H_2S), breakthrough curves were generated by plotting concentration versus time (where C is effluent concentration, and C_o is influent). Breakthrough curves are shown in Figures 4.1 to 4.4. These breakthrough curves were generated by experiments done in the laboratory scale. The slope of the breakthrough curves is representative and proportional to how fast the adsorbent reaches saturation state. The adsorbent reaches saturation state in relatively less time was indicated by a steeper curve.

4.1.1 Effects of gas concentration and temperature

The effect of temperature on adsorption was studied. Simultaneous removal of NH_3 and H_2S at concentrations of 50-50, 100-100, 200-200, 300-300, 400-400, 500-550 ppmv by ZnO and TiO_2 nanoparticles was investigated at a gas flow rate of 100 ± 0.2 mL min^{-1}. These experiments were run at 22, 70, 140 and 280 °C. Figures 4.1, 4.2, 4.3 and 4.4 show the breakthrough curves at different temperatures.

When the temperature is increased from 22 °C to 70 °C and 140 °C and maximum to 280 °C, there was a slight change in equilibrium capacities for ammonia. It can be seen in Figure 4.1 that the slope of the breakthrough curve at 50 ppmv is slanted to the right potentially due to the low ammonia mass transfer rate from the gas phase to the surface of adsorbents (i.e., small driving force). By increasing the concentration to 100 ppmv, the slope of the breakthrough curves increased, indicating the enhancement of the mass transfer rate during the adsorption process but further increase of concentration from 100 to 500 ppmv did not affect the slope. This could be interpreted as an increase in adsorption rate or the rate by which nanoparticles reached their saturation state was higher from 50 ppmv to 100 ppmv compared to 100 ppmv to 500 ppmv of ammonia gas.
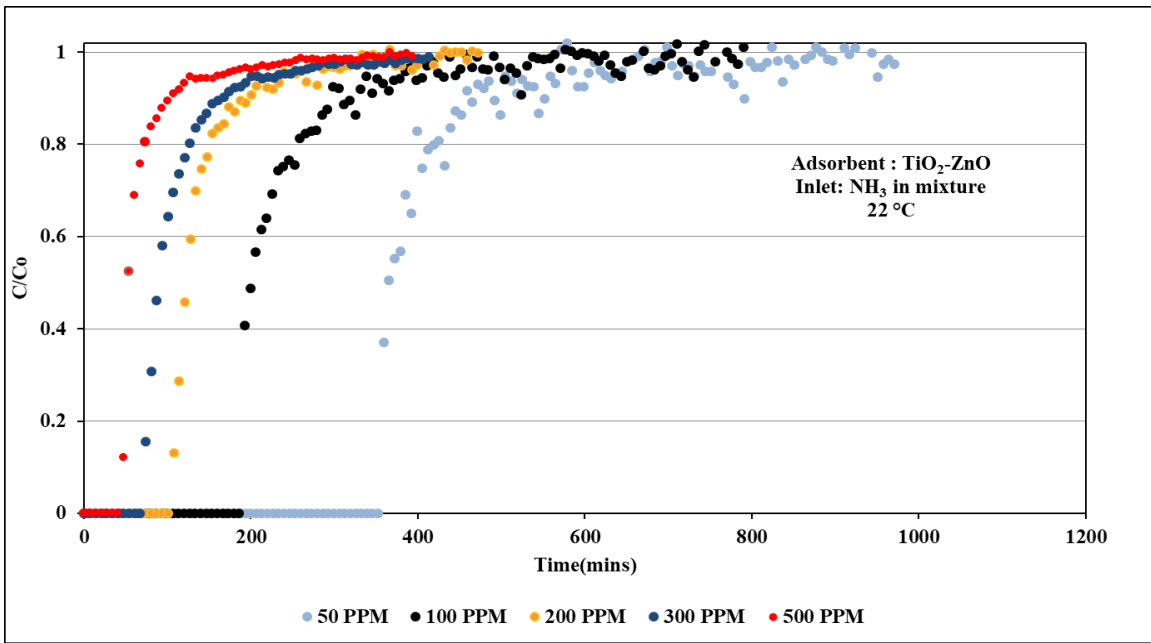
(a)
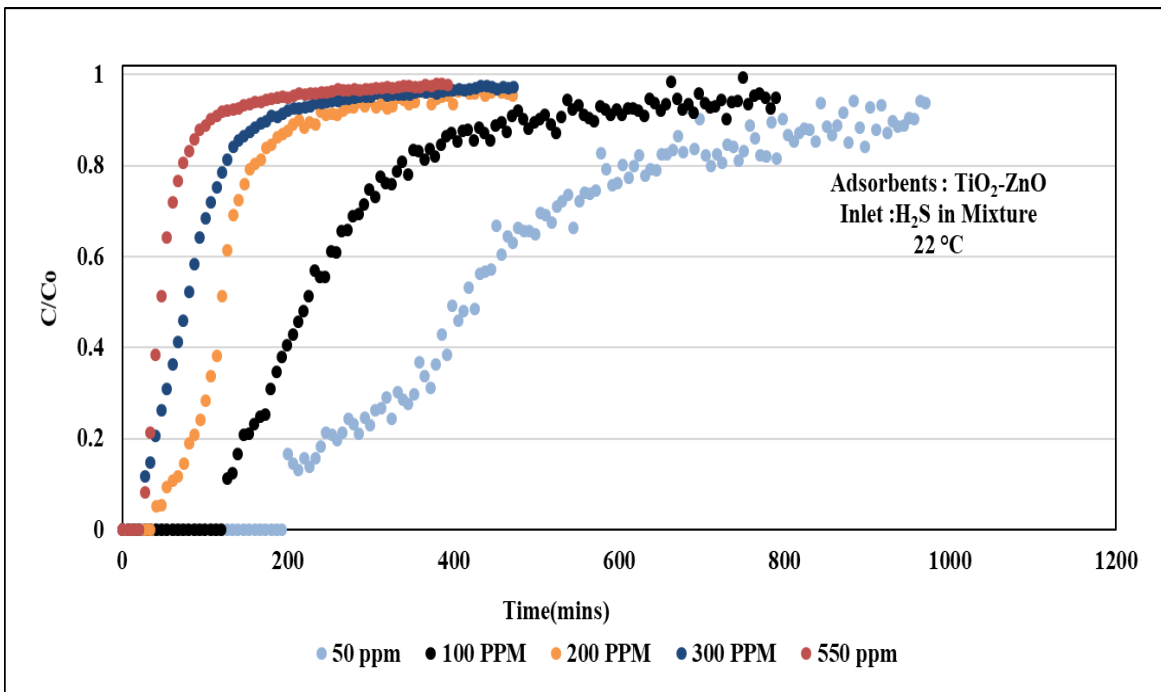
(b)

Figure 4.1. Ammonia and hydrogen sulfide breakthrough curves at 22 $^\circ$C (a) NH$_3$, (b) H$_s$S.

For hydrogen sulfide, as shown in Figure 4.1 (at 22 °C) the adsorbent reached saturation state faster as the concentration of H$_2$S in the feed stream was increased (i.e., the steepness of the slope).

When the concentration of hydrogen sulfide in the feed stream was increased from 50 to 300 ppmv, steepness of the slope increases. The higher concentration of H_2S (200, 300, 550 ppmv) has no sharp change in their slope. This could be interpreted as an increase in adsorption rate or the rate by which nanoparticles reached their saturation state (Simo et al. 2009). Experiments in duplicates were done at each temperature and breakthrough curves were plotted in Appendices B.

The driving force for mass transfer along the pores is enhanced due to H_2S concentration increase, that why equilibrium is reached faster and the slope of the curve in both sets of tests was slightly steeper when the temperature was decreased.
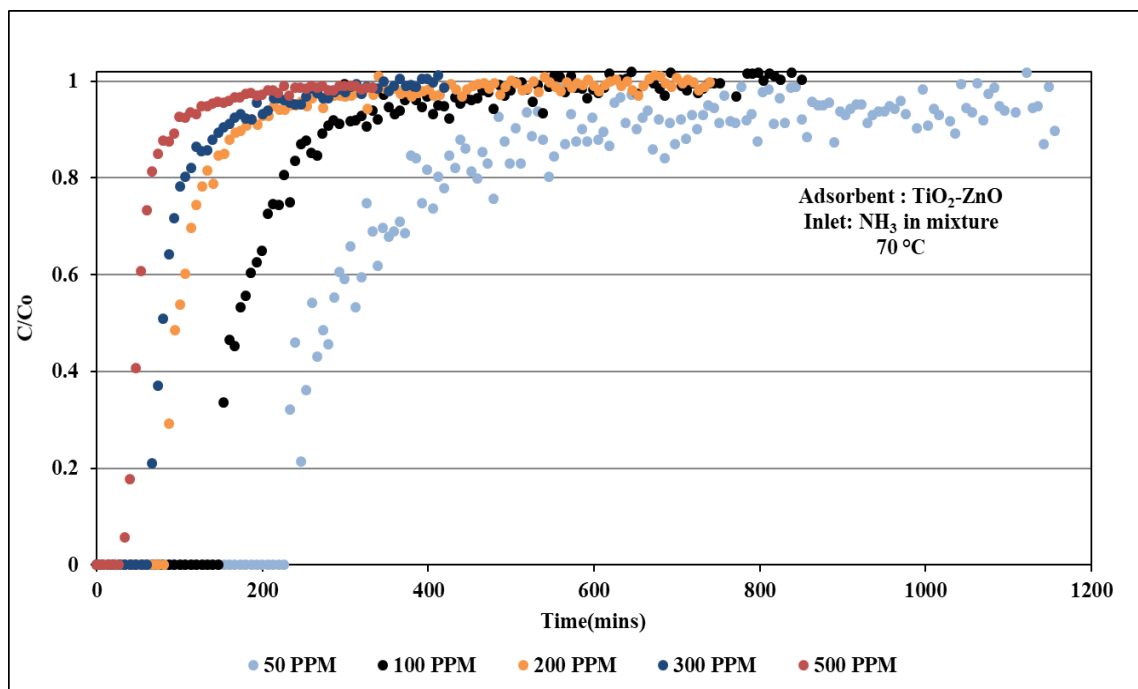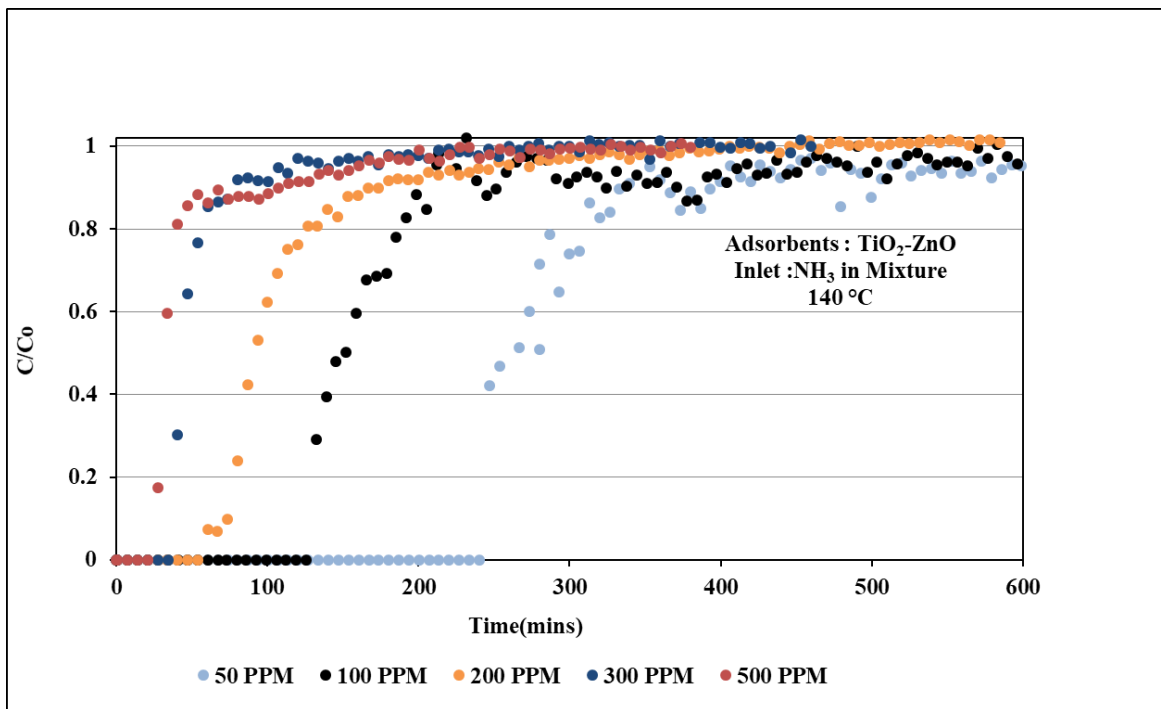
(a)
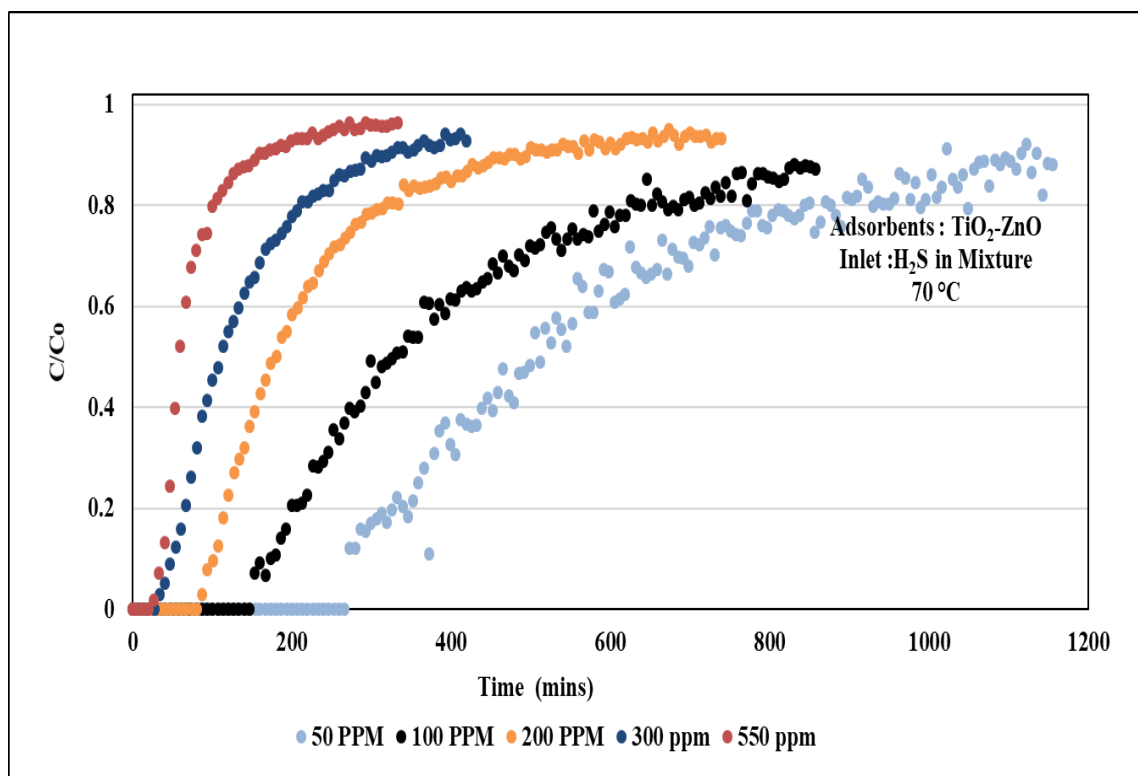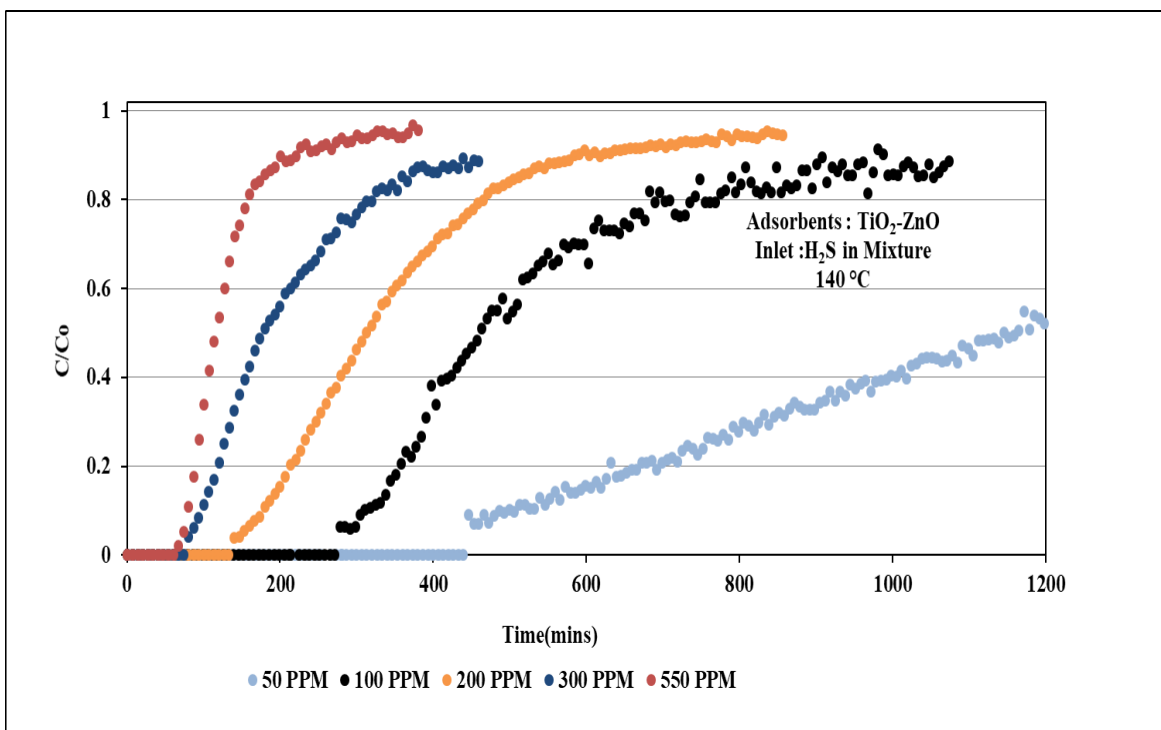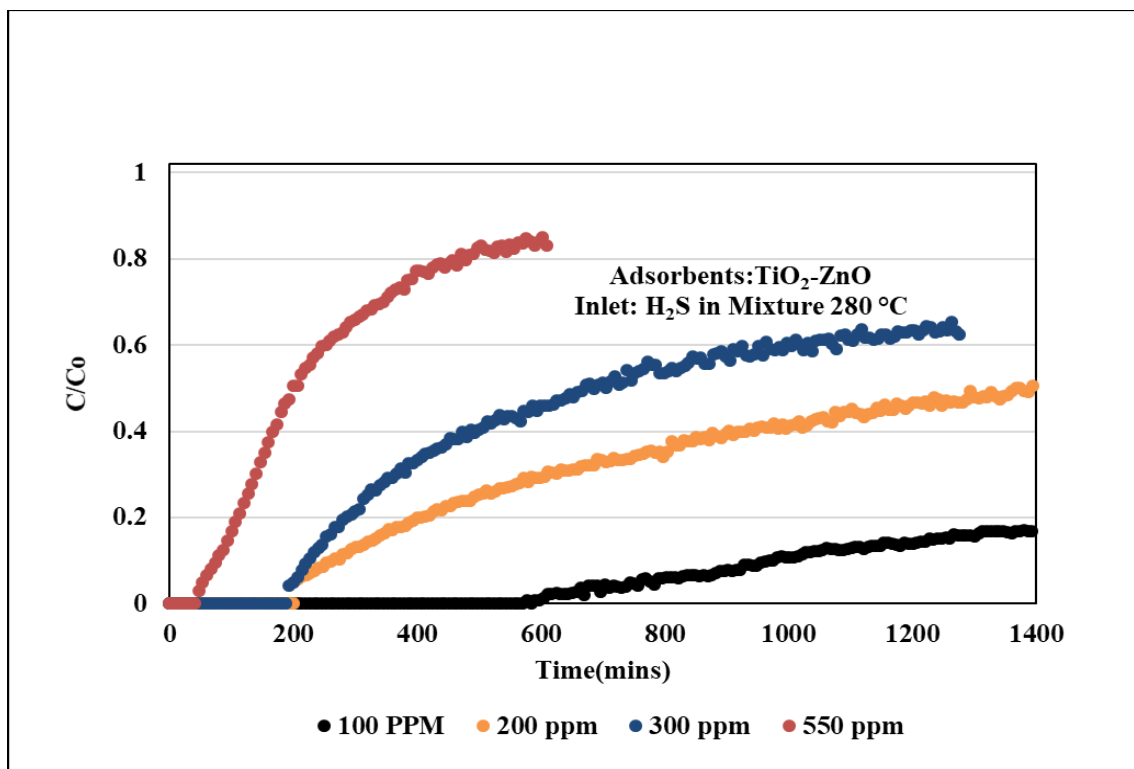

(b)

Figure 4.2. Ammonia and hydrogen sulfide breakthrough curves at 70 °C (a) NH_3, (b) H_sS.

(a)

(b)

Figure 4.3. Ammonia and hydrogen sulfide breakthrough curves at 140 $^\circ$C (a) NH_3, (b) H_sS.
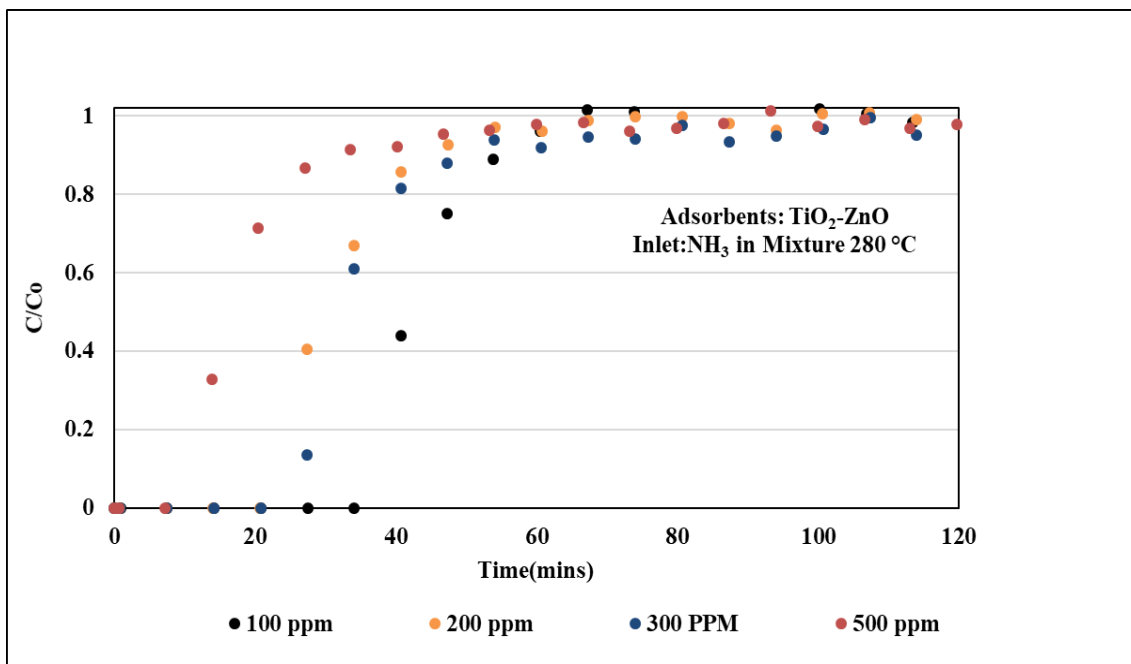
(**a**)

(**b**)

Figure 4.4. Ammonia and hydrogen sulfide breakthrough curves at 280 $^\circ$C (a) NH_3, (b) H_sS.

As shown in Figures 4.1, 4.2, 4.3 and 4.4, the slope of the curve for hydrogen sulfide in both sets of tests was slightly steeper when the temperature was decreased. There was an increase in adsorption capacities when the temperature was increased. The hydrogen sulfide adsorption capacities have been calculated and presented as adsorption isotherms micropore diffusion depends on temperature, while macropore diffusion is not affected by temperature to the same extent (Simo et al. 2009).

Also, in this laboratory scale experiments, it showed that the change in temperature did not affect the adsorption rate because the micropore mass transfer did not limit adsorption at the range of temperatures studied.

As shown in Table 4.1 and 4.2, for NH_3 and H_2S the breakthrough time decreases with increasing gas concentration (at constant temperature, i.e., 22 °C). However, the equilibrium adsorption capacities and breakthrough capacities increase with an increase in concentration. It was observed that for NH_3 as we see in Table 4.1, increase temperature decreased the equilibrium adsorption capacity. In case of H_2S, increase in temperature increases the adsorption capacity.

Table 4.1. Equilibrium adsorption capacities for NH_3 at different temperatures.

Concentration (ppmv)	Equilibrium Adsorption Capacity(mg/g)			
	22 °C	70 °C	140 °C	280 °C
50	6.98	6.37	5.42	-
100	8.06	6.86	6.15	0
200	9.67	8.32	7.32	0.77
300	10.94	10.77	5.70	2.99
500	12.00	11.64	8.41	3.49

Increasing temperature decreases breakthrough capacities for NH_3. At 500 ppmv NH_3 the breakthrough capacity was 7.51 mg g^{-1} at 22 $^{\circ}$C which decreased to 5.68 mg g^{-1} at 70 $^{\circ}$C and 3.94 mg g^{-1} at 140 $^{\circ}$C. It further decreased to 1.45 mg g^{-1} when the temperature was increased to 280 $^{\circ}$C.

Table 4.2. Equilibrium adsorption capacities for H_2S at different temperatures.

Concentration (ppmv)	Equilibrium Adsorption Capacity(mg/g)			
	22 °C	70 °C	140 °C	280 °C
50	16.15	20.56	38.08	-
100	18.87	28.49	38.29	206.70
200	19.22	33.09	49.36	153.85
300	20.17	30.60	45.56	159.12
550	25.15	32.26	52.31	161.45

As we see from Table 4.2, increase in temperature increased the equilibrium adsorption capacity for hydrogen sulfide. This is all because of the higher concentration gradient; the adsorption capacities increase with concentration. Also, temperature plays a critical role to increase the rate of reaction and saturation reaches faster, so there was an increase in adsorption capacities too. In case of H_2S, C/C_o was always below 1 (mostly at higher temperature). This could be due to the chemical oxidation of H_2S in the presence of air and its conversion to other forms of sulfide such as sulphur dioxide.

For some concentration including 300 ppmv (NH_3 and H_2S) and 500 ppmv NH_3 - 550 H_2S, duplicate experiments have been done to determine the reproducibility of results (Appendices B).

Rezaei et al. (2017) reported that among the tested adsorbents (activated charcoal, MgO, CuO, MgO, TiO_2 and ZnO, commercial TiO_2 had the highest equilibrium adsorption capacity of 6.87

mg $NH_3\,g^{-1}$ followed by AC, ZnO, MgO, and CuO. The highest adsorption capacity obtained was 7.07 mg $NH_3\,g^{-1}$ at 22 °C for 500 ppmv ammonia while the lowest was 2.96 mg $NH_3\,g^{-1}$ for 50 ppmv ammonia at 280 °C. While in current work highest and lowest adsorption capacity obtained was 6.98 mg $NH_3\,g^{-1}$ at 22°C and 5.42 mg $NH_3\,g^{-1}$ at 140 °C, respectively, which matches with the previous research work on individual TiO_2 nanoparticles (40 nm) with ammonia adsorption (Rezaei et al. 2017). There was also the same trend of adsorption capacity, i.e., decreases as temperature increases in case of ammonia adsorption with TiO_2.

While in the case of individual H_2S adsorption with ZnO nanoparticles, the adsorption rate and capacities increased with increases of H_2S concentration (80-1700 ppmv) and increasing temperature increases the adsorption capacity (Awume et al. 2017). In current work also, it was observed that adsorption capacities increase with concentration and increasing temperature increases H_2S adsorption capacity.

Nassar and Pereira-Almao (2010) also reported an increase in the slope of the breakthrough curves as the temperature was increased from 25 to 200 °C when they examined the effectiveness of different metal oxides (ZnO, Al_2O_3, NiO, and CuO) on H_2S adsorption. The results obtained were promising demonstrating the capability of this material to remove H_2S and NH_3 simultaneously. Lower temperature (1- 4 °C) did not affect much in adsorption capacities for both ammonia and hydrogen sulfide (Awume et al. 2017).
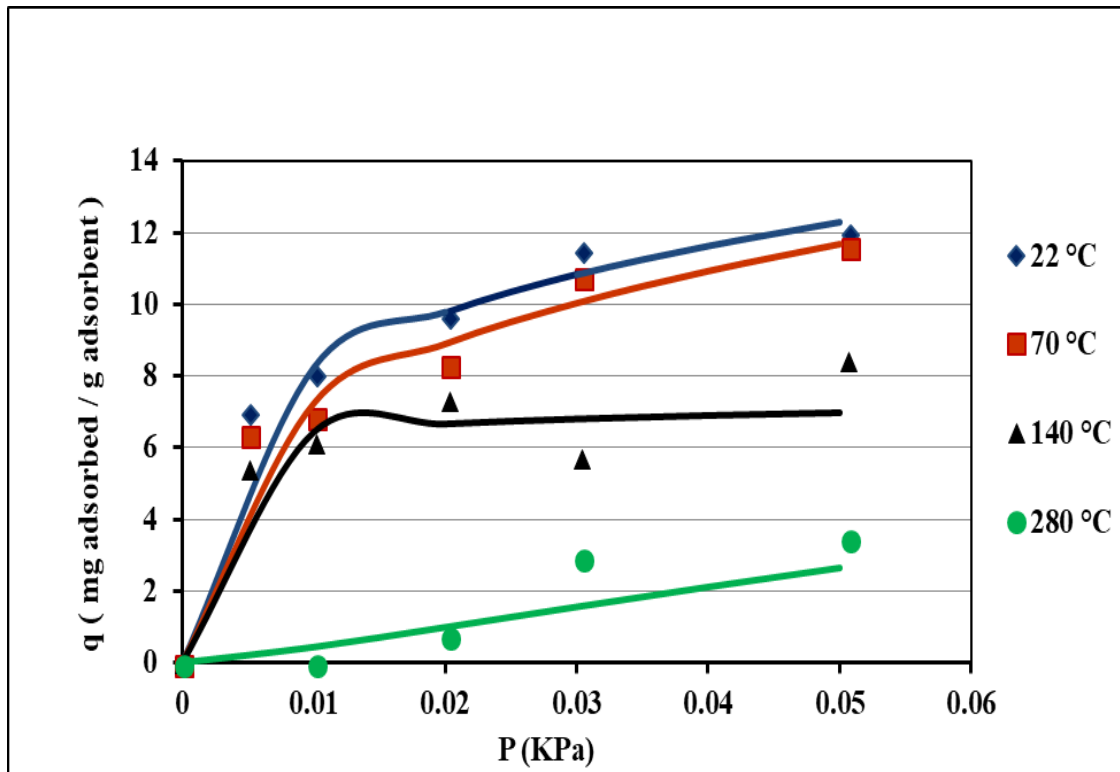
4.1.2 Adsorption isotherms

The ammonia and hydrogen sulfide adsorption capacities have been calculated and presented as adsorption isotherms for TiO_2 and ZnO nanoparticles in Figures 4.5 and 4.6. The data were modeled using Langmuir, Freundlich, and Langmuir Freundlich isotherms using Equations 2.5, 2.6 and 2.7.
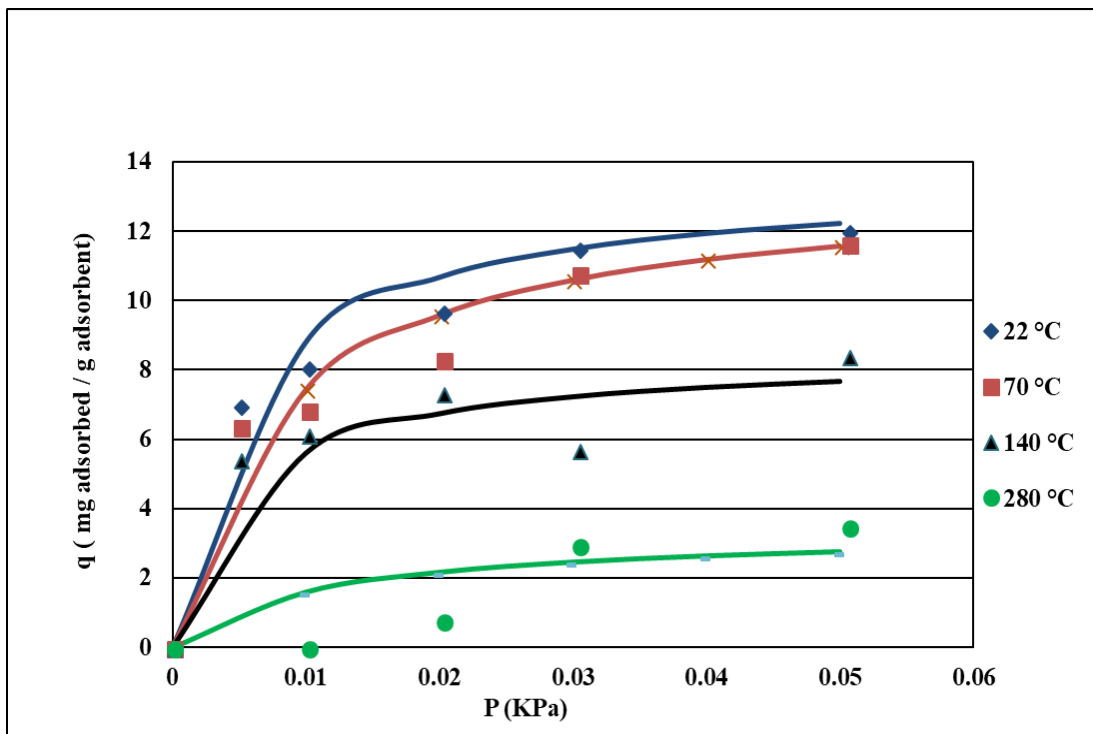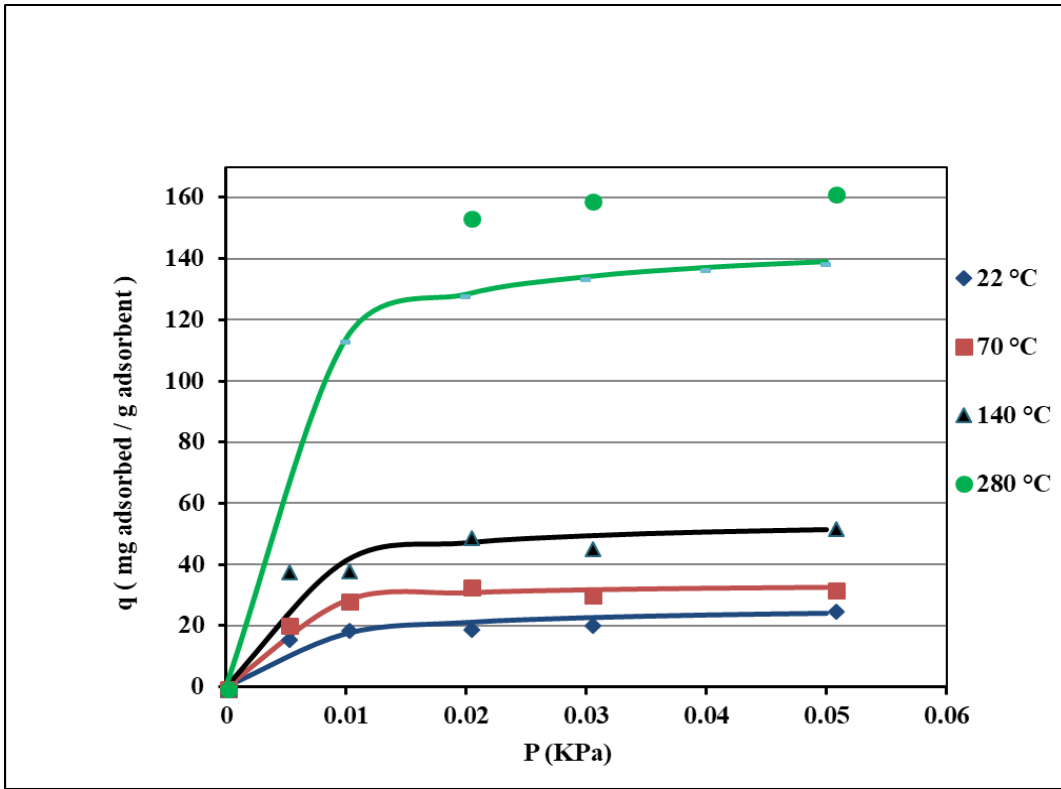
(a)
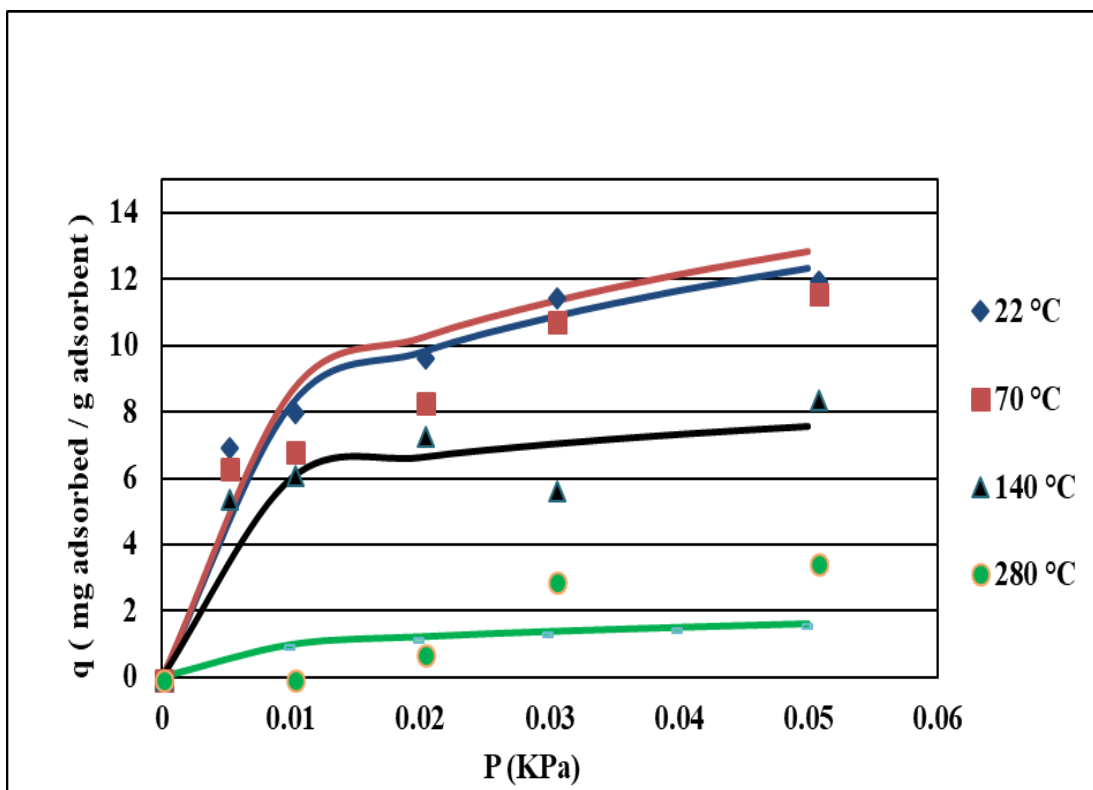
(b)

(c)

Figure 4.5. Ammonia adsorption isotherms; (a) Langmuir, (b) Freundlich, (c) Langmuir-Freundlich. Symbols are experimental data, and solid lines are model predictions.

Langmuir isotherm (Figure 4.5a) shows the experimental results with $R^2 = 0.99$. Freundlich isotherm (Figure 4.5b) did not predict the experimental equilibrium adsorption capacities accurately showing an average R^2 value of 0.74. As shown in Figure 4.5 c Langmuir-Freundlich show $R^2 = 0.99$ in the case of ammonia.
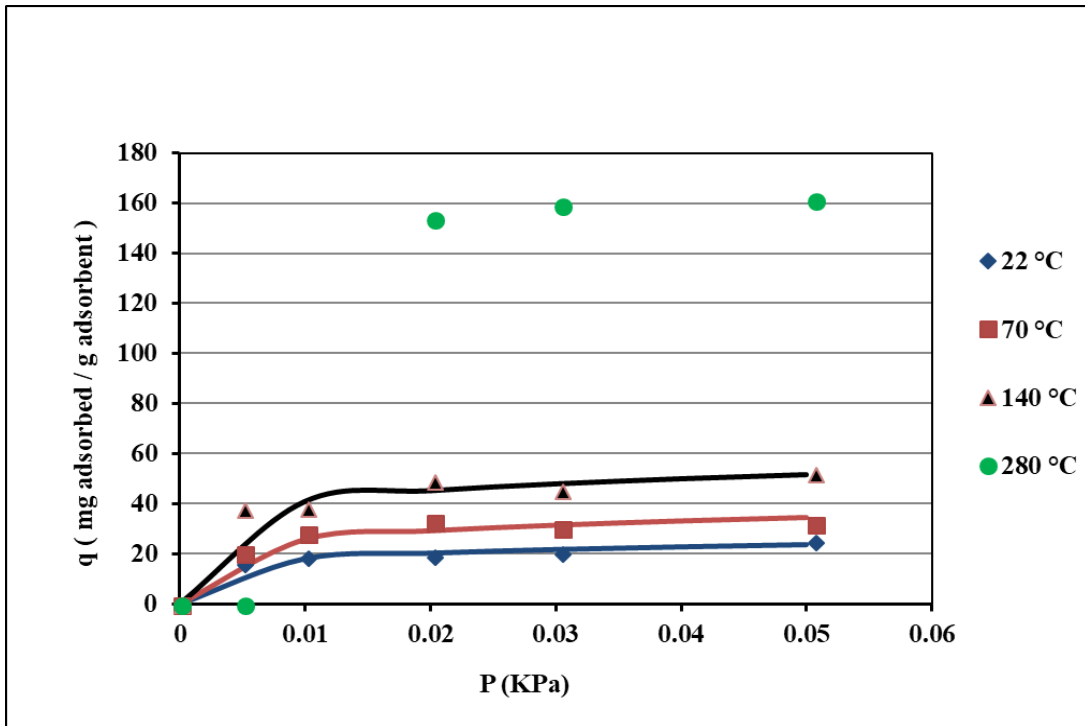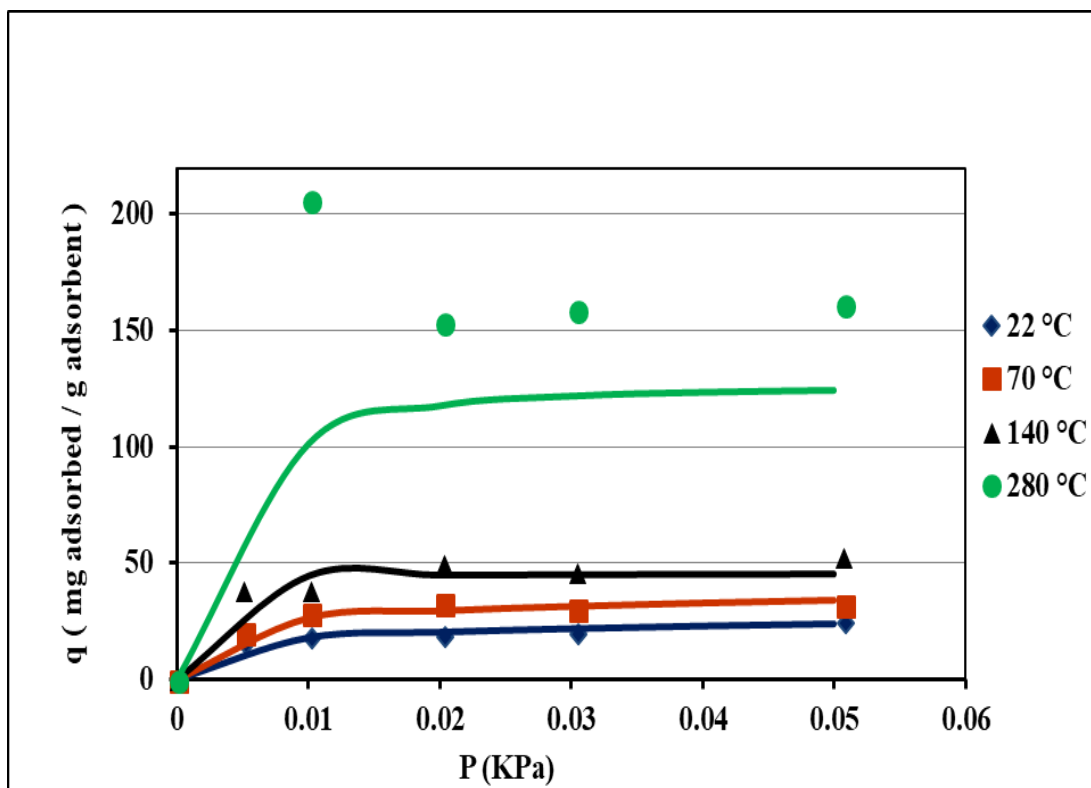
(a)

(b)

(c)

Figure 4.6. Hydrogen sulfide adsorption isotherms; (a) Langmuir, (b) Freundlich, (c) Langmuir Freundlich; Symbols are experimental results, and solid lines are model predictions.

For hydrogen sulfide, Langmuir isotherm (Figure 4.3a) did not accurately predict the experimental equilibrium adsorption as the curve did not fit the experimental data well ($R^2 = 0.91$) compared to Langmuir-Freundlich which predicted the results with higher accuracy (regression coefficient = 0.98) than Langmuir and Freundlich expressions.

The goodness of fit for each model is presented in Figures 4.5 and 4.6, and the associated constants and coefficient regression are listed in Tables 4.3 and 4.4, respectively. As ammonia adsorption capacities increase with an increase in concentration and decrease with increase in temperature.

Table 4.3. Equilibrium isotherms and associated coefficients for NH_3 adsorption on TiO_2/ZnO nanoparticles.

Isotherm model	T (˚C)	q_s (g NH_3 adsorbed g adsorbent^{-1})	K (B)	n	R^2
Langmuir	22	26.80	33.91	-	0.99
	70	26.60	75.00	-	0.98
	140	8.00	311.75	-	0.48
	280	3.00	166.20	-	0.34
Freundlich	22	-	26.14	3.97	0.97
	70	-	27.03	4.02	0.93
	140	-	11.67	6.91	0.51
	280	-	15.81	1.72	0.56
Langmuir-Freundlich	22	5.93	3.73	4.02	0.99
	70	3.92	5.77	3.36	0.98
	140	2.67	3.33	6.46	0.93
	280	11.56	12.47	0.80	0.87

(T - temperature, q_s - saturation limit, K(B) and n - isotherm coefficients, R^2 - coefficient of determination)

The trend is attributed to the exothermic nature of ammonia adsorption on TiO_2 (Rezaei et al. 2017). The results are consistent adsorption mechanism where ammonia is adsorbed mainly through the exothermic step in its molecular form on Lewis acid site (Rezaei et al. 2017).

Regardless of the temperature applied, as shown in Figure 4.5 the equilibrium adsorption capacity increase with the increase in concentration. The enhancement effect of concentration on the adsorption capacity is due to the increase in mass driving force.

Table 4.4. Equilibrium isotherms and associated coefficients for H_2S adsorption on TiO_2/ZnO nanoparticles.

Isotherm model	T (°C)	q_s (g H_2S adsorbed g adsorbent^{-1})	K (B)	n	R^2
Langmuir	22	26.52	188.50	-	0.97
	70	33.78	493.33	-	0.99
	140	52.63	475.00	-	0.99
	280	153.84	650.00	-	0.98
Freundlich	22	-	39.08	5.95	0.89
	70	-	59.71	5.50	0.72
	140	-	79.59	6.92	0.81
	280	-	-	0.53	0.54
Langmuir-Freundlich	22	7.90	4.56	5.64	0.98
	70	6.45	7.29	6.36	0.93
	140	17.82	4.25	6.88	0.98
	280	12.73	34.00	3.22	0.55

(T - temperature, q_s - saturation limit, K(B) and n - isotherm coefficients, R^2 - coefficient of determination)

The experimental data were fitted in all three adsorption models, i.e., Langmuir, Freundlich, and Langmuir-Freundlich model. The coefficients in Table 4.3 and 4.4 are calculated using equations 2.8, 2.9 and equation 3.1.

The effect of temperature on H_2S adsorption was different from NH_3 adsorption as breakthrough curves are more separated at a higher temperature range at different concentration range (50 to 550 ppmv). At lower concentration and higher temperature (i.e. 140 and 280 °C), the breakthrough time increases, and the breakthrough curves are more inclined towards x-axis. Increase in adsorption capacity with an increase in concentration is due to the enhancement in mass transfer driving force. Increasing temperature leads to an increase in adsorption capacity in case of hydrogen sulfide,

which is also seen in the case of adsorption of individual hydrogen sulfide on ZnO (Awume et al. 2017).

Wang et al. (2008) reported on the chemisorption of H_2S by ZnO nanoparticles supported on mesoporous silica SBA-15 at room temperature and atmospheric pressure. The highest H_2S uptake at the breakthrough point was 100 mg H_2S (g adsorbent)$^{-1}$ and achieved with the adsorbent that contained 1.2 wt.% zinc. Habibi et al. (2010) also reported a decrease in breakthrough adsorption capacity of rod-shaped ZnO nanoparticles due to a decrease in temperature from 250 to 150 °C.

The decrease in the breakthrough adsorption capacity ZnO on H_2S with increases in temperature from 300 to 400 °C was also reported by Novochinskii et al. (2004). The equilibrium adsorption capacity increases when the temperature for hydrogen sulfide increases which could be from exothermic reaction in the simultaneous adsorption of NH_3 and H_2S at high temperature (Awume et al. 2017). That could be the reason why Freundlich isotherm at high temperature (280 °C) did not fit with experimental data in case of hydrogen sulfide.

## 4.2 Effect of nanoparticles configuration and their homogeneity

The effect of orientation of nanoparticles and homogeneity was studied at room temperature (22 °C) for a gas containing 500 ppmv NH_3 and 550 ppmv H_2S in the mixture by switching the nanoparticles layers (i.e., the top layer was TiO_2 separated by glass wool, and the bottom layer was ZnO) and by using a relatively homogeneous mixture of nanoparticles (i.e., ZnO and TiO_2 and silicon carbide were mixed and packed as one layer). The amount (0.2 g ZnO and TiO_2 and 0.8 g silicon carbide) remained the same as previous experiments. As given in Appendices (figure B.2), the equilibrium adsorption capacity was calculated and found to be 11.96 mg g^{-1} for NH_3 and 27.21 mg g^{-1} for H_2S, compared to 12 mg g^{-1} for NH_3 and 25.15 mg g^{-1} for H_2S in the previous orientation of nanoparticles. For the homogeneous mixture of nanoparticles, the equilibrium adsorption capacity was found to be 11.9 mg g^{-1} for NH_3 and 24.6 mg g^{-1} for H_2S in the mixture of gases (NH_3 and H_2S). The figure for a homogeneous mixture of nanoparticles is shown in Appendices (Figure B.1). These experiments showed that the orientation did not affect the equilibrium adsorption capacity for both NH_3 and H_2S.

4.3 Semi pilot scale trials

Batches of manure (5 containers) were used for the semi-pilot scale trials. The average flow rate was set at 27 L s^{-1}. The concentrations of NH_3 and H_2S in the feed and treated gas samples were determined using gas sensors (NH_3 and H_2S) installed on the semi-pilot scale setup. Figure 4.7 shows the results obtained in these runs. The highest inlet NH_3 and H_2S concentration recorded were 300 ppmv and 200 ppmv, respectively. As the maximum limit for both sensors was 300 ppmv. The variation in the feed concentration (NH_3 reaches to 300 ppmv while H_2S around 150-200 ppmv) can be attributed to the variation in the collected manure samples and the extent of anaerobic digestion in the stored manure. Therefore, there were differences in the level of NH_3 and H_2S gas produced in each container.

The treated gas concentration of NH_3 and H_2S recorded was almost negligible for containers 1 and 2, while for containers 3, 4 and 5 the gas levels decreased to 100 ppmv, as the adsorbent was saturated during the experiment of container 1 and 2.

Awume et al. (2017) studied the adsorption of H_2S gas using ZnO nanoparticles in semi-pilot scale trials. They reported in the first cycle (container 1), feed gas H_2S concentration had an initial value of 238.4 ppmv that decreased to 90.4 ppmv after 12 min of withdrawing the gas from the headspace of manure container. In the third cycle (container 3), the feed gas H_2S concentration decreased from an initial value of 248.5 to 48.9 ppmv after 15 min of operation. This is also true in the current research work. These experiments showed that nanoparticles (ZnO and TiO_2) were effective in the removal of gases from swine manure.
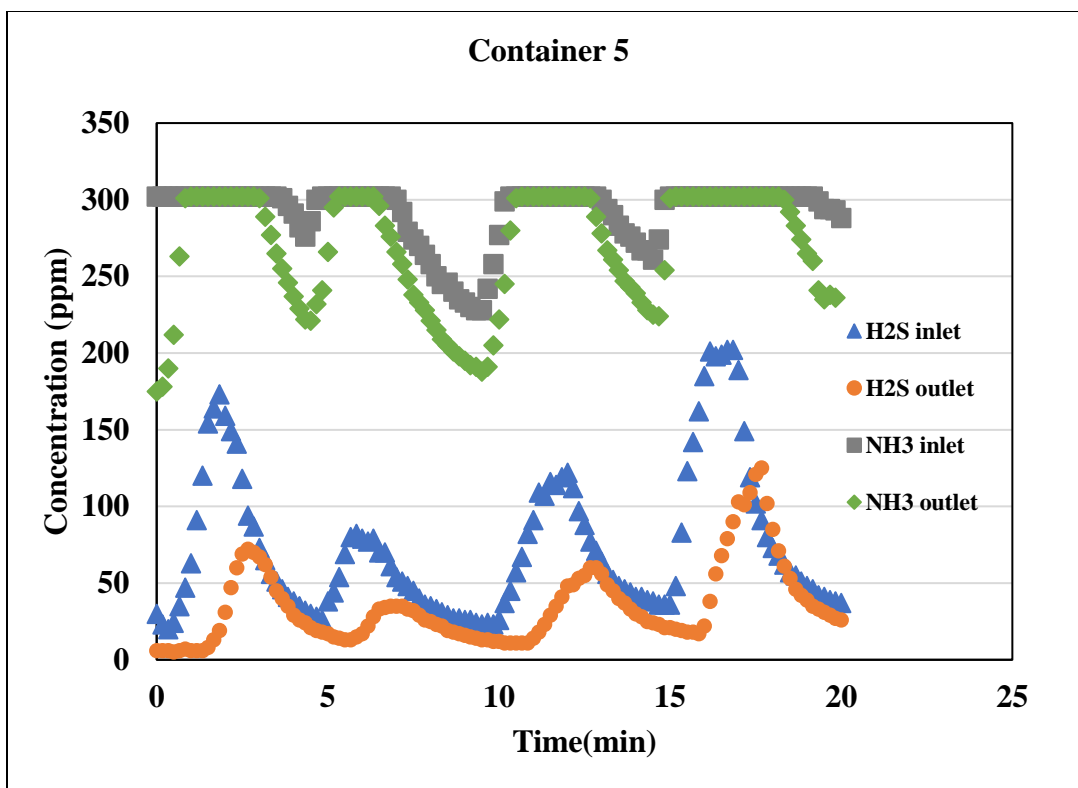
Container 1

Container 2

Container 3

Container 4
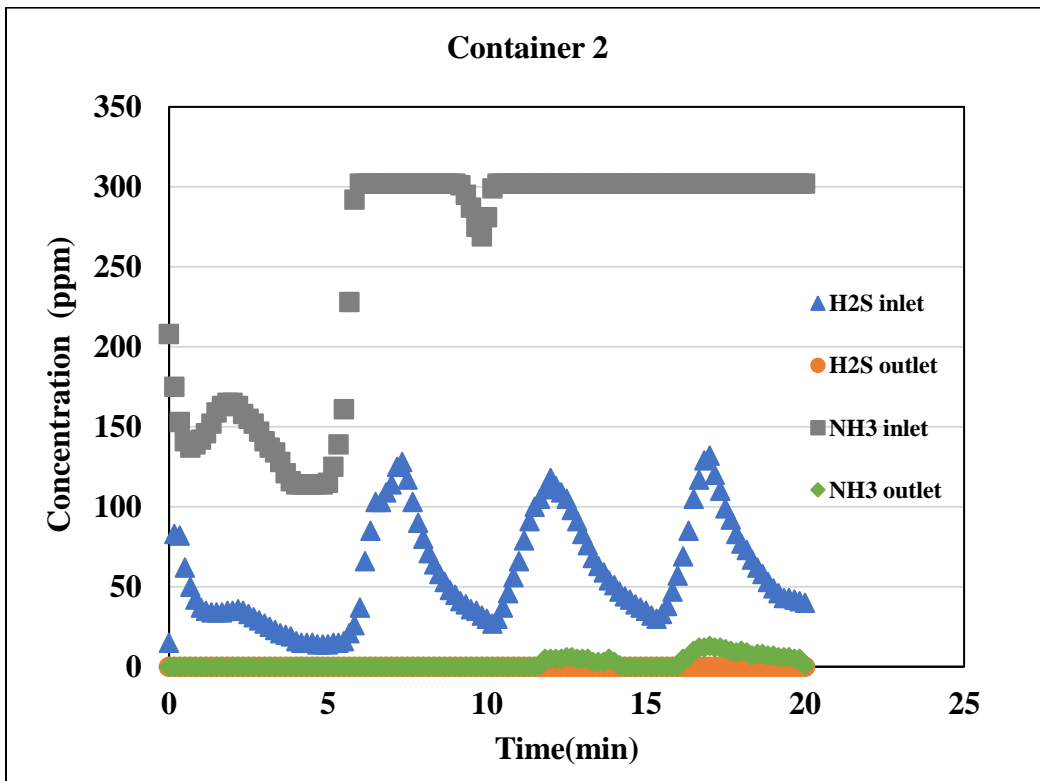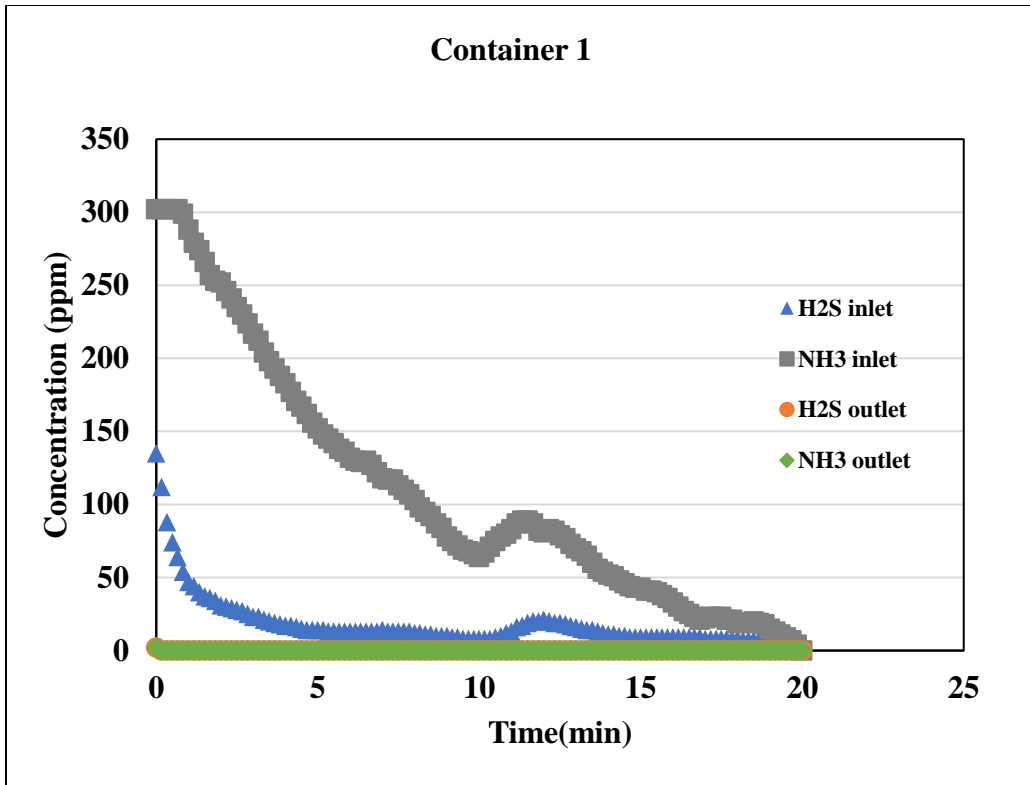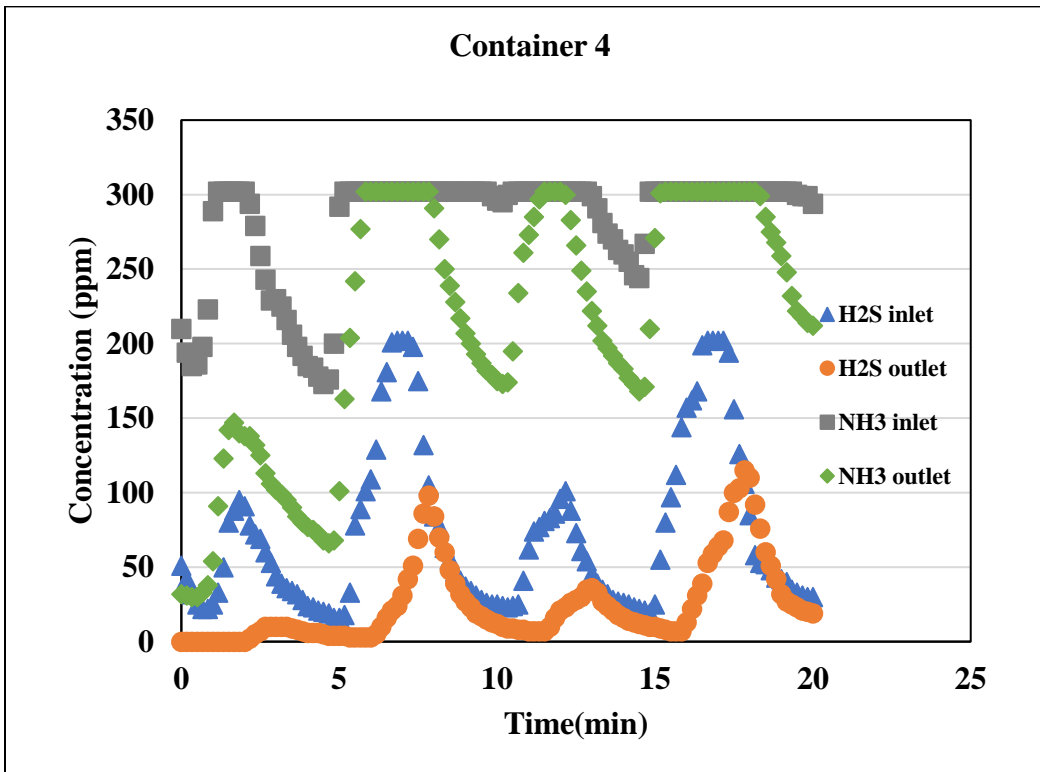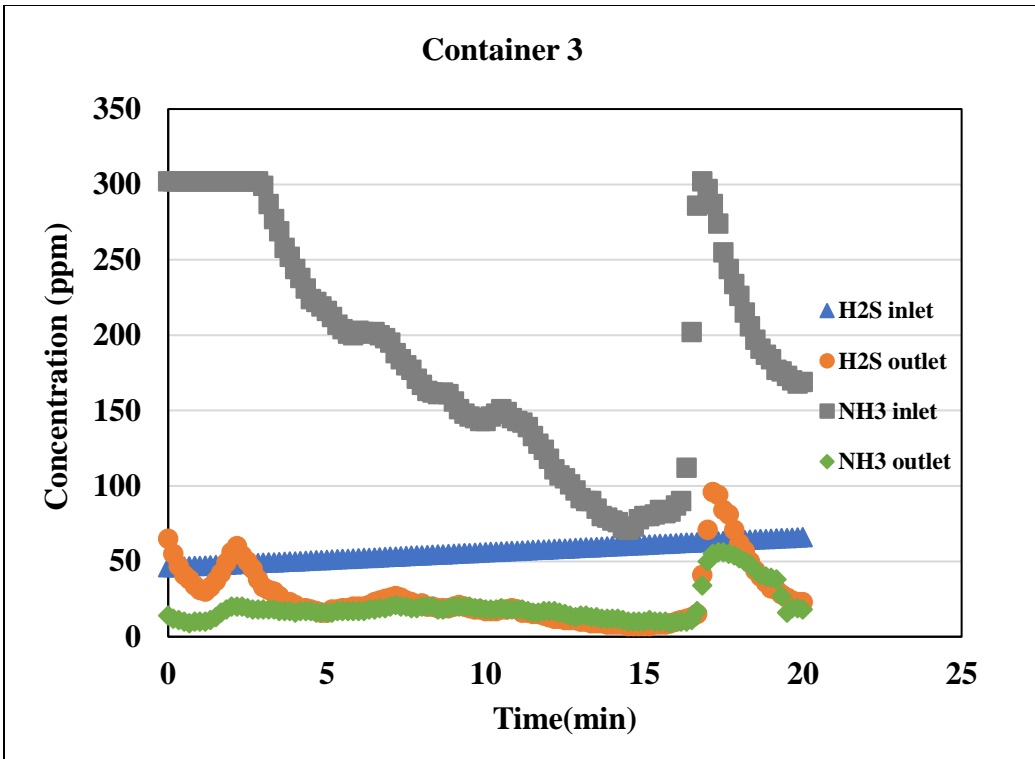
Figure 4.7. NH_3 and H_2S concentration profiles of the gases emitted from swine manure (influent gas) and treated gas (effluent gas).

Also, as explained in the Materials and Methods (section 3.4.2), a second trial was performed one week after the first run to assess the reproducibility of the results with the results shown in Figure 4.8. In the first trial, ZnO and TiO_2 were effective in removal for NH_3 and H_2S, which was reproduced in the second run as well. Compared to the first run, the highest concentration observed of NH_3 was 300 ppmv, and H_2S was 200 ppmv (maximum reading sensors were exceeded in the run), and lowest was around zero for both NH_3 and H_2S. However, in this trial, the manure was mixed for one minute for every six minutes to generate the maximum level of H_2S and NH_3 for short time duration and avoid early saturation of nanoparticles. A control test was carried out in the semi-pilot scale set-up in the absence of nanoparticles to verify if any component of the set-up influence NH_3 and H_2S adsorption and it was found that there was no significant difference in the inlet and outlet concentrations.
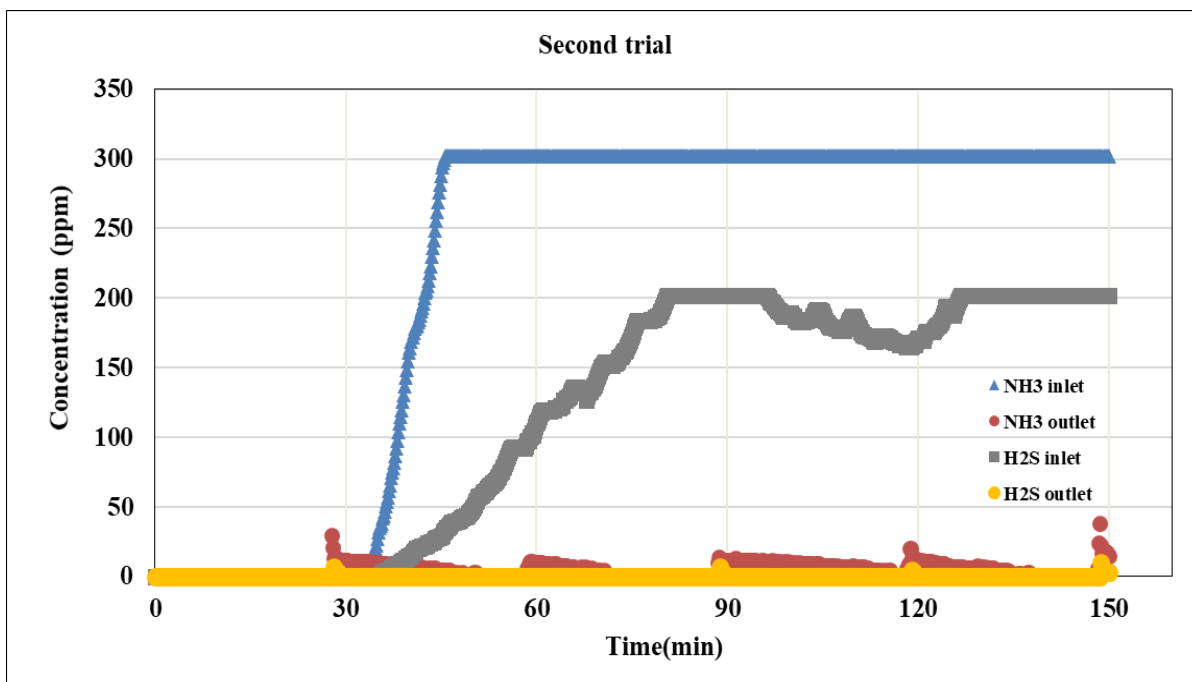
Figure 4.8. NH_3 and H_2S concentration profiles of the gases emitted from swine manure (influent gas) and treated gas (effluent gas) in the second trial.

Monitoring the concentration of NH_3 and H_2S in the treated gas revealed that TiO_2/ ZnO nanoparticles effectively removed the NH_3 and H_2S from the manure gas and the level of NH_3 and H_2S in the treated gas in all five cycles was negligible. Earlier research was based on the direct addition of ZnO or other nanoparticles to the manure as a means to inhibit microbial activity (Alvarado et al. 2015) and formation of NH_3 and H_2S in the manure or using only one nanoparticle ZnO for removal of NH_3 and H_2S (Awume et al. 2017). Thus, the present work emerges to be one of the first that reports on the use of ZnO and TiO_2 nanoparticles (together) for the treatment of gases emitted from swine manure.

4.4 Characterization

Saturated adsorbents from the experimental run with 500 ppmv ammonia and 550 hydrogen sulfide mixture and gas flow rate of 100 mL min^{-1} and the lowest (22°C) and highest temperatures (280 °C) were collected and examined with TGA and CHNS. Figure 4.9, 4.10 and 4.11 showed the TGA (Thermogravimetric analysis) for unused and exposed ZnO.
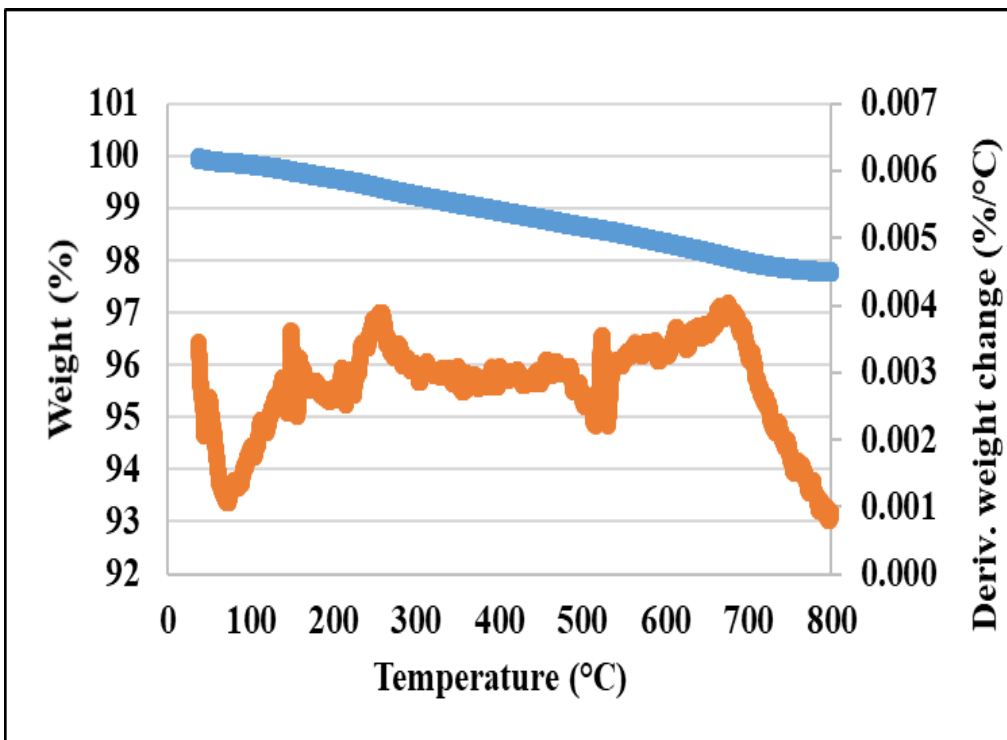
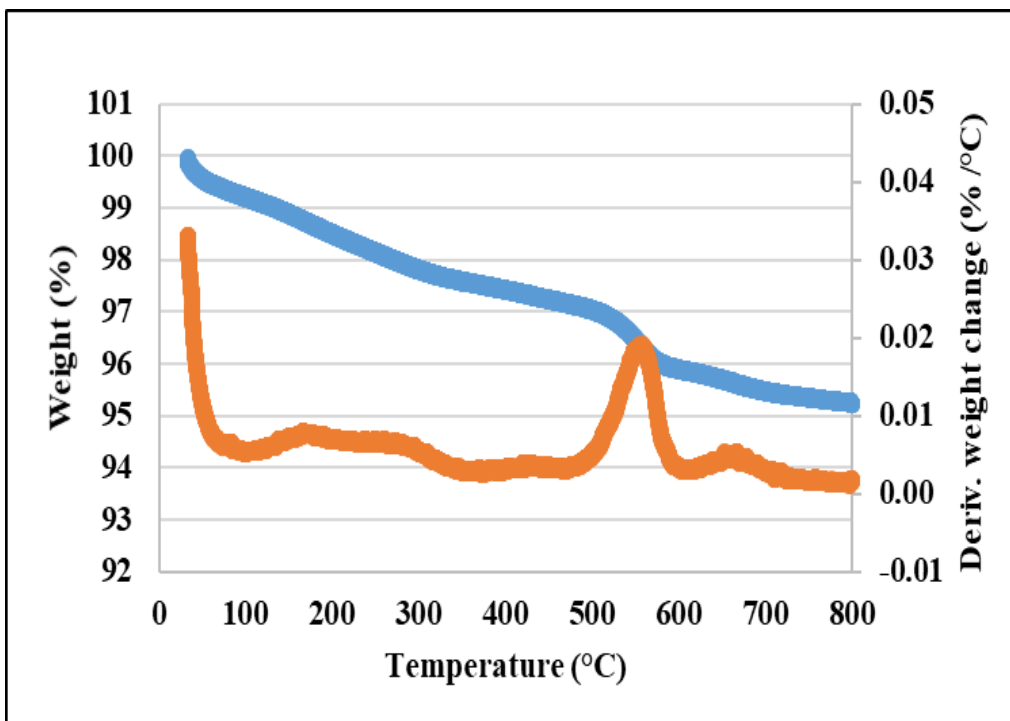**Figure 4.9.** TGA characterization of unused ZnO nanoparticles.

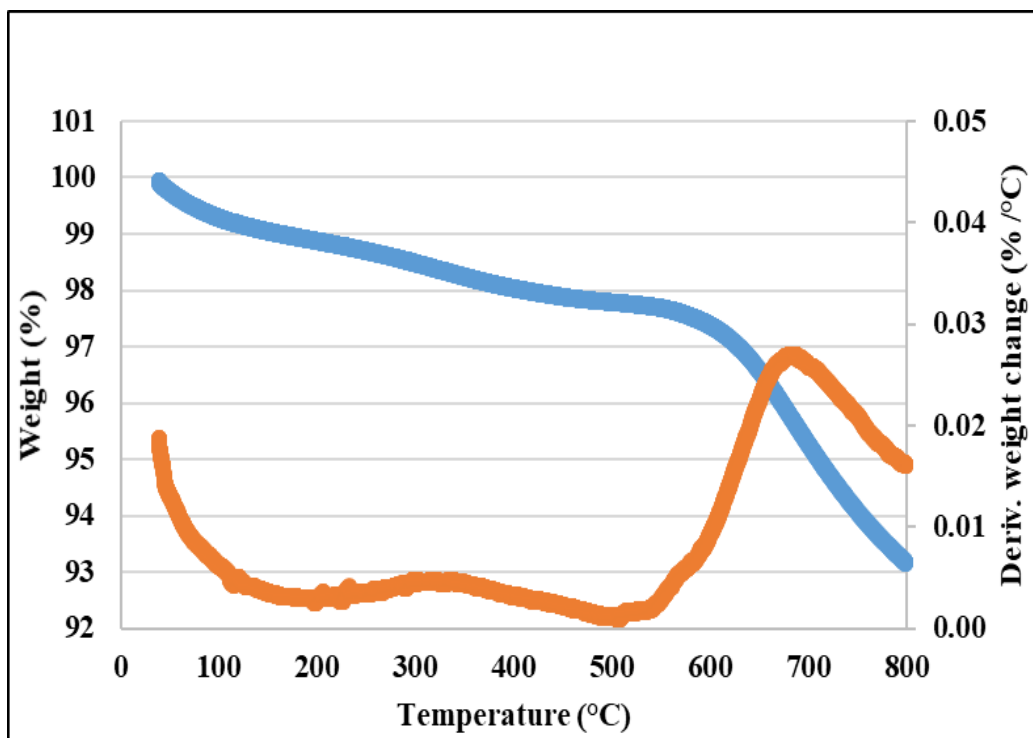**Figure 4.10.** TGA characterization of ZnO (22 °C) nanoparticles.

Figure 4.11. TGA characterization of exposed ZnO nanoparticles from the run at 280 $^{\circ}$C.

The saturated ZnO lost more weight than the unused sample due to the loss of surface adsorbed species. As seen in Figure 4.9, 4.10 and 4.11, blue color represents weight (%) with a change in temperature while the orange color represents derivative weight change (% / °C). Comparing to exposed ZnO at 22 °C and 280 °C, ZnO weight loss is higher at 22 °C.

Also, the rate of weight loss for the saturated sample was higher than that of the unused TiO_2 (Figure 4.12) which shows the presence of various adsorbed species (molecular ammonia or sulfur) with different affinities for the TiO_2 surface.
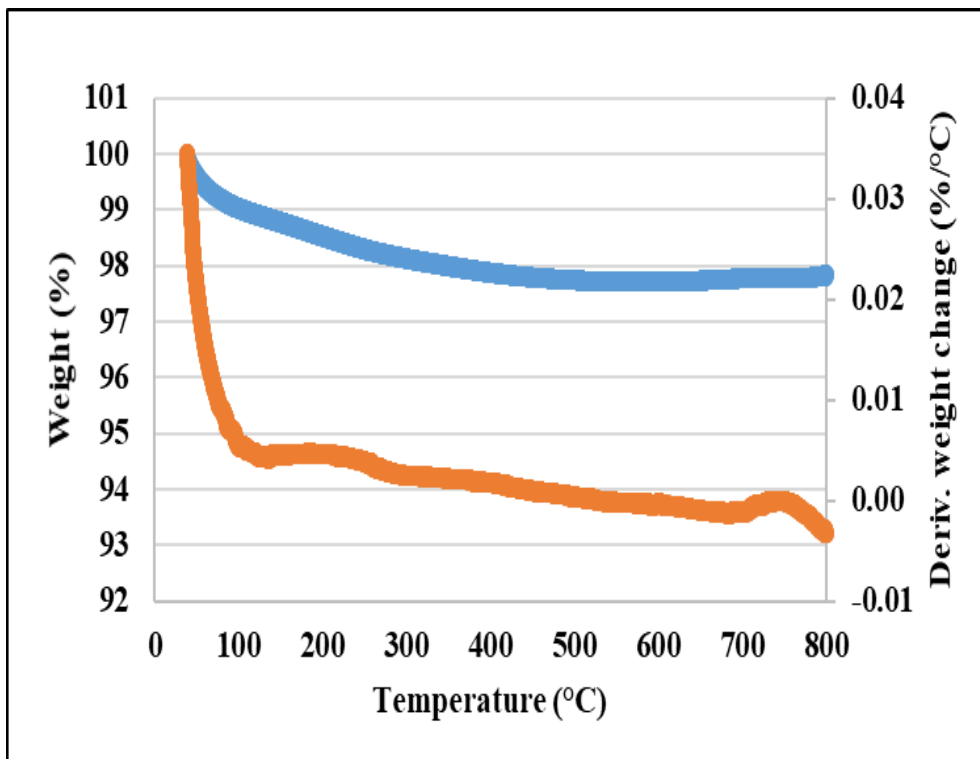
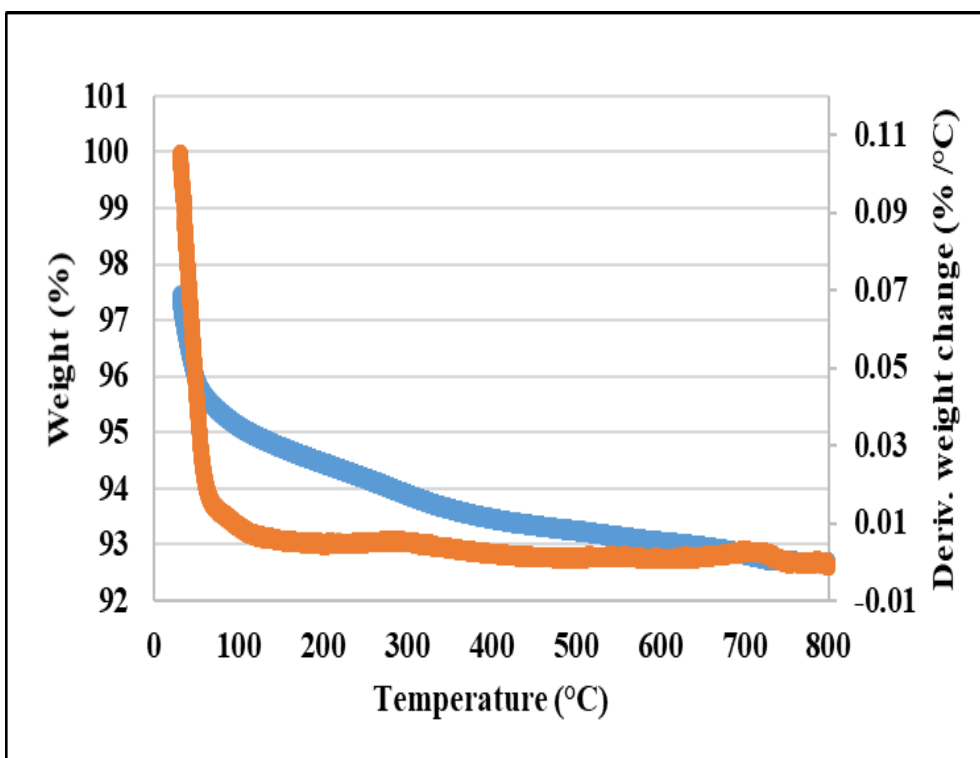**Figure 4.12.** TGA characterization of unused TiO_2 nanoparticles.

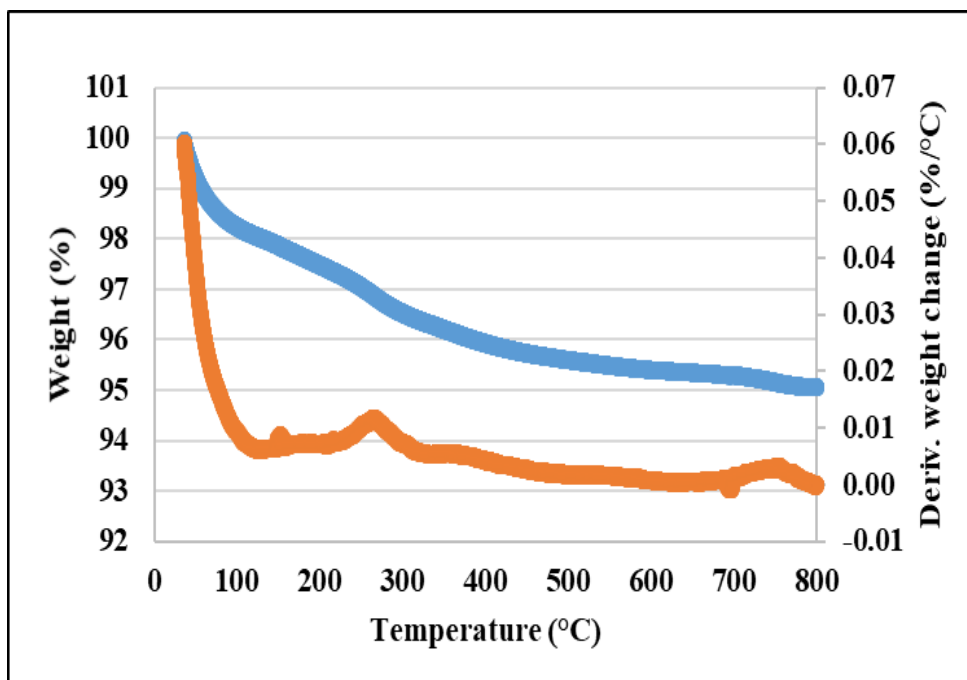**Figure 4.13.** TGA characterization of TiO_2 (22 $^{\circ}$C) nanoparticles.

Figure 4.14. TGA characterization of TiO_2 (280 $^\circ$C) nanoparticles.

In Figures 4.12, 4.13 and 4.14, the blue line represents the primary y-axis while the orange line represents the secondary y-axis. The saturated adsorbent lost more weight than unused adsorbents as same case as ZnO. The saturated TiO_2 and ZnO lost more weight than the unused sample due to the loss of surface adsorbed species. TGA results of the unused and saturated samples, two distinct regions of 22- 100 °C and 100-350 °C were identified in which the rate of weight loss for the saturated sample was higher than that of the unused TiO_2, which shows the presence of various adsorbed species with different affinities for the TiO_2 surface assuming the surface species were in the form of molecular ammonia or sulfur.

The weight percent of nitrogen on the saturated samples was determined using a CHNS analyzer (Vario EL III, Elementar Americans Inc, USA). The nitrogen contents on TiO_2 and ZnO at 280 °C was 0.45 mg Ng $^{-1}$ and 0.43 Ng $^{-1}$, respectively, while at 22 °C the respective contents were 0.513 Ng $^{-1}$ and 0.531 Ng $^{-1}$, respectively.

The amount of carbon and sulfur content on TiO_2 is 0.03 wt. % and 0.36 wt.% respectively at 22 °C. While on ZnO it is 0.05 wt. % and 1.44 wt.% of carbon and sulfur. At 280 °C, the amount of

carbon and sulfur content on TiO_2 is 0.37 wt.% and 0.69 wt.%, respectively, while for ZnO it is 0.68 wt.% and 10.97 wt.% for carbon and sulfur.

Based on the results ammonia adsorption capacity calculated for TiO_2 was 5.31 mg NH_3 g^{-1} which was lower than experimental NH_3 adsorption capacity of 12 mg NH_3 g^{-1} at 22 °C but it is higher, i.e., 4.48 mg NH_3 g^{-1} than experimental NH_3 adsorption capacity of 3.49 at 280 °C. However, for ZnO, both at 22 °C and 280 °C, calculated adsorption capacity based on CHNS results are lower, i.e., 14.4 mg H_2S g^{-1} (at 22 °C) and 107.1 mg H_2S g^{-1} (at 280 °C) compared to 25.15 and 161.4 mg H_2S g^{-1} experimental adsorption capacity respectively. The difference of adsorption capacity calculated from CHNS, and experimental adsorption capacity in case of H_2S, showed chemisorption could be playing an essential role in H_2S adsorption at higher temperature.

CHAPTER 5

SUMMARY, CONCLUSIONS, AND RECOMMENDATIONS FOR FUTURE WORK

5.1 Summary

The research work focused on the simultaneous capture of NH_3 and H_2S by a binary mixture of ZnO (35-45nm) and TiO_2 (40 nm) nanoparticles. Experiments to evaluate the effects of NH_3 and H_2S concentrations were conducted by varying NH_3 and H_2S concentrations within the range of 50 to 500 ppmv of each gas in the mixture (i.e., NH_3-H_2S concentrations: 50-50, 100-100, 200-200, 300-300, 400-400, 500-550 ppmv, respectively). Experiments with all indicated concentrations were carried out at temperature 22, 70, 140 and 280˚C to investigate the effect of temperature on simultaneous NH_3 and H_2S adsorption. The premixed gases (1000 ppmv NH_3-balanced He and 1000 ppmv H_2S – balanced He) were diluted with helium to achieve desired ammonia and hydrogen sulfide concentrations in the range 50-550 ppmv through an adsorption column packed with the designated adsorbent (0.2 g) to generate breakthrough curves. The adsorbent consisting of a layer of ZnO and silicon carbide (0.8 g) and another layer TiO_2 and silicon carbide (0.8 g). The outlet of the adsorption column was directed to an online gas chromatograph (GC) to measure the concentration of NH_3 and H_2S.

The generated data have been then used to develop suitable adsorption isotherms (Langmuir, Freundlich, and Langmuir-Freundlich) and other information required for the application of these adsorbents in large-scale systems.

To understand the mechanism of simultaneous removal of NH_3 and H_2S from gaseous streams, characterization (TGA and CHNS) of the unused and exposed adsorbents were conducted.

Finally, Experiments were conducted using gases emitted from swine manure stored in containers to simulate the actual conditions in the swine barn and to assess the performance of adsorbent in the removal of NH_3 and H_2S from manure gas. The five containers were used in sequence to

generate manure gas for approximately 100 minutes (20 minutes for each manure container). In each cycle, a manure container was agitated intermittently (2 min agitation at 5 min intervals) during which centrifugal fan withdrew the headspace gas and passed it through the adsorption column. Following this, the next container was connected to the feed line, and the cycle was repeated. Later, another five containers were used to repeat experiment and reproducibility of the results.

5.2. Conclusions

Based on the results of the studies in the laboratory and semi-pilot tests, the following conclusions can be drawn:

1. TiO_2 and ZnO nanoparticles were effective in simultaneous adsorption of ammonia and hydrogen sulfide.

2. The equilibrium adsorption capacities of both ammonia and hydrogen sulfide increase as gas concentration increases (50 -550 ppmv).

3. Equilibrium adsorption capacity of hydrogen sulfide increases with the increase of temperature in the range (22°C to 280 °C) while there is a decrease in adsorption capacity of ammonia due to an increase of temperature. The results showed that adsorption was mainly of a physical nature but in the case of H_2S chemisorption seems to be the governing mechanism.

4. The highest adsorption capacity observed for NH_3 was 12 mg/g at 500 ppmv NH_3- 550 ppmv H_2S (22 °C) while highest adsorption capacity for H_2S was 206.7 mg/g at 100 ppmv NH_3 - 100 ppmv H_2S (280 °C).

5. Among Langmuir, Freundlich, and Langmuir- Freundlich isotherms the latter best-described equilibrium data.

6. The semi-pilot scale experiments showed the effectiveness of ZnO and TiO_2 nanoparticles in the capture of NH_3 and H_2S from gases representing those emitted from a swine production facility.

5.3. Recommendations for future work

1. An extensive characterization study of both unused and used nanoparticles for a complete understanding of reaction mechanism is required.

2. Desorption and regeneration of exposed nanoparticles should be studied for cost-effectiveness.

3. A more detailed study on various operating conditions in the semi-pilot scale setup should be done for better understanding of the design of an effective system for the removal of hazardous gases.

REFERENCES

Allen, A. G., Harrison, R. M., & Wake, M. T. (1988). A meso-scale study of the behavior of atmospheric ammonia and ammonium. *Atmospheric Environment (1967)*, *22*(7), 1347-1353.

Alvarado, A. C., Predicala, B. Z., & Asis, D. A. (2015). Mixing nanoparticles with swine manure to reduce hydrogen sulfide and ammonia emissions. *International Journal of Environmental Science and Technology*, *12*(3), 893-904.

Aneja, V. P., Bunton, B., Walker, J. T., & Malik, B. P. (2001). Measurement and analysis of atmospheric ammonia emissions from anaerobic lagoons. *Atmospheric Environment*, *35*(11), 1949-1958.

Aneja, V. P., Nelson, D. R., Roelle, P. A., Walker, J. T., & Battye, W. (2003). Agricultural ammonia emissions and ammonium concentrations associated with aerosols and precipitation in the southeast United States. *Journal of Geophysical Research: Atmospheres*, *108*(D4).

Anstrom, M., Dumesic, J. A., & Topsøe, N. Y. (2002). Theoretical insight into the nature of ammonia adsorption on vanadia-based catalysts for SCR reaction. *Catalysis Letters*, *78*(1-4), 281-289.

ApSimon, H. M., Kruse, M., & Bell, J. N. B. (1987). Ammonia emissions and their role in acid deposition. *Atmospheric Environment*, *21*, 1939-1946.

Apsimon, H. M., & Kruse-Plass, M. (1991). The role of ammonia as an atmospheric pollutant. *Odour and ammonia emissions from livestock farming*, 17-20.

Armeen, A., Feddes, J. J. R., Leonard, J. J., & Coleman, R. N. (2008). Biofilters to treat swine facility air: Part 1. Nitrogen mass balance. *Canadian Biosystems Engineering*, *50*-57.

Arogo, J., Zhang, R. H., Riskowski, G. L., & Day, D. L. (2000). Hydrogen sulfide production from stored liquid swine manure: a laboratory study. *Transactions of the ASAE*, *43*(5), 1241-1245.

ASABE. (2007). Management of manure odours. American Society of Agricultural and Biological Engineers standard EP379.4. St. Joseph, MI.

Assaad, V., Jofriet, J., & Hayward, G. (2008). Sulphate and sulphide corrosion in livestock buildings, Part I: Concrete deterioration. Biosystems Engineering 99, 372-381.

Atia, A., Haugen-Kozyra, K., & Amrani, M. (2013). Ammonia and hydrogen sulfide emissions from livestock production. Manure Research Findings and Technologies: From science to social issues [Online]. Alberta, Canada.
<http://www1.agric.gov.ab.ca/$department/deptdocs.nsf/all/epw8313/$FILE/chapter7.pdf>
Accessed: 1 August 2017.

ATSDR (Agency for Toxic Substances & Disease Registry)(2006). Public health statement: Hydrogen sulfide. CAS no. 7783-06-4. Division of toxicology and environmental medicine, Atlanta, GA.

Awume, B., Tajallipour, M., Nemati, M., & Predicala, B. (2017). Application of ZnO nanoparticles in control of H_2S emission from low-temperature gases and swine manure Gas. *Water, Air, & Soil Pollution*, *228*(4), 147-163.

Bandosz, T. J. (1999). Effect of pore structure and surface chemistry of virgin activated carbons on removal of hydrogen sulfide. *carbon*, *37*(3), 483-491.

Barpaga, D., & LeVan, M. D. (2016). Functionalization of carbon-silica composites with active metal sites for NH_3 and SO_2 adsorption. *Microporous and Mesoporous Materials*, *221*, 197-203.

Barthelmie, R. J., & Pryor, S. C. (1998). Implications of ammonia emissions for fine aerosol formation and visibility impairment: A case study from the Lower Fraser Valley, British Columbia. *Atmospheric Environment*, *32*(3), 345-352.

Battye, R., Battye, W., Overcash, C., & Fudge, S. (1994). Development and selection of ammonia emission factors. EPA contract number 68-D3-0034, US Environmental Protection Agency.

Behera, S. N., & Sharma, M. (2011). Degradation of SO_2, NO_2, and NH_3 leading to formation of secondary inorganic aerosols: An environmental chamber study. *Atmospheric Environment*, *45*(24), 4015-4024.

Bejan, D., Graham, T., & Bunce, N. J. (2013). Chemical methods for the remediation of ammonia in poultry rearing facilities: a review. *Biosystems Engineering*, *115*(3), 230-243.

Brezonik, P., & Arnold, W. (2011). *Water Chemistry: An Introduction to the Chemistry of Natural and Engineered Aquatic Systems*. New York: Oxford University Press.

Brown, A.M. A step-by-step guide to non-linear regression analysis of experimental data using a Microsoft Excel spreadsheet, Comput. Methods Programs Biomed. 65 (2001) 191-200

Casey, K. D., Bicudo, J. R.,Schmidt, D. R., Singh, A., Gay, S. W., Gates, R. S., Jacobson, L. D., Hoff, S. J. (2006). Air quality and emissions from livestock and poultry production/ waste management systems. In Animal agriculture and the environment: National Center for Manure and Animal Waste Management White Papers, 1-40. J. M. Rice, D. F. Caldwell, F. J. Humenik (eds.). American Society for Agricultural and Biological Engineers St. Joseph, Michigan.

Chénard, L., Lemay, S. P., & Laguë, C. (2003). Hydrogen sulfide assessment in shallow–pit swine housing and outside manure storage. *Journal of agricultural safety and health*, *9*(4), 285-302.

Clark, O. G., Moehn, S., Edeogu, I., Price, J., & Leonard, J. (2005). Manipulation of dietary protein and nonstarch polysaccharide to control swine manure emissions. *Journal of environmental quality*, *34*(5), 1461-1466.

Clarisse, L., Clerbaux, C., Dentener, F., Hurtmans, D., & Coheur, P. F. (2009). Global ammonia distribution derived from infrared satellite observations. *Nature Geoscience*, *2*(7), 479-483.

Dąbrowski, A. (2001). Adsorption—from theory to practice. *Advances in colloid and interface science*, *93*(1-3), 135-224.

EPA. (2007). Nanotechnology white paper. *US Environmental Protection Agency, EPA 100/B-07/001*, (February), 136

Froment, G.F., Bischoff, K.B. , De Wilde, J. Chemical Reactor Analysis and design, 3rd ed., John Wiley & Sons, Inc., United States of America, 2011.

Godbout, S., Lemay, S. P., Joncas, R., Larouche, J. P., Martin, D. Y., Bernier, J. F., Zijlstra, R., Chénard, L., Marquis, A., Barber E., & Massé. D. 2001. Oil sprinkling and dietary manipulation to reduce odour and gas emissions from swine buildings–laboratory scale experiment. In *Livestock Environment VI, Proceedings of the 6th International Symposium 2001* (p. 671). American Society of Agricultural and Biological Engineers St. Joseph, Michigan.

Guo, J., Luo, Y., Lua, A. C., Chi, R. A., Chen, Y. L., Bao, X. T., & Xiang, S. X. (2007). Adsorption of hydrogen sulphide (H_2S) by activated carbons derived from oil-palm shell. *Carbon*, *45*(2), 330-336.

Habibi, R., Rashidi, A. M., & Daryan, J. T. (2010). Study of the Rod-Like and spherical nano-ZnO morphology on H_2S removal from natural gas. *Applied surface science*, *257*(2), 434-439.

Hartung, J., & Phillips, V. R. (1994). Control of gaseous emissions from livestock buildings and manure stores. *Journal of Agricultural Engineering Research*, *57*(3), 173-189.

Heald, C.L., Collett Jr, J.L., Lee, T., Benedict, K.B., Schwandner, F.M., Li, Y., Clarisse, L., Hurtmans, D.R., Van Damme, M., Clerbaux, C. & Coheur, P.F. (2012). Atmospheric ammonia and particulate inorganic nitrogen over the United States. *Atmospheric Chemistry and Physics*, *12*(21), 10295-10312.

Heber, A. J., Lim, T. T., Tao, P. C., & Ni, J. Q. (2004). Control of air emissions from swine finishing buildings flushed with recycled lagoon effluent. In *2004 ASAE Annual Meeting* (p. 1). American Society of Agricultural and Biological Engineers St. Joseph, Michigan.

Helminen, J., Helenius, J., Paatero, E., & Turunen, I. (2000). Comparison of sorbents and isotherm models for NH_3-gas separation by adsorption. *AIChE Journal*, *46*(8), 1541-1555.

Hines, A. L., & Maddox, R. N. (1985). *Mass transfer: fundamentals and applications* (Vol. 434). Englewood Cliffs, NJ: Prentice-Hall.

Hobbs, P. J., Misselbrook, T. H., & Cumby, T. R. (1999). Production and emission of odours and gases from ageing pig waste. *Journal of Agricultural Engineering Research*, *72*(3), 291-298.

Horvath, & Suzuki. (1999). Advanced technical tools for the solution of high capacity adsorption separation. *Studies in Surface Science and Catalysis, 120*, 275-300.

Hu, J., Chen, G., & Lo, I. M. (2005). Removal and recovery of Cr (VI) from wastewater by maghemite nanoparticles. *Water Research*, *39*(18), 4528-4536.

Huang, C. C., Li, H. S., & Chen, C. H. (2008). Effect of surface acidic oxides of activated carbon on adsorption of ammonia. *Journal of Hazardous Materials*, *159*(2-3), 523-527.

Ismadji, S., Soetaredjo, F. E., & Ayucitra, A. (2015). *Clay materials for environmental remediation* (Vol. 25, pp. 1-124). Berlin: Springer.

Jun, H. K., Lee, T. J., Ryu, S. O., & Kim, J. C. (2001). A study of Zn− Ti-based H_2S removal sorbents promoted with cobalt oxides. *Industrial & Engineering Chemistry Research*, *40*(16), 3547-3556.

Kaneko, K., Katori, T., Shimizu, K., Shindo, N., & Maeda, T. (1992). Changes in the molecular adsorption properties of pitch-based activated carbon fibres by air oxidation. *Journal of the Chemical Society, Faraday Transactions*, *88*(9), 1305-1309.

Kim, K. Y., Ko, H. J., Kim, H. T., Kim, Y. S., Roh, Y. M., Lee, C. M., & Kim, C. N. (2008). Odor reduction rate in the confinement pig building by spraying various additives. *Bioresource Technology*, *99*(17), 8464-8469.

Koerkamp, P.G., Metz, J.H.M., Uenk, G.H., Phillips, V.R., Holden, M.R., Sneath, R.W., Short, J.L., White, R.P.P., Hartung, J., Seedorf, J. & Schröder, M. (1998). Concentrations and emissions of ammonia in livestock buildings in Northern Europe. *Journal of Agricultural Engineering Research*, *70*(1), 79-95.

Kurvits, T., & Marta, T. (1998). Agricultural NH3 and NOx emissions in Canada. *Environmental Pollution*, *102*(1), 187-194.

Le Leuch, L. M., Subrenat, A., & Le Cloirec, P. (2005). Hydrogen sulfide and ammonia removal on activated carbon fiber cloth-supported metal oxides. *Environmental Technology*, *26*(11), 1243-1254.

Lew, S., Sarofim, A. F., & Flytzani-Stephanopoulos, M. (1992). Sulfidation of zinc titanate and zinc oxide solids. *Industrial & Engineering Chemistry Research*, *31*(8), 1890-1899.

Li, Z., & Flytzani-Stephanopoulos, M. (1997). Cu− Cr−O and Cu− Ce−O regenerable oxide sorbents for hot gas desulfurization. *Industrial & Engineering Chemistry Research*, *36*(1), 187-196.

Mangun, C. L., Benak, K. R., Daley, M. A., & Economy, J. (1999). Oxidation of activated carbon fibers: effect on pore size, surface chemistry, and adsorption properties. *Chemistry of Materials*, *11*(12), 3476-3483.

Maghirang, R. G., Riskowski, G. L., Christianson, L. L., & Manbeck, H. B. (1995). Dust control strategies for livestock buildings - a review. ASHRAE Transactions SD-95-15-1:1161-1168.

Masciangioli, T., & Zhang, W.X. (2003). Environmental technologies at the nanoscale. *Environmental Science & Technology*, *37*(5), 102A–108A.

McAllister, J. S. V., & McQuitty, J. B. (1965). Release of gases from slurry. *Res. Exp. Rec. Minist. Agric. Nth. Ire*, *14*, 73-78.

McCrory, D. F., & Hobbs, P. J. (2001). Additives to reduce ammonia and odor emissions from livestock wastes. *Journal of environmental quality*, *30*(2), 345-355.

Meisinger, J. J., Lefcourt, A. M., & Thompson, R. B. (2001). Construction and validation of small mobile wind tunnels for studying ammonia volatilization. *Applied Engineering in Agriculture*, *17*(3), 375-381.

Moore, P. A., Daniel, T. C., Edwards, D. R., & Miller, D. M. (1995). Effect of chemical amendments on ammonia volatilization from poultry litter. *Journal of Environmental Quality*, *24*(2), 293-300.

Morán, M., Ferreira, J., Martins, H., Monteiro, A., Borrego, C., & González, J. A. (2016). Ammonia agriculture emissions: From EMEP to a high-resolution inventory. *Atmospheric Pollution Research*, *7*(5), 786-798.

Moreno, L., Predicala, B., & Nemati, M. (2010). Laboratory, semi-pilot and room scale study of nitrite and molybdate mediated control of H_2S emission from swine manure. *Bioresource technology*, *101*(7), 2141-2151.

Nassar, N. N., & Pereira-Almao, P. (2010). Capturing H_2S (g) by in situ-prepared ultradispersed metal oxide particles in an oilsand-packed bed column. *Energy & Fuels*, *24*(11), 5903-5906.

Ni, J.Q., Heber, A.J., Fakhoury, K.J., Shao, P., Sutton, A.L., Kelly, D., Patterson, J.A. & Kim, S.T. (2000). Laboratory measurement of hydrogen sulfide and sulfur dioxide releases from swine manure of different solid contents. *2000 ASAE Annual International Meeting, Technical Papers: Engineering Solutions for a New Century*, *2*(4082), 4401–4413.

Ni, J. Q., Heber, A. J., Diehl, C. A., Lim, T. T., Duggirala, R. K., & Haymore, B. L. (2002). Summertime concentrations and emissions of hydrogen sulfide at a mechanically ventilated swine finishing building. *Transactions of the ASAE*, *45*(1), 193-199.

Nicolai, R. E., & Janni, K. A. (2001). Biofilter media mixture ratio of wood chips and compost treating swine odors. *Water science and technology*, *44*(9), 261-267.

Noble, R. D., Noble, R. D., & Terry, P. A. (2004). *Principles of chemical separations with environmental applications*. (Cambridge series in chemical engineering). Cambridge, UK; New York: Cambridge University Press.

Novochinskii, I. I., Song, C., Ma, X., Liu, X., Shore, L., Lampert, J., & Farrauto, R. J. (2004). Low-temperature H_2S removal from steam-containing gas mixtures with ZnO for fuel cell application. 1. ZnO particles and extrudates. *Energy & Fuels*, *18*(2), 576-583.

Oliver, J. P. (2015). *Role of fungi in the biofiltration of livestock housing and manure storage emissions* (Doctoral dissertation, University of Minnesota).

Olivier, J. G. J., Bouwman, A. F., Van der Hoek, K. W., & Berdowski, J. J. M. (1998). Global air emission inventories for anthropogenic sources of NO_x, NH_3, and N_2O in 1990. *Environmental Pollution*, *102*(S1), 135-148.

OSHA. 2018. Hydrogen Sulfide: OSHA Chemical Sampling Information. Washington, D.C., Occupational Safety and Health Administration.
http://www.osha.gov/dts/chemicalsampling/data/CH_246800.html > Accessed: 31 January 2018

Ouellette, C., Lemay, S., Godbout, S., & Edeogu, I. (2006). Oil application to reduce dust and odour emissions from swine buildings Ouellette. CSBE/SCGAB 2006 Annual Conference. No. 06-147. Edmonton, Alberta.

Palmquist, R. B., Roka, F. M., & Vukina, T. (1997). Hog operations, environmental effects, and residential property values. *Land Economics*,73, 114-124.

Park, S. J., & Jin, S. Y. (2005). Effect of ozone treatment on ammonia removal of activated carbons. *Journal of colloid and interface science*, *286*(1), 417-419.

Paszek, D. A., Jacobson, L. D., Johnson, V. J., & Nicolai, R. E. (1998). Design and management of an oil sprinkling system to control dust, odor, and gases in and from a curtain-sided pig finishing barn. In *2001 ASAE Annual Meeting* (p. 1). American Society of Agricultural and Biological Engineers St. Joseph, Michigan.

Petit, C., Karwacki, C., Peterson, G., & Bandosz, T. J. (2007). Interactions of ammonia with the surface of microporous carbon impregnated with transition metal chlorides. *The Journal of Physical Chemistry C*, *111*(34), 12705-12714.

Rezaei, E., Azar, R., Nemati, M., & Predicala, B. (2017). Gas phase adsorption of ammonia using nano TiO_2-activated carbon composites–Effect of TiO_2 loading and composite characterization. *Journal of Environmental Chemical Engineering*, *5*(6), 5902-5911.

Rezaei, E., Schlageter, B., Nemati, M., & Predicala, B. (2017). Evaluation of metal oxide nanoparticles for adsorption of gas phase ammonia. *Journal of Environmental Chemical Engineering*, *5*(1), 422-431.

Riskowski, G. L. (2003). Overview of methods to reduce odorant emissions from confinement swine buildings. *Food and Agricultural Research*, 122-143.

Rodrigues, C. C., de Moraes Jr, D., Da Nobrega, S. W., & Barboza, M. G. (2007). Ammonia adsorption in a fixed bed of activated carbon. *Bioresource Technology*, *98*(4), 886-891.

Romero, J. V., Smith, J. W., Sullivan, B. M., Croll, L. M., & Dahn, J. R. (2011). SO_2 and NH_3 gas adsorption on a ternary $ZnO/CuO/CuCl_2$ impregnated activated carbon evaluated using combinatorial methods. *ACS combinatorial science*, *14*(1), 31-37.

Rouquerol, J., Rouquerol, F., Llewellyn, P., Maurin, G., & Sing, K. S. (2013). *Adsorption by powders and porous solids: principles, methodology, and applications*: *Second Edition.* Elsevier. Ruthven, D. M. (1984). *Principles of adsorption and adsorption processes*. New York: John Wiley & Sons.

Schiffman, S. S., Walker, J. M., Dalton, P., Lorig, T. S., Raymer, J. H., Shusterman, D., & Williams, C. M. (2000). Potential health effects of odor from animal operations, wastewater treatment, and recycling of byproducts. *Journal of Agromedicine*, *7*(1), 7-81.

Schmidt, A. M., & Heber, A. J. (2004). Dust, Odor and Gas control in swine finishing barns through oil sprinkling. *Extension publications (MU)*. University of Missouri-Columbia.

Shi, Y., Parker, D. B., Cole, N. A., Auvermann, B. W., & Mehlhorn, J. E. (2001). Surface amendments to minimize ammonia emissions from beef cattle feedlots. *Transactions of the ASAE*, *44*(3), 677-682.

Simo, M., Sivashanmugam, S., Brown, C. J., & Hlavacek, V. (2009). Adsorption/desorption of water and ethanol on 3A zeolite in near-adiabatic fixed bed. *Industrial & Engineering Chemistry Research*, *48*(20), 9247-9260.

Soccol, C. R., Woiciechowski, A. L., Vandenberghe, L. P., Soares, M., Neto, G. K., & Soccol, V. T. (2003). Biofiltration: An Emerging Technology.

Sommer, S. G., & Hutchings, N. (1995). Techniques and strategies for the reduction of ammonia emission from agriculture. *Water, Air, and Soil Pollution*, *85*(1), 237-248.

Statistics Canada. 2016. Livestock estimates. Catalogue no. 11-001-X.

Takai, H., & Pedersen, S. (1999). Design concept of oil sprayer for dust control in pig buildings. In *Dust Control in Animal Production Facilities, Aarhus (Denmark), 30 May-2 Jun 1999*. DJF.

Wang, X., Sun, T., Yang, J., Zhao, L., & Jia, J. (2008). Low-temperature H_2S removal from gas streams with SBA-15 supported ZnO nanoparticles. *Chemical Engineering Journal*, *142*(1), 48-55.

Watts, P. J. (2000). Development of a pig effluent emissions database and analysis of promising control strategies. *A final report prepared for the Pig Research and Development Corporation, Australia*.

Webb, J., Thorman, R. E., Fernanda-Aller, M., & Jackson, D. R. (2014). Emission factors for ammonia and nitrous oxide emissions following immediate manure incorporation on two contrasting soil types. *Atmospheric Environment*, *82*, 280-287.

Westmoreland, P. R., & Harrison, D. P. (1976). Evaluation of candidate solids for high-temperature desulfurization of low-Btu gases. *Environmental Science & Technology*, *10*(7), 659-661.

Xue, S. K., Chen, S., & Hermanson, R. E. (1998). Measuring ammonia and hydrogen sulfide emitted from manure storage facilities. *Transactions of the ASAE*, *41*(4), 1125-1130.

Zhang, R. H., North, J. R., & Day, D. L. (1990). Operation of a field scale anaerobic digester on a swine farm. *Applied Engineering in Agriculture*, *6*(6), 771-776.

Zhang, Y., Tanaka, A., Barber, E. M., & Feddes, J. J. R. (1996). Effects of frequency and quantity of sprinkling canola oil on dust reduction in swine buildings. *Transactions of the ASAE*, *39*(3), 1077-1081.

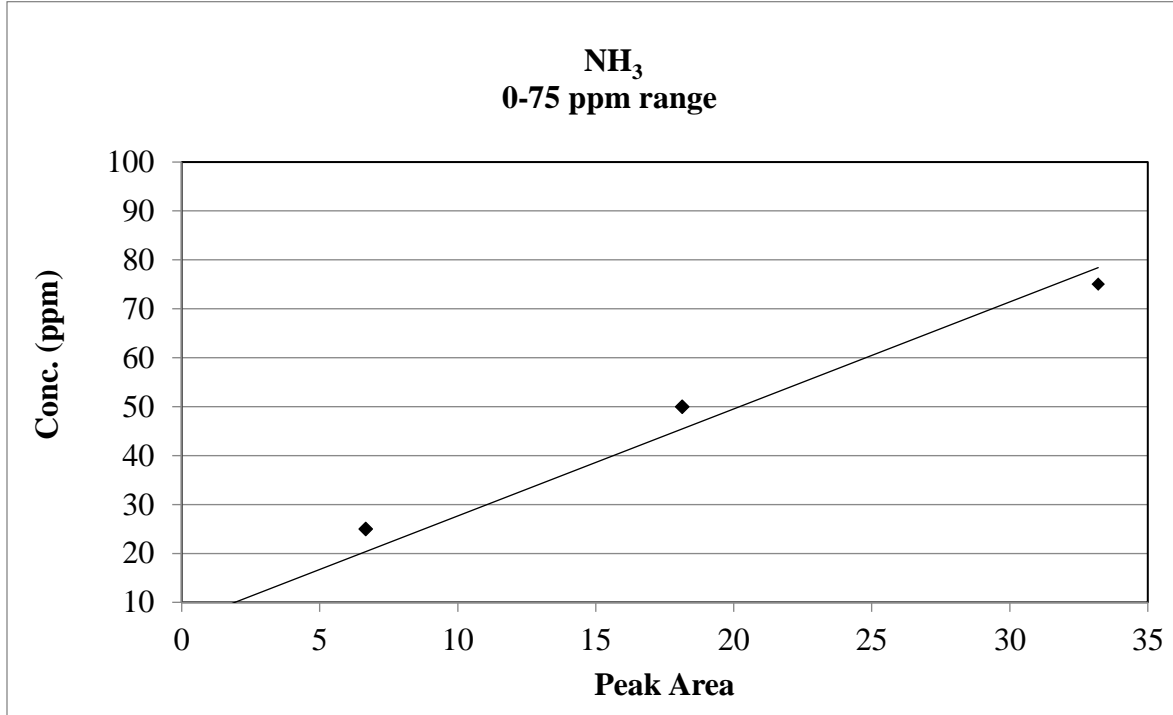# APPENDICES

A. Gas chromatograph calibration curves for NH$_3$ and H$_2$S

Figure A.1. Gas chromatograph calibration curve (NH$_3$) for 0 to 75 ppmv range.
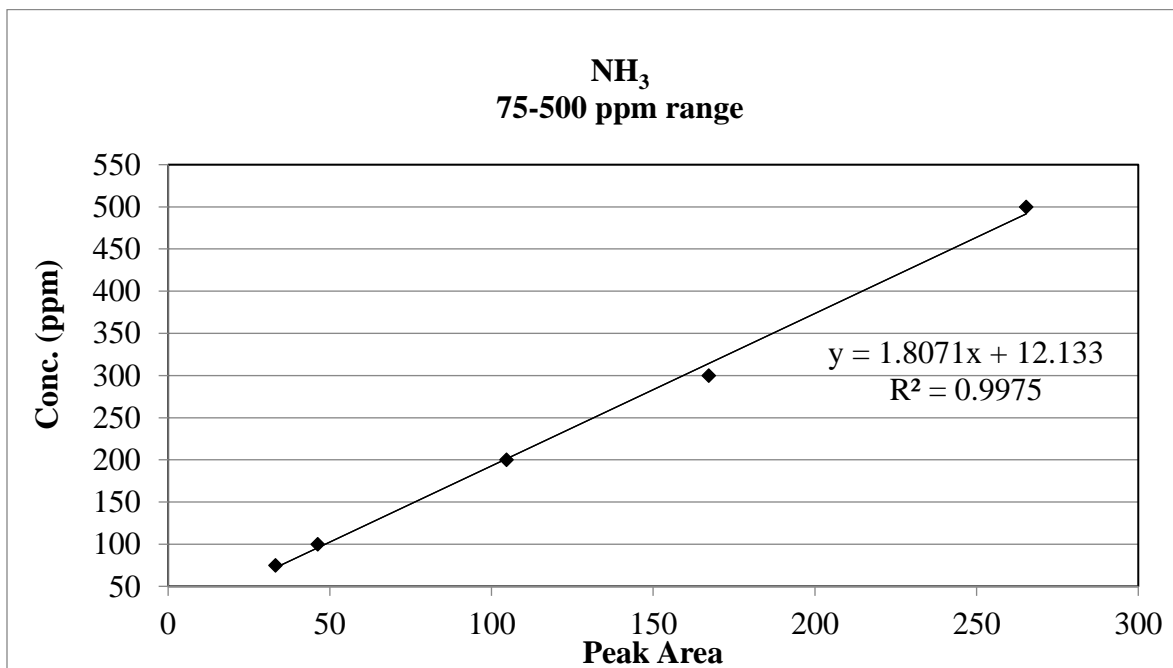
$$y = 1.8071x + 12.133$$
$$R^2 = 0.9975$$

Figure A.2. Gas chromatograph calibration curve (NH$_3$) for 75 to 500 ppmv range.
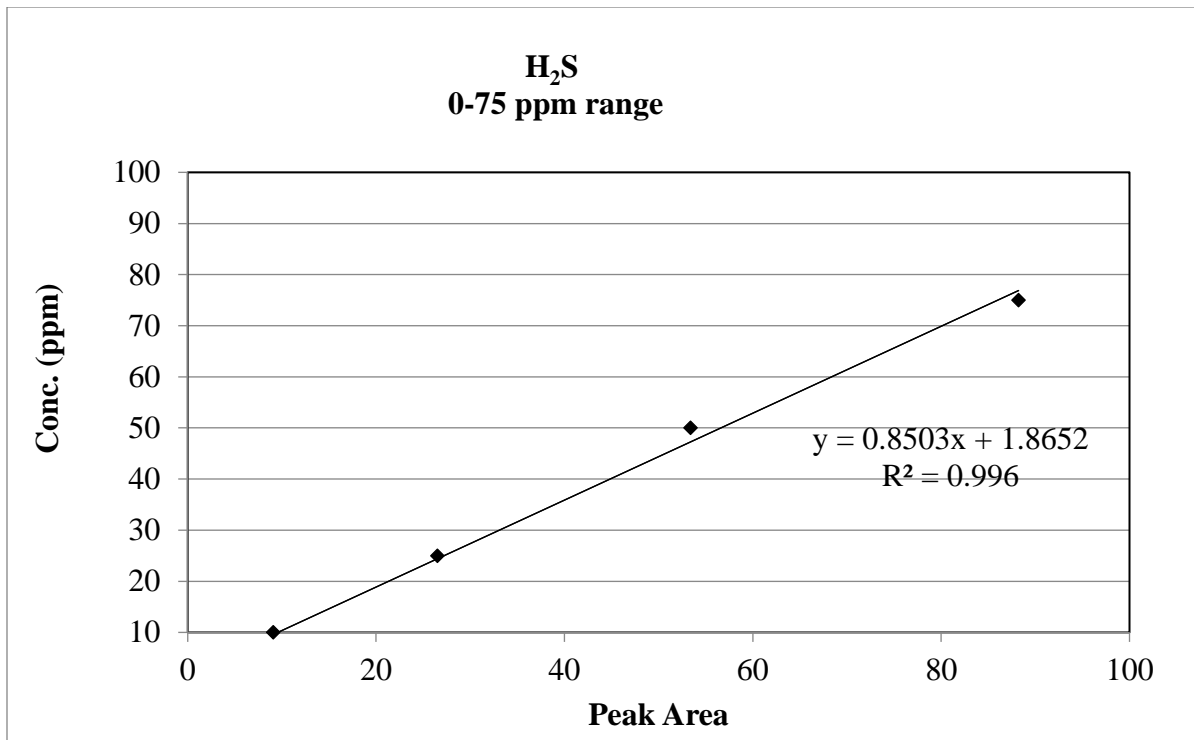
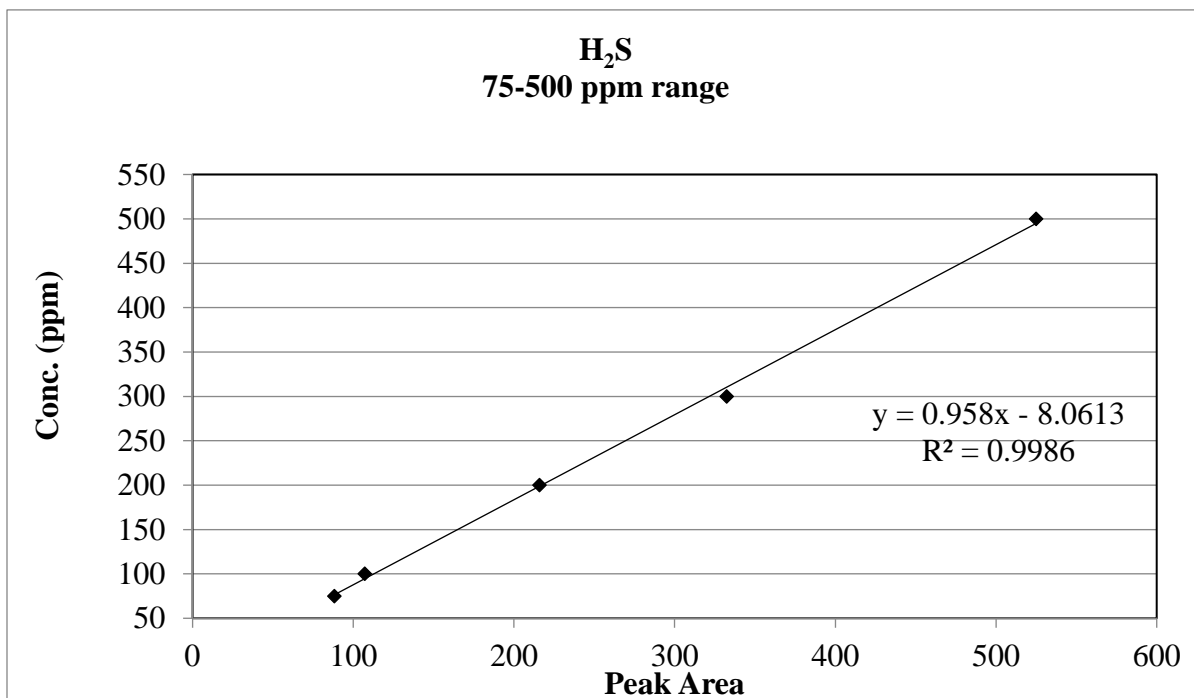**Figure A.3.** Gas chromatograph calibration curve (H_2S) for 0 to 75 ppmv range.

Figure A.4. Gas chromatograph calibration curve (H_2S) for 75 to 500 ppmv range.

B. Supplementary experimental data
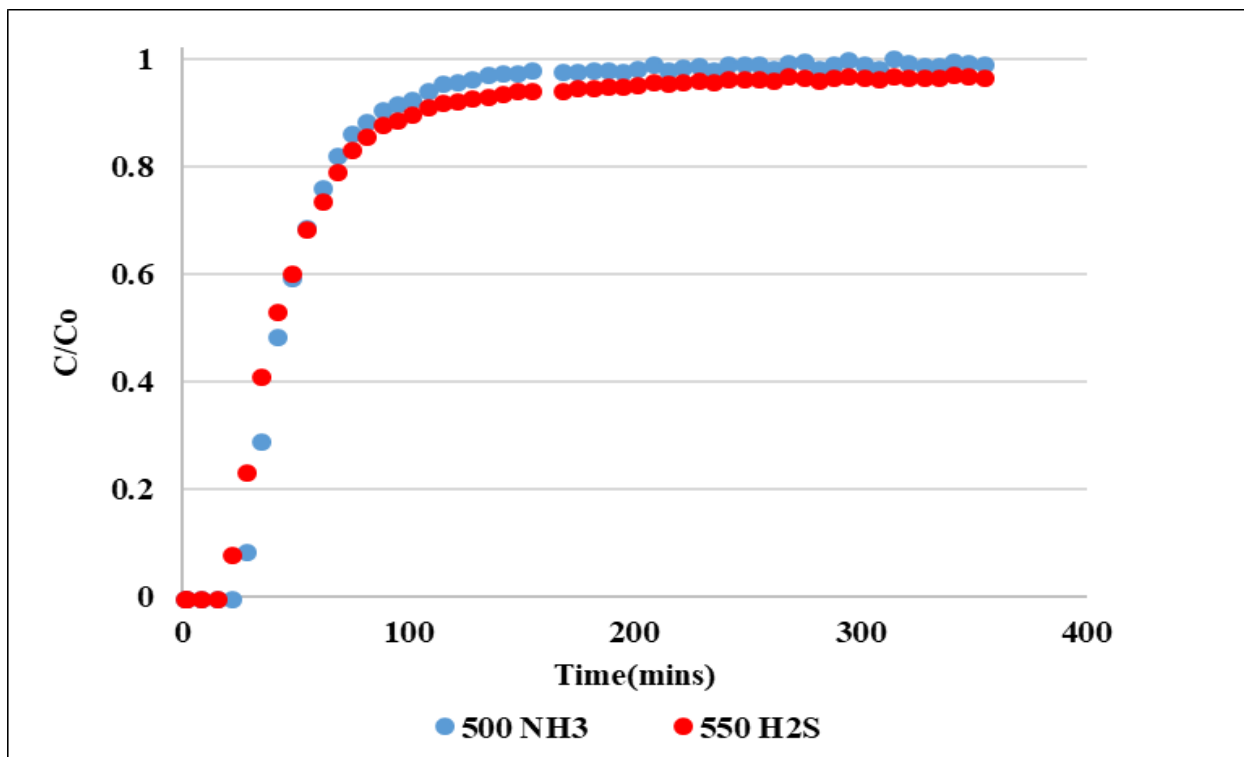
Figure B.1. Breakthroughcurve of NH$_3$ and H$_2$S at 22 °C (Homogeneous mixture of nanoparticles)**.**
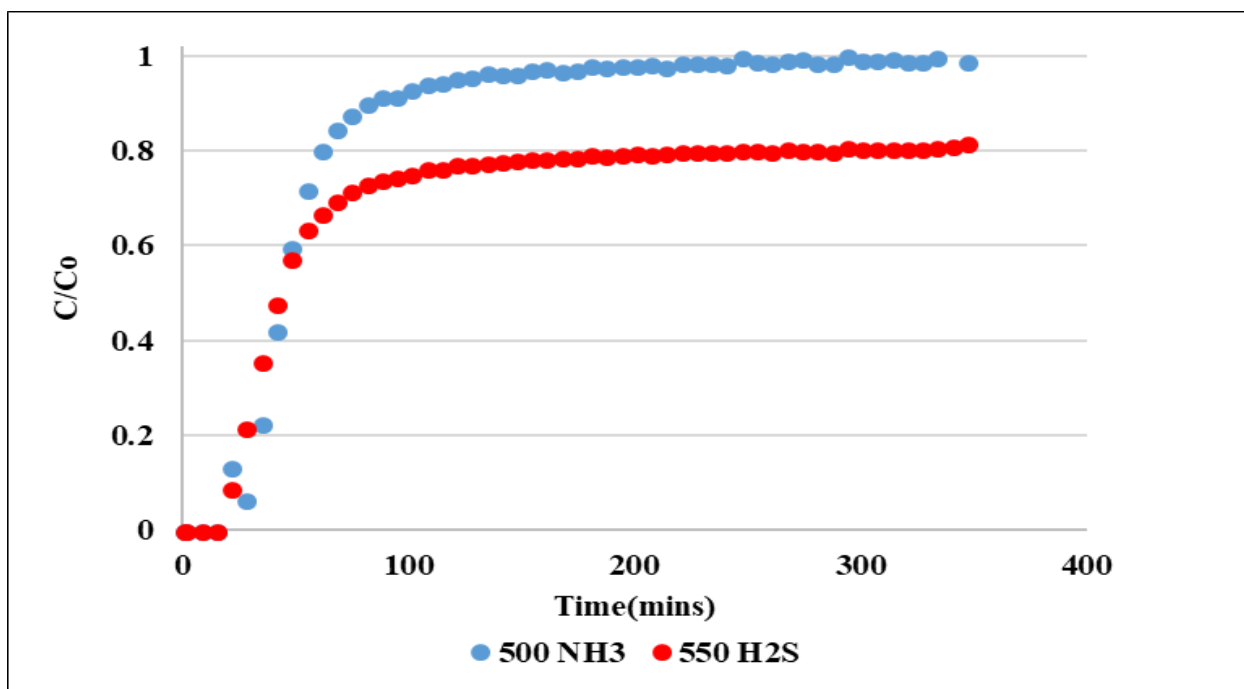
Figure B.2. Breakthrough curve of NH$_3$ and H$_2$S at 22 °C (Effect of orientation/bi-layer).
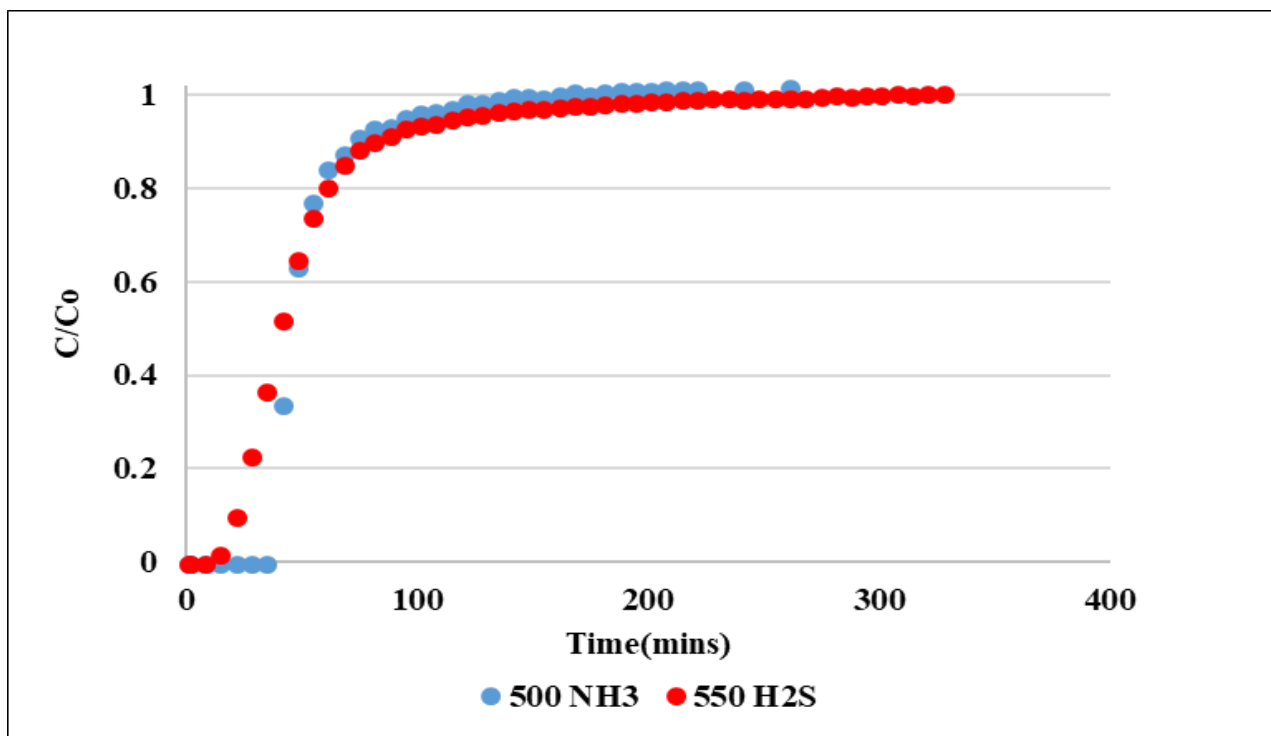
Figure B.3. Breakthrough curve of 500 NH_3 and 550 H_2S at 22 °C in the repeated experiment.
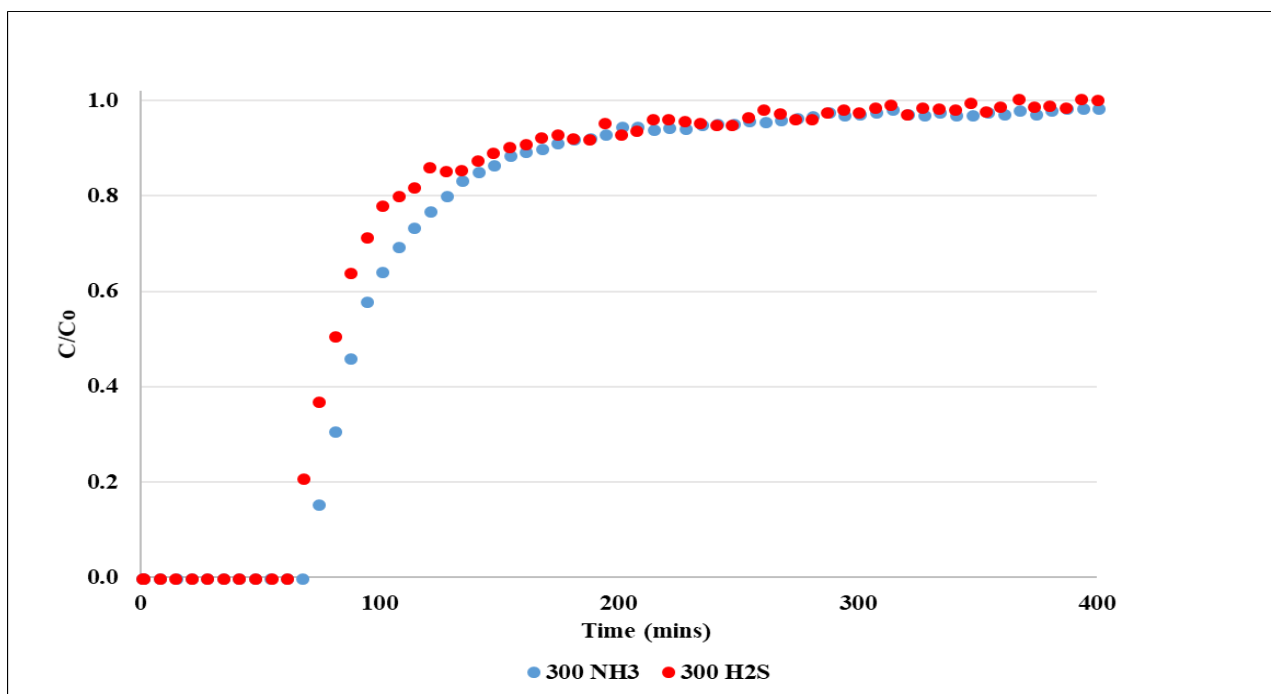
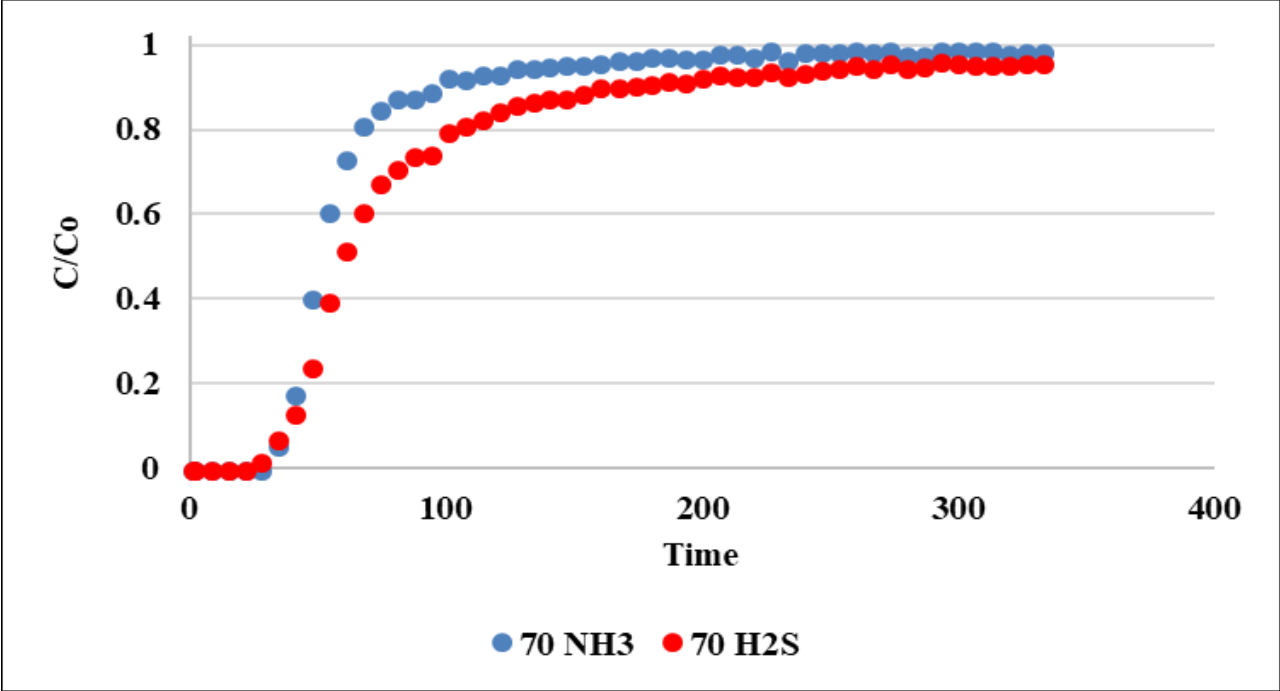**Figure B.4.** Breakthrough curve of 300 NH_3 and 300 H_2S at 22 °C in the repeated experiment.

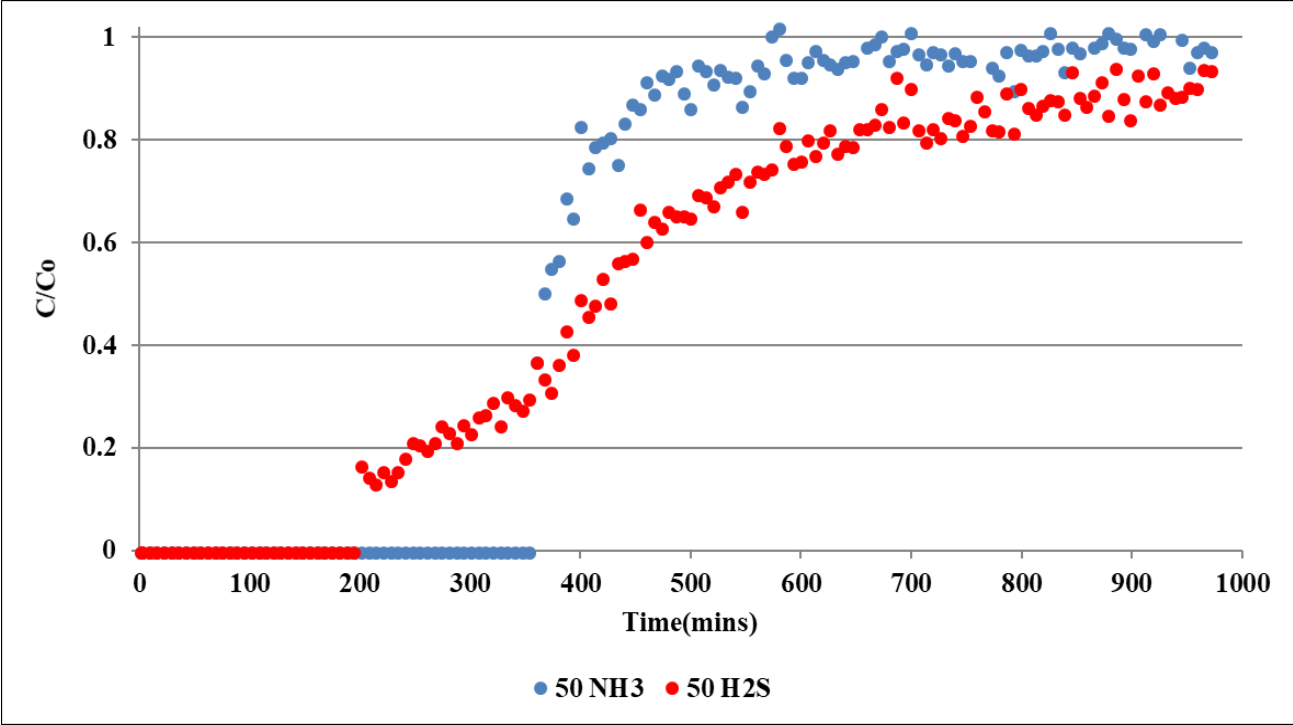**Figure B.5.** Breakthrough curve of 500 NH_3 and 550 H_2S at 70 °C in the repeated experiment.

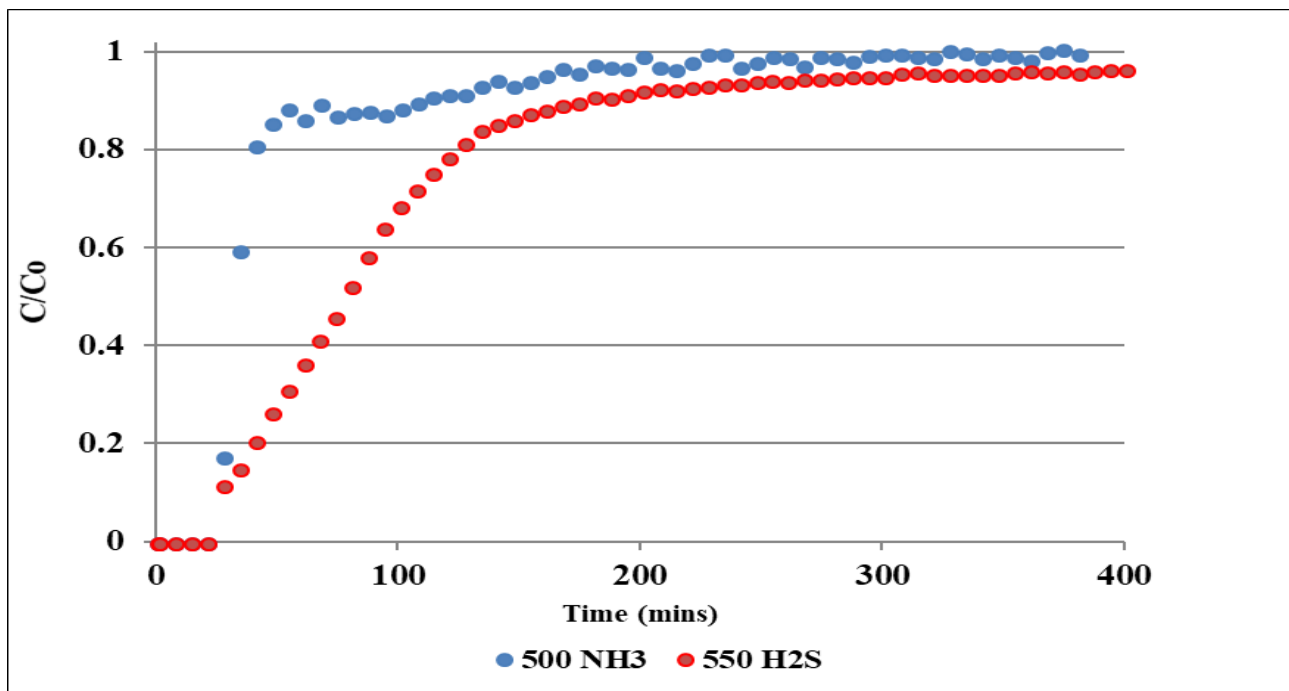**Figure B.6.** Breakthrough curve of 50 NH_3 and 50 H_2S at 70 °C in the repeated experiment.

Figure B.7. Breakthrough curve of 500 NH_3 and 550 H_2S at 140 °C in the repeated experiment.
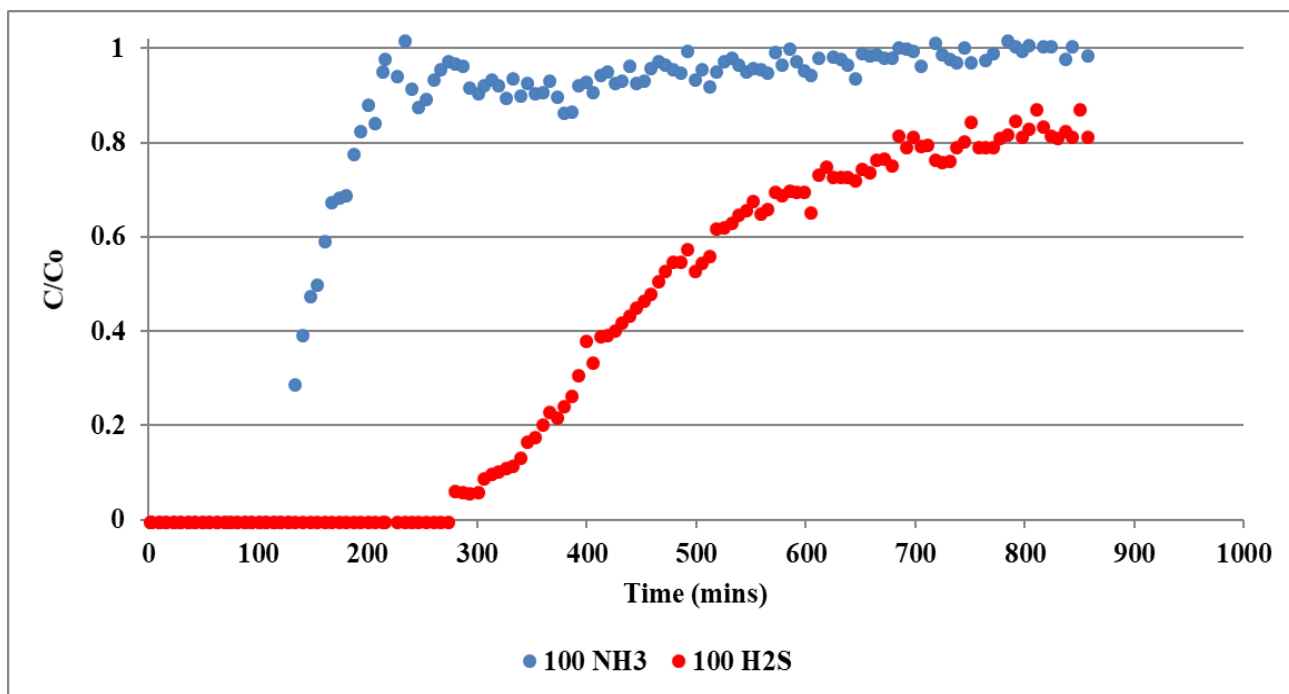

Figure B.8. Breakthrough curve of 100 NH_3 and 100 H_2S at 140 °C in the repeated experiment.
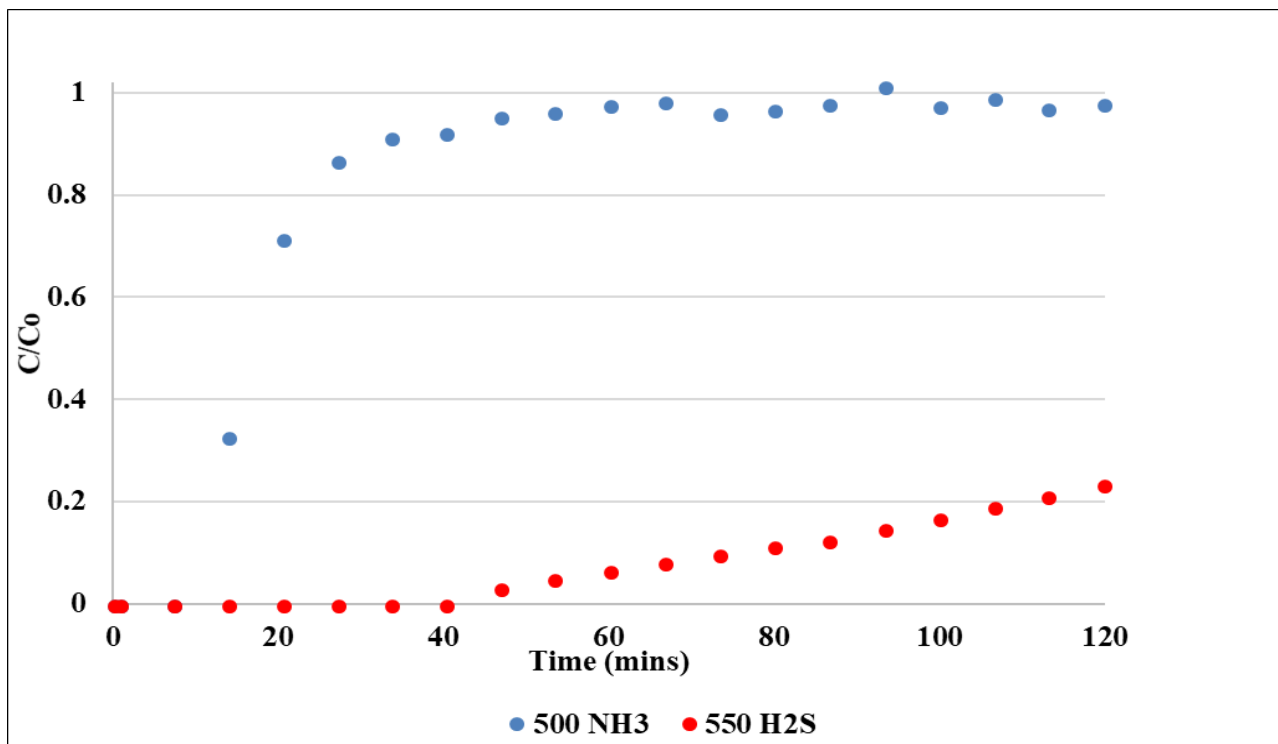
Figure B.9. Breakthrough curve of 500 NH_3 and 550 H_2S at 280 °C in the repeated experiment.
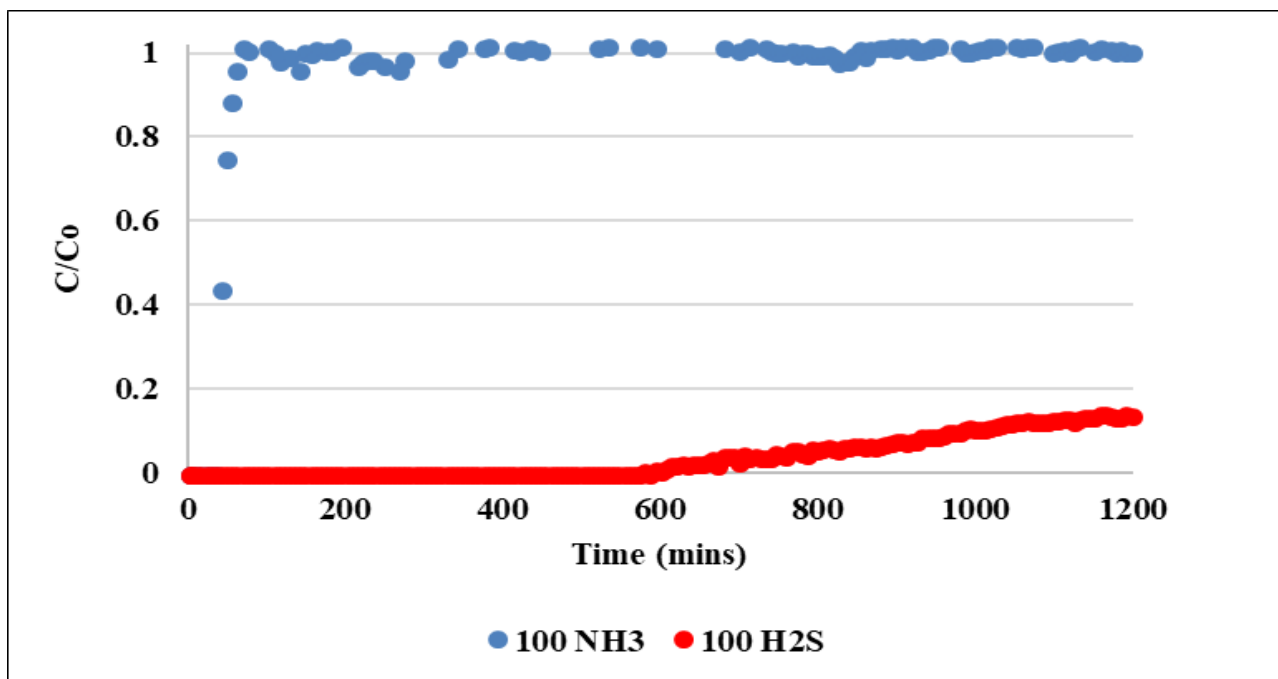

Figure B.10. Breakthrough curve of 100 NH_3 and 100 H_2S at 280 °C in the repeated experiment.

C. Adsorption capacity calculation

Data generated in the laboratory scale system and Equation C.1 was used to determine equilibrium adsorption capacities of nanoparticles (Awume et al. 2017).

$$q = \frac{Q \, C_O}{M} \int_0^t \left(1 - \frac{C}{C_O} \right) dt \tag{C.1}$$

where q is adsorption capacity (mg adsorbate g^{-1}), t is time (min; breakthrough point or saturation point), M is the quantity of adsorbents (g), Q is the gas flow rate (L min^{-1}), and C_o and C are inlet and outlet concentrations of adsorbate (mg L^{-1}), respectively. The breakthrough time was defined as the time when the ratio of H_2S concentrations in the effluent (C) and influent (C_o) approached approximately 0.05. Equilibrium conditions were assumed when the breakthrough curve leveled off and concentration of NH_3 or H_2S in the effluent changed by less than 10%. MATLAB Software (R2013a, MathWorks, USA) was used to carry out the required integration.

Table C. 1. Calculation adsorption capacity using CHNS data.

Adsorbent	Temp (°C)	wt.%	Mass of sample (g)	N capacity mg/g	Experiment results	Difference
TiO₂	22	0.51	0.20	5.13	12.00	6.87
	280	0.44	0.05	4.48	3.49	-0.99
ZnO	22	1.44	0.20	14.40	25.15	10.75
	280	10.71	0.05	107.10	161.45	54.35